

A Novel Model System to Study the Role of Catecholamines in Cardiac Lineage Commitment of Embryonic Stem Cells and Functional Response to Proarrhythmic Drugs

In a u g u r a l D i s s e r t a t i o n

zur

Erlangung des Doktorgrades

Dr. nat. med.

der Medizinischen Fakultät

und

der Mathematisch-Naturwissenschaftlichen Fakultät

der Universität zu Köln

vorgelegt von

Martin Lehmann

aus Hoyerswerda

Köln 2014

Berichterstatter/Berichterstatterin: Prof. Dr. M. Paulsson

Prof. Dr. G. Plickert

Tag der letzten mündlichen Prüfung: 11.02.2014

„Die einzige Quelle des Wissens ist Erfahrung.“

(A. Einstein)

Meinen Eltern und meiner Familie

I Table of Content

| | | |
|------------|--|-------------|
| I | Table of Content | I |
| II | Table of Figures | VI |
| III | Abbreviations | VIII |
| IV | Abstract | XIII |
| V | Zusammenfassung | XV |
| 1 | Introduction | 1 |
| 1.1 | Pluripotent stem cells | 1 |
| 1.1.1 | Embryonic stem (ES) cells | 1 |
| 1.1.2 | Induced pluripotent stem cells (iPSCs) | 1 |
| 1.1.3 | Direct reprogramming | 3 |
| 1.2 | Application fields of ES and iPS cells | 3 |
| 1.3 | Catecholamines | 4 |
| 1.3.1 | Catecholaminergic regulation of the heart function | 4 |
| 1.3.2 | Synthesis | 4 |
| 1.3.3 | Characterization, Function and Distribution of Adrenoceptors | 7 |
| 1.3.4 | Cellular effects of adrenoceptor signal transduction | 9 |
| 1.3.5 | Reserpine action | 9 |
| 1.4 | Embryonic heart development | 10 |
| 1.4.1 | Specification of myo- and endocardial precursors | 10 |
| 1.4.2 | Development of the tubular heart | 11 |
| 1.4.3 | Looping of the tubular heart | 11 |
| 1.4.4 | Development of the four-chambered heart | 12 |
| 1.5 | Electrophysiology of the heart | 13 |
| 1.5.1 | Resting membrane potential | 13 |
| 1.5.2 | The cardiac action potential (AP) | 13 |

Table of Content

| | | |
|----------|---|-----------|
| 1.6 | Microelectrode arrays (MEA) | 16 |
| 1.6.1 | Extracellular vs. intracellular recordings | 16 |
| 1.6.2 | Comparison of APs and FPs..... | 17 |
| 1.6.3 | Technical MEA Applications..... | 18 |
| 1.7 | Aims of the work | 18 |
| 1.7.1 | The role of catecholamines in cardiac lineage commitment in mouse ES cells. | 19 |
| 1.7.2 | MEA-based QT-screen using pluripotent stem cell derived CMs | 19 |
| 2 | Materials and Methods | 21 |
| 2.1 | Cell culture | 21 |
| 2.1.1 | Feeder culture and inactivation | 21 |
| 2.1.2 | ICR-feeder (Charles Rivers Laboratories, Germany)..... | 21 |
| 2.1.3 | neomycin-resistant mouse embryonic fibroblasts (NEO-feeder)..... | 21 |
| 2.1.4 | CF1-feeder (Charles Rivers Laboratories, Germany) | 22 |
| 2.1.5 | Murine embryonic stem cells (mESCs; D3 aPIG44) | 22 |
| 2.1.6 | Puromycin purification of cardiomyocytes | 23 |
| 2.1.7 | Rhesus monkey embryonic stem cells (rESCs; R366.4 and MF12) | 23 |
| 2.1.8 | Human embryonic and induced pluripotent stem cells (hESCs and hiPSCs).... | 25 |
| 2.1.9 | EB size assay | 25 |
| 2.1.10 | Ratio of beating clusters | 25 |
| 2.2 | Flow cytometry..... | 26 |
| 2.2.1 | Cell preparation | 26 |
| 2.2.2 | Measurement | 26 |
| 2.3 | Immunohistochemistry | 26 |
| 2.3.1 | Cryosliced EBs | 26 |
| 2.3.2 | Single cells/ whole EBs..... | 27 |
| 2.3.3 | Permeabilization and immunostaining procedures | 27 |
| 2.4 | Molecular biology..... | 27 |
| 2.4.1 | RNA Isolation | 27 |

| | | |
|----------|--|-----------|
| 2.4.2 | DNase I digestion of RNA isolations | 28 |
| 2.4.3 | cDNA Synthesis | 28 |
| 2.4.4 | Semiquantitative-RT-PCR | 28 |
| 2.4.5 | Quantitative-RT-PCR..... | 29 |
| 2.4.6 | Agarose gel electrophoresis | 29 |
| 2.5 | Extracellular recordings using Microelectrode Arrays (MEA) | 30 |
| 2.6 | Impedance measurement | 31 |
| 2.6.1 | Cell preparation | 31 |
| 2.6.2 | Measurement procedure | 32 |
| 2.7 | Data analysis..... | 32 |
| 3 | Results | 33 |
| 3.1 | The role of catecholamines in cardiac lineage commitment in mouse ES cells..... | 33 |
| 3.1.1 | Cell culture and morphology..... | 33 |
| 3.1.2 | Reserpine application protocols | 33 |
| 3.1.3 | Reserpine reduces numbers of beating clusters..... | 35 |
| 3.1.4 | Quantification of CMs in EBs using flowcytometry..... | 36 |
| 3.1.5 | Reserpine inhibits expression of cardiac marker proteins..... | 38 |
| 3.1.6 | Effects of reserpine on proliferation and cell viability..... | 40 |
| 3.1.7 | Reserpine effects on gene expression - Quantitative Real Time-PCR (qRT-PCR) | 43 |
| 3.1.8 | Expression of α - and β -adrenergic receptor subtypes..... | 48 |
| 3.1.9 | Positive effects on neuronal differentiation..... | 49 |
| 3.1.10 | Immunohistochemical stainings for β -III-tubulin and DBH..... | 50 |
| 3.1.11 | Functional expression of the adrenergic and muscarinic system | 51 |
| 3.1.12 | Prove of reserpine's catecholamine depleting action..... | 54 |
| 3.1.13 | Isoproterenol (ISO) partially rescues the long-term effects of reserpine | 56 |
| 3.1.14 | α - and β -AR antagonists mimic the reserpine effect..... | 58 |
| 3.2 | MEA-based QT-screen using pluripotent stem cell derived CMs..... | 61 |

Table of Content

| | | |
|-------------|--|--------------|
| 3.2.1 | Rhesus monkey cell culture..... | 61 |
| 3.2.2 | rESC differentiation using mass culture and END2 protocols..... | 62 |
| 3.2.3 | rESC differentiation applying activinA/BMP4..... | 62 |
| 3.2.4 | Summary of the optimized differentiation | 64 |
| 3.2.5 | Efficiency of the optimized differentiation | 65 |
| 3.2.6 | rESCMs express cardiac α Actinin | 66 |
| 3.2.7 | Negative FP _{Dur} / frequency (FP/f) correlation in hESCMs under physiologic conditions | 67 |
| 3.2.8 | Negative FP/f correlation in hiPSCMs under physiologic conditions | 70 |
| 3.2.9 | Negative FP/f correlation during negative chronotropic stimulation..... | 71 |
| 3.2.10 | FP/f correlation during successive positive and negative chronotropic stimulations | 71 |
| 3.2.11 | Effects of class III antiarrhythmic drugs on FP/f correlations in hESCMs and rESCMs | 72 |
| 4 | Discussion | 76 |
| 4.1 | Role of catecholamines in cardiac lineage commitment in mouse ES cells..... | 76 |
| 4.1.1 | Effects of reserpine on cardiac differentiation | 77 |
| 4.1.2 | Underlying mechanisms | 81 |
| 4.1.3 | Effects on neuronal Differentiation..... | 83 |
| 4.1.4 | Conclusions | 85 |
| 4.2 | MEA-based QT-screen using pluripotent stem cell-derived CMs | 86 |
| 4.2.1 | Optimization of rESC culture and differentiation | 86 |
| 4.2.2 | Qualitative classification of drug effects by FP/f correlation | 87 |
| 4.2.3 | Limitations and suggested improvements | 88 |
| 4.2.4 | Conclusions | 90 |
| VI | References | XVII |
| VII | Primers | XXXIV |
| VIII | Antibodies | XXXV |

| | |
|---------------------------------|--------------|
| IX Materials | XXXVI |
| X Curriculum Vitae | XL |
| XI Declaration | XLI |
| XII Publications..... | XLII |
| XIII Danksagungen..... | XLIII |

II Table of Figures

| | |
|--|----|
| Figure 1.1: Schematic overview of catecholamine synthesis and corresponding enzymes | 5 |
| Figure 1.2: Correlation of APs and ECG intervals and segments | 16 |
| Figure 1.3: Linear relationship between APD ₉₀ and FP _{Dur} | 18 |
| Figure 2.1: Depiction of common FP features | 31 |
| Figure 3.1: Colony of pluripotent D3 α PIG44 ES cells | 33 |
| Figure 3.2: Scheme of culture protocols | 34 |
| Figure 3.3: eGFP positive cardiomyocyte containing EBs representative of the time course of differentiation | 35 |
| Figure 3.4: Visual counting of beating clusters..... | 36 |
| Figure 3.5: Flowcytometry for CM quantification..... | 38 |
| Figure 3.6: Immunohistochemical staining for cardiac markers..... | 40 |
| Figure 3.7: Cross-section areas during the course of differentiation | 41 |
| Figure 3.8: Impedance measurements to exclude cytotoxic effects of reserpine on CMs | 43 |
| Figure 3.9: qRT-PCR results of <i>Zfp42 (Rex1)</i> , <i>Oct4</i> , <i>Nanog</i> and <i>Fgf-5</i> | 44 |
| Figure 3.10: qRT-PCR results of cardiac marker genes <i>Myh6</i> , <i>Mlc2a</i> and mesodermal markers <i>Nkx2-5</i> , <i>T-bra</i> and <i>Gata4</i> | 46 |
| Figure 3.11: qRT-PCR results of catecholamine synthesis genes <i>Th</i> , <i>Ddc</i> , <i>Dbh</i> and <i>Pnmt</i> | 47 |
| Figure 3.12: qRT-PCR results of endodermal and ectodermal /neuronal marker genes..... | 48 |
| Figure 3.13: Time course of α - and β -AR subtype expression..... | 49 |
| Figure 3.14: Neuronal cells in reserpine-treated EBs | 50 |
| Figure 3.15: Immunohistochemical staining with anti- β -III-tubulin and anti-DBH antibodies | 51 |
| Figure 3.16: Comparison of β -adrenergic and muscarinic modulation of beating rate in control and reserpine-treated ES cell-derived cardiomyocytes | 53 |
| Figure 3.17: Effect of catecholamines on spontaneously beating clusters of EBs after acute application of reserpine | 55 |
| Figure 3.18: Long-term rescue experiment with ISO | 57 |
| Figure 3.19: Isoprenaline long-term rescue effect on neuronal development..... | 58 |
| Figure 3.20: Blocking of α - and β -ARs mimics the reserpine-induced effect on cardiomyogenesis | 60 |
| Figure 3.21: Alkaline phosphatase staining of R366.4 and MF12 rESCs..... | 61 |

| | |
|---|----|
| Figure 3.22: Optimization of rESCM differentiation by mass culture and END2 differentiation protocols | 62 |
| Figure 3.23: Optimization of rESCM differentiation protocols by activinA and BMP4..... | 64 |
| Figure 3.24: Scheme of the rESC cardiac differentiation protocol using growth factors activinA and BMP4 for MEA QT-screen | 65 |
| Figure 3.25: Efficiency of rESC differentiation into contracting EBs..... | 66 |
| Figure 3.26: Anti- α Actinin immunohistochemical staining of an rESC-derived contracting EB | 67 |
| Figure 3.27: Negative FP/f correlation in H1 hESCMs under physiological positive chronotropic conditions..... | 69 |
| Figure 3.28: Negative FP/f-correlation in hiPSCMs under physiological positive chronotropic conditions FP _{Dur} /frequency plots representative of ISO treatment of NP0017, NP0014c5 and Royan d25-35 hiPSCMs..... | 70 |
| Figure 3.29: Negative FP/f correlation in hESCMs under physiologic positive chronotropic conditions FP _{Dur} /frequency plots representative of CCH treatment of H1 d25-35 hESCMs... | 71 |
| Figure 3.30: Negative FP/f correlation in hESCMs under physiologic positive and negative chronotropic conditions..... | 72 |
| Figure 3.31: Positive FP/f correlation in hESCMs and rESCMs induced by class III antiarrhythmic drug application | 73 |
| Figure 3.32: Positive FP/f correlation in hESCMs and rESCMs induced by different antiarrhythmic drug applications..... | 74 |
| Figure 4.1: Illustration of drug effect classification based on positive and negative FP/f correlations | 87 |

III Abbreviations

| | |
|-------------------|---|
| % | percent |
| °C | degree celsius |
| μ (SI-prefix) | micro (10 ⁻⁶) |
| AA | arachidonic acid |
| AADC | aromatic L-amino acid decarboxylase (see DDC) |
| Afp | alpha-fetoprotein (gene name) |
| Alb | albumin (gene name) |
| AP | action potential |
| APD | action potential duration |
| APD ₉₀ | action potential duration at 90 % repolarization |
| AP _{Dur} | action potential duration |
| AR | adrenoceptor/adrenergic receptor |
| ATP | adenosine-5'-triphosphate |
| AV-node | atrioventricular node |
| bFGF | basic fibroblast growth factor |
| β-ME | β-Mercaptoethanol |
| BMP | bone morphogenic protein |
| bp | base pairs |
| Ca ²⁺ | calcium ion |
| cAMP | cyclic adenosine-5'-monophosphate |
| CCH | carbachol |
| cDNA | complementary deoxyribonucleic acid (DNA) |
| cGMP | cyclic guanosine-5'-monophosphate |
| CI | cell index |
| CICR | Ca ²⁺ -induced Ca ²⁺ -release |
| Cl ⁻ | chloride ion |
| CO ₂ | carbondioxide |
| COMT | catechol-O-methyltransferase |
| ct | cycle threshold |
| cTnT | cardiac troponinT |
| d | day of differentiation |
| DA | dopamine |
| DAG | diacylglycerol |
| DBH | dopamine-β-hydroxylase |
| DDC | L-dopa-decarboxylase (see AADC) |
| DMEM | Dulbecco's Modified Eagle Medium |
| DMSO | dimethylsulfoxide |
| DNA | deoxyribonucleic acid |
| DNase | deoxyribonuclease |
| DOPA | 3,4-dihydroxyphenylalanine |
| E | embryonic day (e.g. E9, etc.) |

| | |
|-------------------|---|
| EB | embryoid body |
| ECG | electrocardiogram |
| EDTA | ethylenediaminetetraacetic acid |
| eGFP | enhanced green fluorescent protein |
| EPI | epinephrine/adrenaline |
| ES (cell)/ESC | embryonic stem cell |
| ESCM | embryonic stem cell-derived cardiomyocyte |
| EtBr | ethidium bromide |
| FBS | fetal bovine serum |
| FGF | fibroblast growth factor |
| Fgf-5 | gene name |
| Fig. | figure |
| Foxa2 | forkhead box A2 (gene name) |
| FP | field potential |
| FP/f | FP _{Dur} / frequency |
| FP _{Dur} | field potential duration |
| FP _{max} | field potential maximum |
| FP _{min} | field potential minimum |
| g | gramm |
| G418 | neomycin |
| Gapdh | glyceraldehyde-3-phosphate dehydrogenase (gene name) |
| Gata4 | Gata binding factor 4 (gene name) |
| GFP | green fluorescent protein |
| G _i | inhibitory G-protein |
| GPCR | G protein-coupled receptor |
| G-protein | guanosine nucleotide-binding protein |
| G _s | stimulating G-Protein |
| H ₂ O | water |
| hESCM | human embryonic stem cell-derived cardiomyocyte |
| HMMA | vanillylmandelic acid |
| Hnf4a | hepatocyte nuclear factor 4a (gene name) |
| hr | hour |
| HVA | homovanillic acid |
| Hz | Hertz |
| I | (membrane) current (e.g. I _{Kr} , I _{CaL} , etc.) |
| ICA (cells) | intrinsic cardiac adrenergic (cells) |
| ICM | inner cell mass (of blastocyst) |
| IHC | immunohistochemistry |
| IMDM | Iscove's Modified Dulbecco's Medium |
| IP ₃ | inositol 1,4,5-trisphosphate |
| iPS (cell)/iPSC | induced pluripoten stem cell |
| iPSCM | induced pluripoten stem cell-derived cardiomyocyte |
| ISI | interspike interval |

Abbreviations

| | |
|--------------------|---|
| ISO | isoproterenol/isoprenaline |
| k (SI-prefix) | kilo (10^3) |
| K ⁺ | potassium ion |
| KO-DMEM | Knock-out™ Dulbecco's Modified Eagle Medium |
| l | litre |
| LDCG | large dense core granule |
| L-DOPA | L-Dihydroxyphenylalanine |
| LDVC | large dense core vesicle |
| LIF | leukemia inhibitory factor |
| M | mol/liter |
| m | meter |
| m (SI-prefix) | milli (10^{-3}) |
| MAB | monoclonal antibody |
| MAO | monoamine oxidase |
| Map2 | microtubule-associated protein 2 (gene name) |
| MEA | microelectrode array |
| MEF | mouse embryonic fibroblast |
| mESCM | mouse embryonic stem cell-derived cardiomyocyte |
| Mg ²⁺ | magnesium ion |
| min | minute |
| Mlc2a | myosin light chain 2a (gene name) |
| mRNA | messenger ribonucleic acid |
| Myh6 | myosin heavy chain 6 (gene name) |
| n | number of samples |
| n (SI-prefix) | nano (10^{-9}) |
| Na ⁺ | sodium ion |
| Nanog | gene name |
| NCAM | neuronal cell adhesion molecule |
| NE | norepinephrine/noradrenaline |
| NEAA | non-essential amino acids |
| Nes | nestin (gene name) |
| NH ₄ Cl | ammonium chloride |
| Nkx2-5 | homeobox protein Nkx2-5 (gene name) |
| NO | nitric oxide |
| Nodal | gene name |
| Oct4/Oct3/4 | gene name |
| PBS | phosphate-buffered saline |
| PCR | polymerase chain reaction |
| PD | parkinson's disease |
| Pen/Strep | Penicillin/Streptomycin |
| PI | propidium iodide |
| PNMT | phenylethanolamine N-methyltransferase |
| Prod# | product number |

| | |
|---------------|--|
| Puro | puromycin |
| qRT-PCR | quantitative real-time polymerase chain reaction |
| Res | reserpine |
| rESCM | rhesus monkey embryonic stem cell-derived cardiomyocyte |
| RNA | ribonucleic acid |
| RNase | ribonuclease |
| RP | resting potential |
| RQ | relative quantity |
| RR-interval | ECG-derived time interval between two R-peaks |
| s.e.m. | standard error of the means |
| SA-node | sinoatrial-node |
| SD | standard deviation |
| sec | second |
| Sox17 | gene name |
| sqRT-PCR | semiquantitative reverse-transcription polymerase chain reaction |
| SR | sarcoplasmatic reticulum |
| SR | Serum replacement |
| SV | synaptic vesicles |
| TAE (-buffer) | Tris base, acidic acid, EDTA (-buffer) |
| T-bra | T brachyury (gene name) |
| TdP | torsade de pointes |
| TGF- β | tumor growth factor- β |
| TH | tyrosine hydroxylase |
| Tris | Tris-(hydromethyl)-aminomethane |
| Tubb3 | β -III-tubulin (gene name) |
| U | enzyme units |
| V | Volt |
| v/v | volume per volume |
| VAT | vesicular amine transporter |
| VMA | vanillylmandelic acid |
| VMAT | vesicular monoamine transporters |
| w/o | without |
| w/v | weight per volume |
| Wnt | gene name |
| x g | gravitation [m/s^2] |
| Zfp42(Rex1) | gene name |

IV Abstract

Embryonic stem (ES) cells are pluripotent cells derived from the inner cell mass of the blastocyst. These cells possess the ability to differentiate into all cell types of the three germ-layers and to proliferate indefinitely. In defined conditions ES cells are committed to the mesodermal lineage and differentiate, amongst other cell types, into cardiomyocytes (CMs). The processes underlying mesodermal and subsequent cardiac differentiation are yet only partially understood. Catecholamine release is well known to modulate heart rate and force in adult mammals. Despite first evidence, only little is known about an involvement of catecholamines during embryonic heart development. Therefore the work aimed to investigate in more detail whether catecholamines are involved in the process of ES cell cardiac differentiation *in vitro*.

Effects of catecholamine depletion induced by reserpine were investigated during murine D3 α PIG44 ES cell differentiation. Reserpine is a drug blocking vesicular storage of monoamines, and as a result depletes cells of the catecholamines norepinephrine and epinephrine. Cardiac differentiation was assessed by quantification of beating clusters, immunocytochemistry, molecular biology, flowcytometry and pharmacological approaches. Proliferation and cytotoxicity was evaluated by embryoid body cross-section measurements and impedance monitoring, while functional characterization of CMs was performed using extracellular field potential (FP) recordings with microelectrode arrays (MEAs). Involvement of β -adrenoceptor signaling was studied differentiating ES cells in the presence of reserpine and isoproterenol. To further discriminate between drug-specific effects of reserpine and catecholamine action via adrenergic receptors we applied the unspecific α - and β -receptor antagonists phentolamine and propranolol during differentiation.

Reserpine treatment led to a remarkable reduction of beating cardiac clusters, down-regulation of cardiac proteins α -actinin and troponinT and delayed mesodermal and cardiac gene expression. In more detail, the average ratio of ~40% spontaneously beating control clusters was significantly reduced by 100%, 91.1% and 20.0% on days 10, 12, and 14, respectively. In line, significant reduction by 71.6% (n=11) of eGFP expressing CMs after reserpine treatment was revealed by flowcytometry. Reserpine neither reduced EB size nor acted cytotoxic on CMs, while an increased numbers of neuronal cells were observed. MEA measurements with reserpine-treated EBs showed lower FP frequencies and weak responsiveness to adrenergic and muscarinic stimulation. Co-application of isoproterenol and reserpine during differentiation partially rescued cardiac development. The developmental

inhibition after α - and β -adrenergic blocker application mimicked developmental changes with reserpine and proved an involvement of adrenergic receptors in the process. We conclude that catecholamines and adrenergic signaling play a critical role during cardiac development in ES cells.

Since we experienced the ES cell/MEA model as useful for pharmacological approaches, we wondered as a next step whether pluripotent ES cell-derived CMs could be used for safety pharmacological drug screening with cardio-active compounds. Concentration/response was tested in rhesus monkey and human ES cell- and human induced pluripotent stem cell-derived CMs (rESCMs, hESCMs and, hiPSCMs, respectively) for different drugs at increasing concentrations.

Empirical observation under physiologic positive and negative chronotropic drug-stimulation showed negative correlations of FP duration (FP_{Dur}) and beating frequency (negative FP/f correlation). Negative FP/f correlation persisted independent of cell lines in hESCMs and hiPSCMs. In contrast, FP/f correlations changed to positive values in the presence of E4031 and sotalolol in a concentration-dependent manner.

Therefore, it was concluded that safety pharmacological drug-screening is feasible using ES cell-derived CMs and MEAs independent of cell lines and species origin. Furthermore a novel method to qualitatively evaluate QT-time/repolarization prolonging drug effects based on FP/f correlations is suggested. The results may help to reduce cost-intensive clinical trials and, above all, to reduce the number of animal experiments.

V Zusammenfassung

Embryonale Stammzellen werden aus der inneren Zellmasse von Blastozysten gewonnen. Diese Zellen besitzen die Eigenschaft in alle Zelltypen der drei Keimblätter zu differenzieren und unendlich zu proliferieren. Unter den geeigneten Bedingungen lassen sich aus embryonalen Stammzellen mesodermale Zellen generieren, die neben anderen Zellen, zu Kardiomyozyten differenzieren. Die Prozesse, die mesodermaler und anschließender kardialer Differenzierung zugrunde liegen sind jedoch erst teilweise erforscht. Man weiß, dass über Katecholamineausschüttung die Herzfrequenz und die Kontraktionskraft des Herzens in adulten Säugetieren reguliert wird. Obwohl vorläufige Ergebnisse darauf hindeuten, weiß man allerdings erst sehr wenig ob Katecholamine während der embryonalen Herzentwicklung eine Rolle spielen. Daher soll in dieser Arbeit detailliert untersucht werden, ob Katecholamine *in vitro* am Prozess der kardialen Differenzierung von Stammzellen beteiligt sind.

Die Effekte, die durch Reserpin-induzierte Katecholamin-Verarmung hervorgerufen wurden, sollten während der Differenzierung muriner embryonaler D3 α PIG44 Stammzellen untersucht werden. Reserpin blockiert den vesikulären Transport von Katecholaminen, und als Folge verarmen die Zellen an Noradrenalin und Adrenalin. Die Auswirkungen auf die kardiale Differenzierung wurden durch die Quantifizierung kontrahierender Cluster, immunhistochemischer und molekularbiologischer Methoden, sowie Durchflusszytometrie und pharmakologischer Methoden ermittelt. Die Prolifertation und Zytotoxizitätseffekte wurden jeweils mit Hilfe von Querschnittsflächen-Messungen von Embryonalkörpern (EBs) beziehungsweise Impedanz Messungen untersucht, wohingegen man extrazelluläre Feldpotential (FP) Messungen durch Microelektroden Arrays (MEA) dazu benutzte, die Funktionalität der Kardiomyozyten zu prüfen. β -Adrenozeptor vermittelte Signale als Ursache der beobachteten Prozesse, wurde durch Differenzierung der Stammzellen unter gleichzeitiger Zugabe von Reserpin und Isoproterenol (ISO) untersucht. Um darüber hinaus zwischen Reserpin-spezifischen Effekten und Katecholamin-vermittelter α - und β -Adrenozeptor Wirkung zu unterscheiden, wurden die Stammzellen während der Differenzierung den entsprechenden Antagonisten, Phentolamin und Propranolol, ausgesetzt.

Reserpin führte zu einer deutlichen Reduktion schlagender kardialer Cluster und zu herab-regulierter Expression der kardialen Proteine α -Actinin und TroponinT sowie mesodermaler und kardialer Gene. Im Detail beobachtete man, dass die in Kontroll EBs bei ungefähr 40% liegende Rate schlagender Areale an den Tagen 10, 12 und 14 signifikant um entsprechend 100%, 91,1% und 20% reduziert waren. Genauso zeigten Durchflusszytometrie

Experimente eine Reduzierung eGFP-exprimierender Kardiomyozyten um 71,6%. Reserpin hatte weder einen Einfluss auf die EB Größe noch auf Zytotoxizität, jedoch wurde interessanterweise eine erhöhte Anzahl von Neuronen beobachtet. Die MEA Versuche ergaben verringerte Schlagraten in Reserpin-behandelten EBs und sehr geringe Empfindlichkeit gegenüber adrenerger und muskarinerger Stimulation. Eine co-Applikation von Reserpin mit ISO bewirkte einen partiellen „Rescue“ der kardialen Entwicklung. Außerdem beobachtete man, dass die kardiale Entwicklungsverzögerung nach α - und β -Blocker Behandlung in hohem Maß der Verzögerung nach der Reserpin Behandlung glich. Dadurch konnte der Einfluss der adrenergen Rezeptoren gezeigt werden. Es lässt sich daher aus dieser Arbeit schlussfolgern, dass Katecholamine eine kritische Rolle bei der Herzentwicklung spielen und dass adrenerge Rezeptoren daran beteiligt sind.

Da sich das ES Zell/MEA Modell als sehr geeignet für pharmakologische Untersuchungen erwiesen hat, stellte sich die Frage ob man pluripotente Stammzellen für sicherheitspharmakologische Screenings kardioaktiver Substanzen nutzen kann. Die Kombination von Stammzellen als unbegrenzte Quelle für Kardiomyozyten zu dienen mit dem Vorteil der MEA-Technik über lange Zeiträume extrazellulär ableiten zu können, stellt eine ideale Methode für Drogen-Screens dar. Die konzentrationsabhängige Antwort verschiedener Drogen wurde daher an verschiedene Rhesusaffen und humanen embryonalen und induziert-pluripotenten Stammzell-abgeleiteten Kardiomyozyten (entsprechend rESCMs, hESCMs und hiPSCMs) getestet.

Unter physiologisch positiven und negativen chronotropen Bedingungen beobachtete man eine negative Korrelation zwischen der FP Dauer (FP_{Dur}) und der Schlagfrequenz (negative FP/f Korrelation). Negative FP/f Korrelation wurden unabhängig voneinander bei ESCMs und iPSCMs beobachtet. Im Gegensatz dazu änderte die Zugabe von E4031 und Sotalol die FP/f Korrelation zu positiven Werten.

Anhand der empirischen Daten kann man zeigen, dass ein sicherheitspharmakologischer Screen, basierend auf pluripotenten Stammzellen und dem MEA System, unabhängig von Zelllinie und Spezies durchgeführt werden kann. Im Rahmen dieser Arbeit schlagen wir eine neue graphische Methode der qualitativen Evaluierung substanz-abhängiger QT-Zeit- bzw. Repolarisations-Effekte vor. Die Ergebnisse daraus können in Zukunft dazu beitragen, Kosten bei der Medikamentenforschung einzusparen und, vor Allem, die Zahl an Versuchstieren deutlich zu verringern.

1 **Introduction**

1.1 **Pluripotent stem cells**

1.1.1 *Embryonic stem (ES) cells*

Embryonic stem (ES) cells are derived from the inner cell mass (ICM) of an early blastocyst. These cells are pluripotent, i.e. they possess the ability to differentiate into all cells of an embryo except for extra-embryonic tissues (e.g. the trophoblast). Pluripotent ES cells are, thus, characterized by their ability to differentiate into cells of the three germ-layers (endoderm, mesoderm and ectoderm) and further by their property to be propagated indefinitely [Evans and Kaufman 1981, Martin 1981, Thomson, Kalishman et al. 1995, Thomson, Itskovitz-Eldor et al. 1998, Itskovitz-Eldor, Schuldiner et al. 2000]. Due to these characteristics ES cells provide a great tool to study embryogenesis *in vitro*. Underlying mechanisms or signaling pathways crucial for ES cell development into mature cells can easily be accessed using this relatively simple model. Furthermore, ES cells are thought to hold great promise for cell replacement therapy of a variety of degenerative diseases like Parkinson's disease, cardiac infarction and diabetes mellitus. However, there is a number of obstacles to overcome before pluripotent cells and their derivatives will be used for clinical approaches. A major issue of the medical application of pluripotent cells is that current differentiation protocols lead to a mixture of randomly occurring cells, even if the used protocol favors a certain direction of cell-type differentiation. Amongst the other cells there is a high probability of remaining pluripotent cells which, after transplantation, have a high potential for teratocarcinoma formation [Thomson, Kalishman et al. 1995, Thomson and Marshall 1998]. And moreover, if for example donor stem cell-derived somatic cells of a certain kind are transplanted into a host (allogenic transfer), the host's immune system can recognize the donor cells as foreign and will induce a variety of immune reactions potentially leading to transplant rejection [Thomson, Itskovitz-Eldor et al. 1998].

1.1.2 *Induced pluripotent stem cells (iPSCs)*

A breakthrough in regard of the issue of immune rejection, hindering clinical application, was the work of S. Yamanaka, his colleagues and other groups. They showed that somatic cells can be reprogrammed into a pluripotent state and being indistinguishable to pluripotent ES

cells derived from embryos [Takahashi and Yamanaka 2006, Takahashi, Tanabe et al. 2007, Wernig, Meissner et al. 2007]. They found that only four factors, OCT4 (also called OCT3/4 or POU5f1), SOX2, c-MYC, and KLF4 (“Yamanaka factors”) are sufficient to reprogram somatic cells into a pluripotent state. Using a different set of reprogramming factors (OCT4, SOX2, NANOG, and LIN28) also led to successful somatic cell reprogramming [Yu, Vodyanik et al. 2007]. These cells are known today as induced pluripotent stem (iPS) cells possessing typical characteristics of ES cells, and amongst those, the ability to differentiate into cells of all three germ-layers. The possibility of reprogramming to generate patient-specific iPS cells was a critical step toward clinical application of pluripotent cell derivatives, because immune rejection could be overcome by this approach. Very recently, however, the supposed advantage of histocompatibility of iPSCs was challenged. A study showed that also syngeneic iPSCs were rejected after transplantation [Zhao, Zhang et al. 2011]. Nevertheless, controversial debate, especially considering the immunogenicity of iPSC-derived differentiated cells, is still going on [Okita, Nagata et al. 2011, Araki, Uda et al. 2013].

However, iPS cells still inherit the risk of teratoma formation after transplantation [Takahashi and Yamanaka 2006, Wernig, Meissner et al. 2007, Yu, Vodyanik et al. 2007, Yoshida and Yamanaka 2010]. Less than 2 years after the first successful generation of iPS cells using the Yamanaka factors, an improved iPS generation protocol was established omitting the oncogene *c-Myc* leading to reduced tumor formation in chimeric offspring [Nakagawa, Koyanagi et al. 2008, Pera and Hasegawa 2008, Wernig, Meissner et al. 2008]. Another study revealed that exogenous expression of only *Oct4* was enough for reprogramming neural stem cells into pluripotent cells, which could again be differentiated, not only into neuronal lineage cells, but also into cardiomyocytes and endothelial cells [Kim, Sebastiano et al. 2009]. This meant a further advance toward clinical application of pluripotent cells. Still, the viral vectors used for transfection of the pluripotency factors represent an important issue, because they integrate into the genome randomly and potentially lead to insertional mutagenesis. Methods for non-integrative reprogramming such as episomal plasmids [Okita, Matsumura et al. 2011], proteins [Kim, Kim et al. 2009, Zhou, Wu et al. 2009] and mRNA [Warren, Manos et al. 2010, Warren, Ni et al. 2012] have already been established. Ultimately, e.g. small molecules for reprogramming would help to make pluripotent stem cell therapy considerably safer.

1.1.3 Direct reprogramming

Within the last 5 years first results of trans-differentiation of one somatic cell-type directly into another somatic cell-type were presented [Feng, Desbordes et al. 2008, Ieda, Fu et al. 2010, Vierbuchen, Ostermeier et al. 2010]. As suggested, cell types can be converted into cell lines of another type. Even though it is at the very beginning, at the moment this research field is the most promising one, because it circumvents the afore-mentioned major risks of pluripotent cell usage for the treatment of diseases. Trans-differentiated cells supposedly avoid the risk of teratoma formation because they will obviate pluripotent cell states, and if the technique is established cells for syngeneic transplantation can be produced within a short period of time [Feng, Desbordes et al. 2008, Ieda, Fu et al. 2010, Vierbuchen, Ostermeier et al. 2010].

1.2 Application fields of ES and iPS cells

ES as well as iPS cells are used as models to study embryogenesis. Especially iPS cells will be valuable tools for studies involving material of human origin, since ethical considerations are avoided when compared to ES cells. One possible field beside basic research on embryogenesis could certainly be the usage of human iPS cells for drug screening [Khan, Lyon et al. 2013]. In this way possible side-effects can be prognosed *in vitro*, thus, reducing the number of experimental animals needed for clinical trials. Possibly harmful or un-specifically acting compounds could be identified early, if negative effects on tissue-specific committed cells, derived from human iPS cells, are detected. One part of this thesis focusses on exactly this question. We have analyzed and will discuss if cardio-active drug effects can reliably be forecasted using microelectrode arrays (MEA). Another application area for iPS cells is the investigation of the pathophysiology of genetic diseases. Therefore, patient-specific fibroblasts were reprogrammed and subsequently differentiated into the cell types affected by the disease. Cardiomyocytes, for example, were generated to analyze if the pathological symptoms seen in patients can be recapitulated phenotypically [Moretti, Bellin et al. 2010, Fatima, Xu et al. 2011, Itzhaki, Maizels et al. 2011]. These approaches will help to understand mechanisms of diseases, to develop new drugs and to optimize treatment strategies [Jung, Moretti et al. 2012].

1.3 Catecholamines

1.3.1 *Catecholaminergic regulation of the heart function*

It is well known that catecholamine secretion induces several physiological changes increasing the performance of the organism in response to dangerous or acute stress situations (fight-or-flight response [Cannon 1920]). These changes are attributed to the sympathetic nervous system and regulate cardiac output as well as vasoconstriction subsequently influencing blood pressure. Moreover, also respiration, digestion, the pupillary response, urinary excretion and sexual arousal are regulated by that system. Already in 1895, George Oliver and Edward Albert Schäfer showed the pharmacological effect of a supra-renal extract on blood pressure [Oliver and Schafer 1895]. Shortly after that Thomas Renton Elliot found that a substance could be produced from the adrenal medulla, which mimicked the effects of the sympathetic nervous system. Then, in 1904 adrenalin synthesis was accomplished by F. Stolz. It took many years until in 1931 a study on isolated embryonic chick hearts and cardiac tissue cultures showed that adrenaline (and also acetylcholine) affects pre-innervation stage cardiac isolates and thus suggested that an “intermediate receptive substance” (i.e. receptors) confers the adrenalin signal [Markowitz 1931]. Today we know that adrenoceptors (adrenergic receptors, ARs) and their second messengers are responsible for signal transduction of NE and EPI across the membrane of the affected cell.

1.3.2 *Synthesis*

The biogenic amines Dopamine (DA), Norepinephrine (NE) and Epinephrine (EPI) are synthesized in amine-handling cells in different organs of the body in mammals, e.g. neurons in the central and peripheral nervous system and in chromaffin cells of the adrenal medulla in the kidneys. While DA functions as the principal neurotransmitter in those parts of the central nervous system associated with motor control, its β -hydroxylated form, NE, is produced in the adrenergic central and peripheral nervous system. The addition of a methyl group to the amino group of NE forming EPI finally takes place in the adrenal medulla [Molinoff and Axelrod 1971, Peaston and Weinkove 2004]. Amine-handling cells are characterized by the expression of proteins related to I) amine synthesis, II) plasma membrane transport for release and recycling of amines from the extracellular space and III) intracellular transport of amines for vesicular storage (reviewed in [Weihe and Eiden 2000]).

1.3.2.1 Catecholamine synthesis cascade

Catecholamine synthesis is schematically depicted in Fig. 1.1 with the amino acid tyrosine as a precursor which is converted into L-Dihydroxyphenylalanine (L-DOPA), DA, NE and EPI by the sequential action of the enzymes tyrosine hydroxylase (TH), aromatic L-amino acid decarboxylase/L-dopa-decarboxylase (AADC/DDC), dopamine- β -hydroxylase (DBH) and phenylethanolamine N-methyltransferase (PNMT). The TH-catalyzed first step within the anabolic cascade is the rate-limiting one.

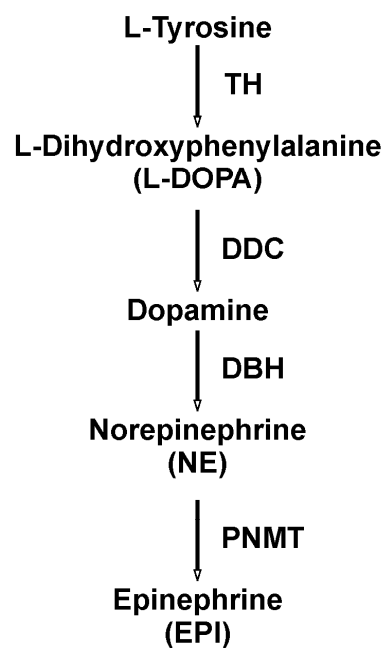


Figure 1.1: Schematic overview of catecholamine synthesis and corresponding enzymes

Adopted from Encycloaedia Britannica.

1.3.2.2 Plasma membrane transport for release and recycling of amines from the extracellular space

During the synaptic transmission process, catecholamines, acting as neurotransmitters, are released from the presynaptic membrane by exocytosis into the synaptic cleft. After release, binding of catecholamines to post-synaptic receptors subsequently induces signal transduction and allows information propagation from one cell to the other. As important as the information propagation, however, is the termination of the signal transduction by an active re-uptake of the amines into the presynaptic membrane (Na^+ -gradient dependent). How important this re-uptake process and the termination of the signaling for a normal function of e.g. the brain is, can be understood by the dramatic effects induced by specific re-uptake

inhibitors like cocaine and amphetamines. After re-uptake amines are either recycled by transport into storage vesicles or degraded by the action of monoamine oxidase (MAO) and catechol-O-methyltransferase (COMT) (reviewed in [Eisenhofer, Kopin et al. 2004, Peaston and Weinkove 2004]).

Only a small fraction of released catecholamines reaches circulation [Bravo, Tarazi et al. 1979], while the majority of the catecholamines is metabolized in the cytosol of neuronal or extra-neuronal cells as well as in the adrenal medulla. During the metabolic degradation of catecholamines which are circulating in the body or are re-uptaken by cells, a number of cytotoxic metabolites are formed. While NE and EPI are metabolized to vanillylmandelic acid (HMMA/VMA), DA is metabolized to homovanillic acid (HVA). These metabolites are then transported to the liver via the blood-stream, before both are eliminated from the system by the kidneys (reviewed in [Eisenhofer, Kopin et al. 2004]).

1.3.2.3 Intracellular transport of Catecholamines for vesicular storage

The intracellular transport of catecholamines in the cells of the adrenergic central and peripheral nervous system and the adrenergic medulla is accomplished by expression of Vesicular Amine Transporters (VATs). Vesicular transport of dopamine is also one of the rate-limiting steps in catecholamine synthesis. In catecholaminergic cells two types of VATs are found depending on the organ or cell type they are located at and are called VMATs (Vesicular Monoamine Transporters). While VMAT1 expressing cells are found in peripheral neuroendocrine cells including the adrenal chromaffin cells (in the adrenal medulla in the kidney), VMAT2 expression is found in all aminergic neurons, some neurons of the guts and in cells of the immune system (e.g. mast cells [Weihe and Eiden 2000]). Monoamine uptake by VMATs can potentially be blocked by reserpine and tetrabenazine [Erickson, Eiden et al. 1992, Schuldiner 1994].

Monoamines are not only stored in synaptic vesicles (SVs), but also in large dense core vesicles (LDCVs) which are analogous to large dense core granules (LDCGs) in neuroendocrine cells [Liu, Krantz et al. 1999, Torrealba and Carrasco 2004]. Both kinds represent different types of secretory vesicles and show distinct differences, e.g. their subcellular sites of release (reviewed in [Fei, Grygoruk et al. 2008]). VMAT2 was found to be localized in SVs as well as LDCVs. Therefore subcellular VMAT2 localization can regulate the site of monoamine release, showing its importance for the regulation of catecholamine effects [Nirenberg, Liu et al. 1995, Nirenberg, Chan et al. 1996, Nirenberg, Chan et al. 1997].

1.3.3 *Characterization, Function and Distribution of Adrenoceptors*

ARs are the targets of the catecholamines epinephrine (adrenaline; EPI) and norepinephrine (noradrenaline; NE) and are found in a variety of tissues within the body. Catecholamine binding induces a sympathetic response ('flight-or-fight' response) with the general result of increased heart rate and force, pupil dilation and energy mobilization preparing the body for improved physiological performance [Bylund, Eikenberg et al. 1994]. Effects of catecholamines in the mammalian body are mediated by the two major classes of adrenergic receptors: alpha- and beta-adrenoceptors (α -ARs and β -ARs; [Powell and Slater 1958]), which are both known to belong to the G protein-coupled receptor superfamily (GPCRs) [Caron and Lefkowitz 1993]. Several receptor-subtypes of both classes were identified and their specific tissue distribution and cellular localization, their distinct pharmacological properties and their different downstream signaling mechanisms explain the variety of actions conferred by catecholamines. ARs are very well investigated because of their widely diversified properties, the following paragraphs will give a rough overview over this complex field.

1.3.3.1 *α -Adrenoceptors*

α -ARs are usually found in nerve terminals of the central and peripheral sympathetic nervous system and are divided into two subclasses, the α_1 -ARs and α_2 -ARs. The α_1 -ARs subclass was further shown to consist of three receptor subtypes (α_{1A} , α_{1B} and α_{1D} ; [Hieble, Bylund et al. 1995]) and the α_2 -AR subclass constitutes another three subtypes (α_{2A} , α_{2B} , α_{2C} ; [Lorenz, Lomasney et al. 1990, Bylund 1992]). Each subtype has specific pharmacological properties and amino acid sequences [Bylund, Eikenberg et al. 1994, Zhong and Minneman 1999]. Originally, α -ARs were classified based on their anatomical localization [Langer 1974]. While α_1 -ARs are located postsynaptically, α_2 -ARs are mostly found presynaptically, even though also postsynaptic localization is found. More recently, however, α -ARs and their subtypes were classified by their pharmacological properties and radio-ligand binding (reviewed in [Bylund, Eikenberg et al. 1994]).

All α_1 -ARs have certain common features: 1.) They are equally activated by NE and EPI, 2.) they are sensitive to blockade by prazosin, 3.) they show a low affinity to α_2 -ARs antagonists yohimbine and rauwolscine, 4.) the activation of each subtype leads to increased intracellular Ca^{2+} (reviewed in [Bylund, Eikenberg et al. 1994]). In the central nervous system α_1 -ARs have excitatory functions on postsynaptic membranes of neurons, whereas, α_1 -ARs in

the periphery are situated on vascular and non-vascular smooth muscle cells and are responsible for their tone. Furthermore, α_1 -ARs were found in the liver responsible for glycogenolysis and potassium release and, in the heart where they exert inotropic effects [Jensen, Swigart et al. 2009, Wang, Yeh et al. 2010].

Also α_2 -ARs have common properties: 1.) they are activated by NE and EPI, 2.) they are blocked by yohimbine and rauwolscine [Bylund 1992, Bylund, Eikenberg et al. 1994]. α_2 -ARs rather serve as an inhibitory system [Stevens, Kuramasu et al. 2004]. On nerve terminals they are found presynaptically, acting as ‘autoreceptors’ or ‘heteroreceptors’ [Starke 1987, Boehm and Huck 1995, Starke 2001]. Activating presynaptic α_2 -ARs with NE or EPI, in turn leads to a feedback inhibition of catecholamine (‘autoreceptor’) or other neurotransmitter (‘heteroreceptor’) release from neuron terminals. Similarly, EPI release from chromaffin cells is regulated in an autoreceptor feedback loop [Gilsbach, Brede et al. 2007]. α_2 -ARs were also found outside the central nervous system, acting in e.g. vascular smooth muscle controlling blood pressure [Link, Desai et al. 1996, Gilsbach, Albarran-Juarez et al. 2011].

Upon stimulation of all three α_1 -subtypes, the $G_{q/11}$ signaling pathway is activated, generating the second messengers inositol-(1,4,5)-triphosphate and diacylglycerol (DAG) by activation of phospholipase C. Furthermore, Ca^{2+} from intracellular stores and especially the sarcoplasmic reticulum (SR) is mobilized upon α_1 -AR stimulation [Chen and Minneman 2005]. In contrast, stimulation of the α_2 -ARs leads to activation of the inhibitory G-protein (G_i) pathway, subsequently inhibiting the activity of the adenylate cyclase enzyme and reducing the cAMP levels in affected cells. Reduced Ca^{2+} influx during action potentials, in turn, reduces the release of NE [Limbird 1988].

1.3.3.2 β -Adrenoceptors

The β -AR subfamily was initially divided into β_1 - and β_2 -receptors classified for their affinity to their natural agonists, NE and EPI. While β_1 -ARs showed equal affinity for NE and EPI, β_2 -ARs show lower affinity for NE than for EPI [Lands, Arnold et al. 1967]. Furthermore, at least one more β -AR subtype (β_3) was identified having pharmacological properties distinct from the other two β -AR agonists [Arch, Ainsworth et al. 1984, Bond and Clarke 1988]. Having an equally strong affinity to the synthetic catecholamine, isoprenaline activation, is one of the common properties of all three subtypes. Also antagonisation with propranolol is found in all subtypes, however, β_3 -ARs are less sensitive to this antagonist. Moreover, β -ARs

are primarily associated with stimulating G-protein (G_s) signaling, activating adenylyl cyclase and producing cAMP as a second messenger.

β_1 -ARs are located mainly in the heart and adipose tissue. Especially their localization in the heart makes them clinically relevant, because upon stimulation they mediate increases in heart rate (chronotropy) and force of contraction (inotropy). Furthermore, they stimulate renin secretion, relaxation of coronary arteries and gastrointestinal smooth muscle. In contrast, β_2 -ARs are responsible for relaxation of vascular, uterine and airway smooth muscle. Also prejunctional β -ARs, responsible for NE release modulation in sympathetic nerve terminals, seem to be of the β_2 -AR subtype (reviewed in [Bylund, Eikenberg et al. 1994]). β_3 -ARs have also been found in adipocytes and, furthermore in the ileum [Arch, Ainsworth et al. 1984, Bond and Clarke 1988]. Nevertheless, β -AR subtypes (as well as α -AR subtypes) are distributed throughout the body and are not exclusively limited to specific tissues and, even more, the distribution is highly species-dependent.

1.3.4 Cellular effects of adrenoceptor signal transduction

Upon catecholamine binding to respective receptor subtypes, dissociation of the G-protein heterotrimers regulates a variety of second messengers, e.g. cAMP, cGMP, Ca^{2+} , inositol 1,4,5-trisphosphate (IP_3), diacylglycerol (DAG) nitric oxide (NO), arachidonic acid (AA), etc. Subsequently, protein kinases and phosphatases regulate the phosphorylation status of proteins involved in almost all areas of cellular function. These functions can roughly be divided into short-term and long-term modulating effects. Short-term effects include e.g. ion channel activity, receptor sensitivity, general metabolism or neurotransmitter synthesis and release, whereas, long-term modulations include synthesis of channels, receptors and intracellular messengers, synaptogenesis and generally gene expression [Keys and Koch 2004, Zheng, Han et al. 2004].

1.3.5 Reserpine action

Reserpine was originally a drug used for the treatment of hypertension, but was soon shown to produce hypokinesia and akinesia as well as other symptoms like rigidity of skeletal muscles, tremor and postural flexion in different treated animal species by changing the catecholamine levels in the brain [Flach 1955, Jurna and Lanzer 1969, Morrison and Webster 1973, Wagner and Anderson 1982]. Inducing these symptoms, resembling human Parkinson's disease (PD), reserpine provided one of the first transient pharmacological PD models. In turn

the decreased motor activity could be counteracted by the administration of 3,4-dihydroxyphenylalanine (L-DOPA) and that was the basis for the L-DOPA substitution therapy of PD [Carlsson, Lindqvist et al. 1957]. Even though, reserpine is not clinically relevant anymore because of its strong psychiatric side-effects, including lethargy and depression [Freis 1954, Freis and Ari 1954], it has been established as a potent drug inhibiting VMAT catalyzed vesicular transport of catecholamines leading to a depletion of catecholamine stores and at the same time preventing re-uptake of catecholamines [Carlsson, Lindqvist et al. 1957, Schuldiner 1994, Bezard, Imbert et al. 1998, Bezard and Przedborski 2011]. The plasma half-life of catecholamines is very short (1-2 min) because secreted extracellular catecholamines are quickly degraded by the action of MAO and COMT. Catecholamines, that after release are re-uptaken into the cytosol or are leaking from storage vesicles, are also degraded by the activity of MAO and COMT. Thus, if reserpine is present and completely inhibits vesicular transport, it prevents new synthesis of NE and EPI and cells will be depleted of those within a short period of time. As a consequence there will be no extracellular catecholamines left for the paracrine effects of these substances.

1.4 Embryonic heart development

The heart is the first organ to be functionally active in vertebrate embryos. During the embryonic development the heart keeps contracting to guarantee circulation, while it is constantly remodeled until it finally becomes the four-chambered organ. Heart development can roughly be divided into four main phases:

1.4.1 Specification of myo- and endocardial precursors

After implantation the three germ layers are formed. In mice the specification of myo- and endocardial precursors is completed within the heart forming fields of the anterior lateral plate mesoderm. Growth factors from different families are involved in this process, i.e. non-canonical Wnt signaling, FGF- and BMP-signaling as well as inhibitors of Wnt/ β -Catenin signaling (reviewed in [Brand 2003, Brade, Manner et al. 2006]). Committed cells of the heart forming field form the cardiogenic crescent. These cells express the earliest cardiac marker, homeodomain transcription factor Nkx2.5. All myo- and endocardial precursors derive from two heart fields: the primary and the secondary heart field. While the first heart field was found to provide cardiomyocytes for the left atria and ventricles, the secondary heart field

mainly contributes the cells for the right ventricle and the outflow tract [Stalsberg and DeHaan 1969, Brade, Manner et al. 2006].

1.4.2 Development of the tubular heart

This stage is characterized by folding processes of the cardiac field subsequently forming the tubular heart. In more detail, during gastrulation and neurulation the primary and secondary heart fields (located at both sides of the embryo midline), fold toward the embryo midline and merge ventrally to form the linear heart tube [Manasek 1968, Brade, Manner et al. 2006, Manner 2006]. At the linear heart tube stage, the tube is rather short and consists of the embryonic ventricles only. From this short linear heart tube stage continuous merging of the heart-forming fields progresses, adding the remaining elements of the embryonic heart to the arterial and venous pole of the linear heart tube. This heart tube finally forms the sinus venosus, a primitive atrium and ventricle, the bulbus cordis, and the aortic arches [Brade, Manner et al. 2006]. As a result of these events the heart is relocated ventrally. The wall of the linear heart tube is already composed of myocardial cells (outer layer) and endocardial cells (inner layer). After folding and relocation the tubular heart shows first peristaltic contractions [Moorman and Lamers 1994]. Also a pacemaking region in the sinus venosus region was described [Brade, Manner et al. 2006, Christoffels and Moorman 2009]. In humans this process takes place in the fourth week of pregnancy.

1.4.3 Looping of the tubular heart

During this stage, principally the already formed tubular heart elongates faster than the surrounding pericardial cavity, resulting in the formation of a loop (looping heart tube). Thereby, the heart tube undergoes positional and morphological changes bringing the future sections of the definitive heart into their topographical proximity [Brade, Manner et al. 2006]. Several functional parts of the final heart are already established at this time: The sinus venosus forming the inflow tract; the atrium primitivum later forming the atria and the left ventricle, respectively; the bulbus cordis forming the right ventricle, the truncus arteriosus which will finally form the aorta; and the aortic arches as the outflow tract [Moorman and Lamers 1994]. Also during this stage, the looping heart tube becomes colonized by primarily extracardiac progenitor cells, subsequently leading to the division of the outflow tract into systemic and pulmonary paths, as well as the entire coronary vasculature [Manner, Perez-Pomares et al. 2001, Brade, Manner et al. 2006].

1.4.4 Development of the four-chambered heart

The final step of the heart development is the formation of the four-chambered heart from the looping heart-tube with its single undivided lumen. Transformation into the four-chambered heart is accompanied by several major morphological changes, including ballooning of the atria and ventricles, remodeling of the inner heart curvature and the outflow tract, valve formation at atrioventricular and ventriculo-arterial junctions and the formation of septa between the four chambers [Christoffels, Habets et al. 2000, Brade, Manner et al. 2006]. Amongst several other signaling molecules, the Wnt/ β -catenin pathways are involved in these remodeling processes [Brade, Manner et al. 2006]. In a final step, the terminal conduction system develops. Thereby, the peristaltic contraction of the heart tube is transformed into the conduction and contraction pattern of the mature four-chambered heart [Christoffels and Moorman 2009].

In conclusion, the development of a complex organ like the heart is well investigated. The general developmental steps (as described above) are well conserved between species. Nevertheless, looking into more detail there are various aspects of heart development that differ between species, are discussed controversially or are just not investigated yet. The findings of e.g. BMP signaling committing mesodermal cells into myo- and endocardial precursor cells laid the basis for approaches to translate these cardiac inducing signaling pathways into ES cell differentiation. For example, activinA and BMP4 (in addition to bFGF) were found to induce cardiomyocyte development during human ES cell differentiation [Yang, Soonpaa et al. 2008]. Moreover, several studies showed that activin/Nodal/TGF- β , Wnt, and BMP pathways all play pivotal roles in the establishment of the cardiovascular system [Conlon, Lyons et al. 1994, Haegel, Larue et al. 1995, Gadue, Huber et al. 2006, Klaus, Saga et al. 2007]. However, a variety of cardiac cell fate determining stimuli like different growth factors, growth factor inhibitors, signaling molecules and further e.g. mechanical or electrical stimulation, are still to be investigated to establish optimal conditions for cardiac differentiation *in vitro*.

1.5 Electrophysiology of the heart

1.5.1 *Resting membrane potential*

The resting membrane potential (RP) is characterized by a specific distribution of ions along the cell membrane. Due to selective permeability of the membrane ions are distributed unequally. In the cytoplasm potassium ions (K^+) and organic ions (e.g. proteins, other organic molecules) are found in high concentration. In lower concentrations also sodium ions (Na^+) are present inside the cells. On the outside of the membrane we find high concentrations of Na^+ and chloride (Cl^-) as well as low concentrations of K^+ . Altogether, the cytoplasm contains more negative charges than the outside of the membrane, resulting in a difference of the distribution of charges which can be detected by e.g. the patch-clamp method as an electric potential across the cell membrane. The resting potential is usually between -70 to -90 mV. The membrane's selective permeability is due to Na^+ - and K^+ - channel proteins in the membrane. Even in the resting state of a cell, the membrane is permeable for both cations, but the membrane permeability is significantly higher for K^+ than for Na^+ . On the other side, the permeability for Cl^- and organic anions is extremely low and can thus be neglected here. However, over time Na^+ and K^+ would be passively transported along their electrochemical gradient resulting in an equilibrium state and vanishing of the membrane potential. The electrochemical gradient itself is defined by the two forces responsible for the movement of ions across the membrane. One force results from the concentration gradient of Na^+ and K^+ between the inside and outside of the membrane, while the other force results from the electromagnetic interaction between the charge carriers. To stabilize the membrane potential, the Na^+/K^+ -ATPase actively transports three Na^+ to the outside and two K^+ to the inside of the membrane under constant ATP-consumption to uphold the unequal ion distribution.

1.5.2 *The cardiac action potential (AP)*

1.5.2.1 *AP formation and contraction of the myocard*

AP formation in the heart mainly depends on voltage-gated Na^+ -, K^+ -, Ca^{2+} - and to a minor degree also Cl^- -ion channels. The initial depolarization is carried by a Na^+ -current into the cell resulting in a very fast reversal of the membrane potential (phase 0). Phase 1 of the AP is characterized by the activation of K^+ -channels initiating repolarization. The channels open to release K^+ from the cytosol resulting in short currents called I_{to} (transient outward) and I_{Kur} (ultra-rapid) [Boyle and Nerbonne 1991]. K^+ -channels are also important in phase 2

(plateauphase) and phase 3 (repolarization). Two types of I_K currents are detected, the faster component is the I_{Kr} while the second and slower component is called I_{Ks} [Sanguinetti and Jurkiewicz 1990, Sanguinetti and Jurkiewicz 1991]. HERG- K^+ -channel open probabilities are responsible for the I_{Kr} current [Abbott, Sesti et al. 1999]. However, in phase 2 most prominent are the Ca^{2+} -currents (I_{Ca-L} and I_{Ca-T}) which are responsible for the plateau phase of the AP. Ca^{2+} influx through L-type Ca^{2+} -channels (I_{Ca} in the sarcolemma) induce Ca^{2+} -release through ryanodine receptors (in the SR membrane), thereby increasing intracellular Ca^{2+} and delaying the depolarization. This process is called Ca^{2+} -induced Ca^{2+} -release (CICR) and triggers the excitation-contraction coupling, finally leading to the contraction of actin and myosin filaments and shortening of sarcomeres. During systolic myocard contraction these processes provide the force for the ejection of blood [Fabiato 1983, Bers 2002]. In contrast, in early human ESCMs and iPSCMs excitation-contraction coupling was found to be dependent on transsarcolemmal Ca^{2+} influx rather than on SR-release [Dolnikov, Shilkrut et al. 2006]. Finally repolarization is completed by the I_{K1} -current in Phase 4, before the RP is stabilized and a new AP can be triggered during the diastole.

1.5.2.2 In cells of the conduction system

Cells of the SA-node (sinoatrial-node), the AV-node (atrioventricular node), bundle of His, tawara's branches, and purkinje fibres show certain differences in comparison to the working myocard. Especially, the cells of the SA- and AV-node show a particularly slow upstroke velocity of the initial depolarization and their RP is less negative. Their depolarization is further mainly carried by a slow Ca^{2+} influx. Additionally, conduction system APs do not possess a pronounced plateau phase due to their relatively weakly developed sarcoplasmic reticulum. All cells of the conduction system show spontaneous depolarization without external stimulation. The leakage channel allowing for spontaneous depolarization is an unspecific anion channel known as the "funny channel" (I_f). This property enables the conduction system cells to work as pacemakers controlling the heart rate. Amongst the cells of the conduction system sinus node cells show the highest spontaneous frequency with decreasing frequencies along the conduction path (i.e. SA-node > AV-node > bundle of His > etc.). In case of e.g. a SA-node failure (e.g. SA block), the AV-node can replace the pacemaking activity, however, exerting lower pacing frequency. The autonomic nervous system strongly innervates the SA-node. In this way the autonomic system is able to adjust the heart rate to adapt to changing conditions. Sympathetic stimulation increases, while parasympathetic stimulation decreases heart rate through the β -adrenergic and muscarinic

receptors, respectively. Upon receptor stimulation by e.g. catecholamines, cAMP and protein kinases induce phosphorylation of the I_f -channel, increasing the velocity of the spontaneous depolarization and with that the heart rate (reviewed in [Baruscotti, Bucchi et al. 2005]).

In Fig. 1.2 the shapes of APs generated by different cells within the heart are depicted. APs can explicitly be distinguished by end-diastolic depolarization (phase 4), their upstroke velocity and the presence and duration of the plateau. A heart cycle consists of the diastolic and the systolic phase during which excitation spreads throughout the heart. Depending on their function, cardiac cells from conduction system, atria and ventricles generate APs at different time-points of the heart cycle. The excitation spread can be monitored by an electrocardiography (ECG) and is represented by its intervals and segments (P-wave, QRS-complex, T-wave and sometimes U-wave). The QT-interval represents the excitation of the ventricles and their recovery. Prolongation of the QT-interval increases the risk of ventricular tachyarrhythmias (e.g. TdP; [Antzelevitch, Shimizu et al. 1999]). QT-interval shortening and resulting decreased refractory time, on the other side, increases the risk of reentry induced cardiac fibrillation [Halbach 2006]. The right panel of Fig. 1.2 depicts AP shapes and correlates them to distinct ECG intervals. Ventricular AP_{Dur} corresponds to the QT-interval of the ECG. In paragraph 1.6.2 the relationship of APs and field potentials (FPs) recorded from MEAs and their significance for this work will further be discussed.

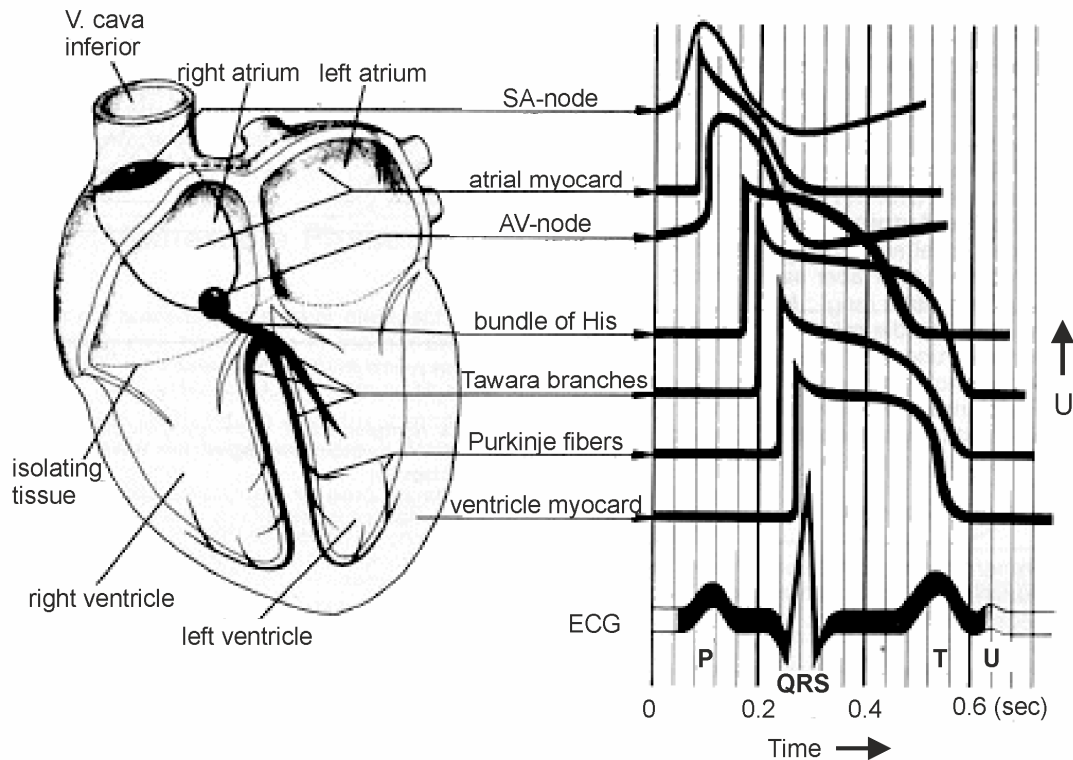


Figure 1.2: Correlation of APs and ECG intervals and segments

APs as they would be recorded from cells of the respective part of the heart. Furthermore, the figure shows the involvement of the functional parts of the heart during a heart cycle presented by the ECG. Different cells generate APs in a coordinated order throughout a heart cycle to guarantee contraction of the heart and ejection of blood. As can be seen, AP durations correlate to respective ECG intervals and segments (From <http://www2.hs-esslingen.de/~johiller/elektrokardiogramm/pics/ekg29.gif>).

1.6 Microelectrode arrays (MEA)

1.6.1 Extracellular vs. intracellular recordings

Extracellular recordings of field potentials (FPs) using the microelectrode array (MEA) technique provide a number of advantages over intracellular recordings like voltage or current clamp and sharp-electrode measurements. One of the most useful advantages of the MEA technique for this work was the fact that it is non-invasive. It therefore allows long recording periods (up to several days) where either different drug concentrations or even different drugs at different concentrations can be applied sequentially to the same preparation (EBs in our case). Analyzing drug effects in identical preparations helps to exclude possible preparation-to-preparation or cell-to-cell differences to improve the reliability of conclusions. Even more, being a non-invasive method guarantees that the recordings are not disturbed by

infringements of cell membranes and subsequently changed electrical physiology of cells. The MEA technique further enables to measure multi-cellular and whole tissue preparations, like retinal tissue, heart and brain slices, and for this work, EBs [Hammerle, Egert et al. 1994, Egert, Heck et al. 2002, Halbach, Egert et al. 2003, Halbach, Pillekamp et al. 2006]. Because MEAs allow simultaneous monitoring of 60 measurement electrodes that are spatially separated from each other (8x8 grid with an inter-electrode distance of 200 μm), tissue preparations can be analyzed in respect to 2-dimensional signal propagation and conduction velocity. This aspect is only insufficiently accessible using traditional intracellular recording techniques [Halbach, Egert et al. 2003].

Using MEAs, cell preparations are cultivated in culture dishes containing the substrate integrated extracellular electrodes and can directly be monitored in the same dishes. Also complicated positioning of the electrodes and penetration of cells, as needed for transmembrane recordings, is not necessary. Thus, in comparison to intracellular recordings of the transmembrane potential, MEA recordings are less work-intensive and, hence, easier to handle.

1.6.2 Comparison of APs and FPs

Compared to intracellular transmembrane potential recordings, a certain downside remains using the MEA technique. Detailed monitoring of single ion channel activity with e.g. patch clamp techniques or monitoring of populations of specific ion channels like from whole-cell voltage clamp recordings cannot be accomplished with MEA. Nevertheless, previous work has shown a linear relationship of FP_{Dur} and APD_{90} recorded by the current clamp sharp electrode technique (see Fig. 1.3; [Halbach, Egert et al. 2003, Halbach 2006]). This relationship allows the estimation of alterations of the cardiac electrical physiology based on FPs similar to AP analysis. Repolarization modulating drug effects, which this work will focus on, can thus be extracted from MEA recordings and drug effects can be analyzed based on FP_{Dur} . As discussed in section 1.5.2 and depicted in Fig. 1.2, durations of APs and ECG intervals correlate. Accordingly, also ECG interval modulations may indirectly be estimated by FP_{Dur} measurements.

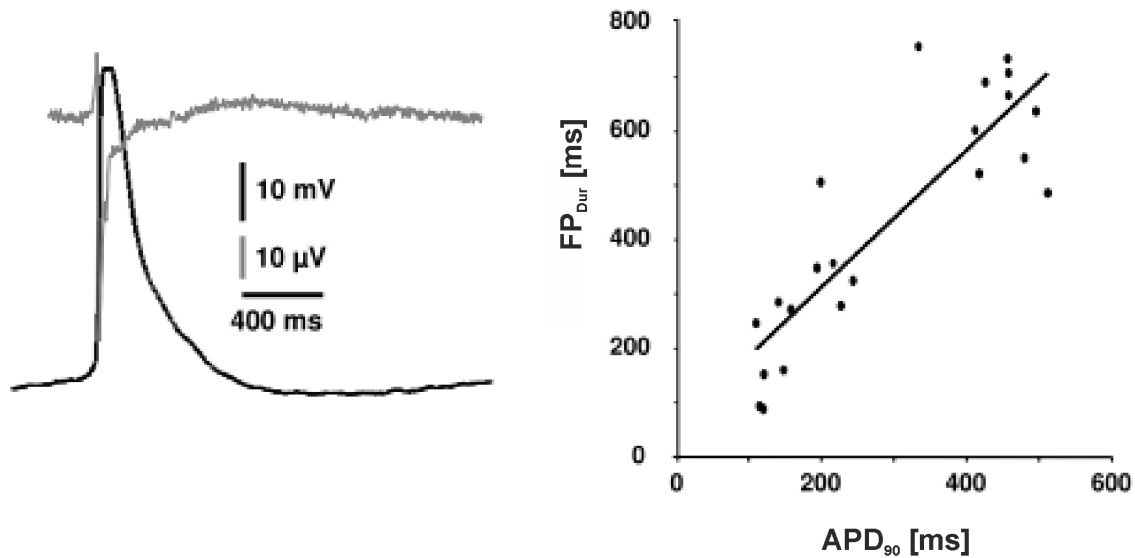


Figure 1.3: Linear relationship between APD₉₀ and FP_{Dur}

Left: Overlay of an action potential from intracellular recording (black) and a FP recorded by MEA (grey). Right: Comparison of APD₉₀ and FP_{Dur}. Each dot represents a value pair of APD₉₀ and FP_{Dur} recorded from the same position of the same preparation to showcase the comparability of both parameters. Both graphs were taken from the doctoral thesis of Dr. M. Halbach, University Hospital Cologne [Halbach 2006].

1.6.3 *Technical MEA Applications*

Drug development is a cost intensive factor for the pharmaceutical industry. The MEA technology with its versatile applications provides different kinds of information on cellular electrical functions. As described in paragraph 1.5.2.2 and 1.6.2 and Fig. 1.2 and 1.3, FPs provide information that allow conclusions to be drawn on drug-effects on AP_{Dur} and the phases of the ECG. Thus, MEAs provide a valuable platform for drug screening purposes. For example, compounds with possible cardio-active side effects can be sorted out before they are tested in cost-intensive clinical trials and, at the same time help reducing the number of experimental animals being used.

1.7 Aims of the work

The current work was conducted to study aspects of embryonic stem cell differentiation into cardiac myocytes. Numerous scientists have produced great knowledge on the field of embryonic stem cells within the last 15 to 20 years. Because the field of stem cell research is broadly diversified, the work itself was subdivided into two separate parts investigating two rather independent aspects.

1.7.1 The role of catecholamines in cardiac lineage commitment in mouse ES cells

The first part was aimed to describe the role of the important class of catecholamines on the differentiation of ES cells, focusing on their role on CM development. Using reserpine enabled us to deplete ES cells of catecholamines during the course of differentiation. Several microscopy, molecular biology, flow cytometry techniques and immunohistochemical stainings were applied for the descriptive analysis. Beside effects on cardiomyogenesis, this work also assessed the expression of pluripotency, catecholamine synthesis and AR genes as well as germ-layer markers. To exclude cytotoxic effects of reserpine EB cross-section areas were measured and a newly developed impedance cytotoxicity assay was used. Functional MEA experiments were employed to investigate the role of catecholamines on the electrophysiology during the course of CM development. Strengthening the conclusion that catecholamines and not reserpine *per se* was responsible for the observation of reduced cardiac development, we tested whether α - and β -AR antagonists mimicked the reserpine effect and if AR stimulation rescued the reduced cardiomyogenesis when co-applied with reserpine.

1.7.2 MEA-based QT-screen using pluripotent stem cell derived CMs

The second part represents series of experiments aimed to investigate the possibility of using the MEA system as a platform for safety-pharmacological screening of drugs with cardiac side effects. One such side effect is known to be life-threatening torsade de pointes (TdP) tachycardia [Selzer and Wray 1964]. TdP is caused by a variety of factors amplifying electrical heterogeneities in the ventricular myocardium. Drugs with antiarrhythmic agent class III actions (potassium channel blockers) reduce the net repolarizing currents and change the spatial dispersion of repolarization within the ventricular myocardium and can therefore result in QT-prolongation and the development of polymorphic reentrant ventricular tachycardia causing TdP [Antzelevitch 2005]. These drug-induced repolarization prolonging effects can be monitored using MEAs. Combining the advantage of long-time recording provided by MEAs with the advantages of pluripotent stem cell-derived cardiomyocytes, we sought to empirically investigate the applicability of that system for drug screenings to identify cardio-active side effects. For this purpose several rhesus monkey and human ES (rES and hES) cell lines as well as human induced pluripotent stem (hiPS) cells were differentiated into CMs. We initially simulated positive and negative chronotropy with specific substances to describe the physiological correlation of FP_{Dur} and the beating rate. As

Introduction

the proof of concept, EBs containing beating cardiac clusters were treated with different concentrations of class III antiarrhythmic agents to investigate if cardiac repolarization prolongation can be qualitatively accessed using our MEA-based analysis system. The correlation of FP_{Dur} and beating rate under the influence of different drugs was further tested in CM lines proving a general feasibility of the screen.

2 Materials and Methods

2.1 Cell culture

Cell culture work was conducted in sterile conditions under laminar-flow work benches. If not delivered in a sterile condition by the manufacturer, materials and solutions used for cell culture work were sterilized by autoclaving or sterile-filtration.

2.1.1 Feeder culture and inactivation

ES cells in culture differentiate spontaneously. Keeping them in a pluripotent state is crucial to guarantee that the initial cell material for differentiations is comparable. Therefore, besides the addition of growth factors, which contribute to cellular growth and proliferation, a cultivation of ES cells on confluent feeder layers is crucial, as those cells secrete factors that support the cells in an undifferentiated state.

2.1.2 ICR-feeder (Charles Rivers Laboratories, Germany)

Purpose: rESC (R366.4 and MF12) propagation

Medium: Dulbeccos Modified Eagle Medium (DMEM), fetal bovine serum (FBS; 10%, v/v), L-glutamine (2 mM) and non-essential amino acids (NEAA; 1x). Medium and supplements were purchased from Invitrogen, Karlsruhe, Germany.

After thawing, ICR-feeders were seeded on cell culture dishes and passaged by enzymatical dissociation (trypsin) to expand the culture for 2 passages. Finally, ICR-feeders were mitotically inactivated using mitomycin C (10 µg/ml; Sigma-Aldrich, Taufkirchen, Germany) for 2-4 hrs. After the inactivation step and cell counting (life/dead staining with Trypan blue in a Neubauer counting chamber), ICR-feeders were seeded at a density of 40,000 cells/cm² for further use.

2.1.3 neomycin-resistant mouse embryonic fibroblasts (NEO-feeder)

Purpose: rESC (R366.4 and MF12) and mESC (αPIG) propagation

Medium: DMEM, fetal bovine serum (FBS; 10%, v/v), L-glutamine (2 mM), non-essential amino acids (NEAA; 1x), β-ME (100 µM), Penicillin/Steptomycin (Pen/Strep; 100 µg/ml and 100 U/ml, respectively).

Mitotically inactivated NEO-feeders (mitomycin C, 10 µg/ml, see above) were seeded at a density of 40,000 cells/cm².

2.1.4 CF1-feeder (Charles Rivers Laboratories, Germany)

Purpose: hESC (H1, H9) and hiPSC propagation

Medium: DMEM, fetal bovine serum (FBS; 10% v/v), L-glutamine (2 mM) and non-essential amino acids (NEAA; 1x), Pen/Strep (100 µg/ml and 100 U/ml, respectively).

Mitotically inactivated CF1-feeders (by radiation with 30 Gray) were provided at a density of 12,000-20,000 cells/cm².

2.1.5 Murine embryonic stem cells (mESCs; D3 αPIG44)

2.1.5.1 Cell propagation

The murine D3 αPIG 44 ES cell line was passaged as published earlier [Kolossoff, Lu et al. 2005]. Passage numbers 15-40 were cultivated on NEO-feeders in IMDM supplemented with fetal bovine serum (FBS; 15% v/v), β-ME (50 µM), non-essential amino acids (1x), leukemia inhibitory factor (LIF; 100 U/ml) and G418 (Neomycin; 0.5 mg/ml). Cells were passaged every 2-3 days by enzymatic dissociation of the mESC for 5 min (0.05% Trypsin/EDTA) at 37°C. Afterwards 0.5*10⁶ single cells were plated on fresh NEO-feeders.

2.1.5.2 Cardiac Differentiation

Differentiation was initialized following a mass culture protocol [Frenzel, Abdullah et al. 2009]. 1*10⁶ of the enzymatically dissociated cells were cultivated in bacteriological dishes under constant horizontal shaking at 37°C in 5% CO₂ atmosphere in IMDM supplemented with: FBS (20%; v/v), β-ME (100 µM), and non-essential amino acids (1x) for the control group. For the solvent control and reserpine-treated group, dimethylsulfoxide (DMSO; 1:1,000 v/v) or reserpine (10 µM in DMSO 1:1,000) was added, respectively. 2 days after the onset of differentiation the culture was split distributing 1,000 EBs per 10 cm bacteriological dish and maintained at 37°C in 5% CO₂ atmosphere under constant horizontal shaking. Afterwards, two separate differentiation protocols were used. In the first protocol, reserpine was added every second day with medium changes every 6 days (chronic application 'd2'; Fig. 3.2), in the second protocol reserpine was added every four days including medium changes at these days (chronic application 'd4'; Fig. 3.2). DMSO was applied and refreshed

like reserpine and served as a second control to exclude unspecific effects of the reserpine solvent.

2.1.6 Puromycin purification of cardiomyocytes

The D3-derived α PIG44 murine ES cell line expresses enhanced green fluorescent protein (eGFP) and a puromycin resistance gene under control of the cardiac specific alpha myosin heavy chain (α MHC) promoter [Kolossoff, Fleischmann et al. 1998]. For purification, day 10 EBs were treated with 8 μ g/ml puromycin and maintained at 37°C in 5% CO₂ atmosphere on a horizontal shaker. Puromycin and medium was changed every 2 days. For most of our experiments purified clusters were harvested at day 14.

2.1.7 Rhesus monkey embryonic stem cells (rESCs; R366.4 and MF12)

The two cell lines were kindly provided in frozen stocks by Prof. U. Martin (Head of the Leibniz Research Laboratories for Biotechnology and Artificial Organs, Hannover, Germany). R366.4 was derived from *macaca mulatta*, while the MF12 line was derived from *macaca fascicularis*.

2.1.7.1 Cell propagation

Rhesus monkey embryonic stem cells were originally isolated by J.A. Thomson and colleagues in 1995 and karyotyped 42, XY, normal [Thomson, Kalishman et al. 1995]. For passages we followed a protocol adopted from K. Schwanke and colleagues [Schwanke, Wunderlich et al. 2006]. RESCs growing as multi-cellular mono-layered colonies, were cultivated on ICR- and NEO-feeders in Knock-out™ Dulbecco's Modified Eagle Medium (Knockout™ -DMEM; Gibco) supplemented with Knockout™-Serum Replacement (20% v/v), β -ME (100 μ M), non-essential amino acids (1x), L-glutamine (1 mM) and basic fibroblast growth factor (bFGF; 4 ng/ml) (all supplements were purchased from Invitrogen). Every 3-4 days pluripotent colonies were enzymatically de-attached by incubation with 1 mg/ml Collagenase IV (Invitrogen) for 15 min at 37°C in 5% CO₂ incubator conditions. Additionally, colonies were mechanically de-attached from the feeder-layer by tapping to guarantee a more efficient yield of colonies. After centrifugation (100 x g, 4°C) and dissociation in 20%-DMEM by gentle pipetting 3-4 times to reduce colony size, colony fragments were distributed 1:4 or 1:6 into wells containing fresh confluent feeders.

2.1.7.2 Cardiac Differentiation

The protocol was adopted from Schwanke et al. [Schwanke, Wunderlich et al. 2006]. In brief, R366.4 and MF12 RESCs were enzymatically and mechanically dissected as described in paragraph 2.1.7.1. For initiation of differentiation, the colony fragments were resuspended in RESC differentiation medium consisting of Iscove's Modified Dulbecco's Medium (IMDM+GlutaMAX™) supplemented with FBS (Hyclone or Invitrogen, 20% v/v), β -ME (100 μ M), non-essential amino acids (1x), L-glutamine (1 mM). Before colony fragments were seeded, 12-well culture dishes were coated with 0.5 ml Agarose (1% Agarose (w/v) in IMDM-GlutMAX™). Next, colony fragments of pluripotent RESCs of 1 well of a 6-well plate were equally distributed on the 12-well plate and incubated at 37°C, 5% CO₂ in RESC differentiation medium. After 7 days RESCs formed 3-dimensional cell aggregates that were transferred to 0.1% Gelatine (w/v in PBS +/-) coated culture dishes and further incubated (37°C, 5% CO₂). Medium was renewed every 2-3 days [Schwanke, Wunderlich et al. 2006].

In addition to the protocol described in the previous section, the rESC colony fragments on agarose coated 12-well plates were treated with activinA (100 ng/ml) for the first 24 hrs of differentiation followed by BMP4 (10 ng/ml; both factors were purchased from PeproTech (Hamburg, Germany) until day 7 as adopted from Laflamme and colleagues [Laflamme, Chen et al. 2007]. No medium was changed within the first 7 days, while in the remaining time until harvesting of EBs for experiments, medium was changed every 2-3 days.

2.1.7.3 END-2-Feeder protocol

END-2 cells are derivatives of the murine embryonic carcinoma cell line P19 and were shown to potently induce endodermal and mesodermal differentiation [Mummery, van Achterberg et al. 1991]. Co-cultivation of pluripotent cells with END-2 cells markedly increases their differentiation efficacy into cells of the cardiac lineage. Therefore we applied an established END-2 co-cultivation protocol to our R366.4 and MF12 RESC culture in an approach to increase the yield of spontaneously beating clusters [Mummery, Ward-van Oostwaard et al. 2003]. RESC colony fragments were dissected as described in the RESC passage section (2.1.7.1). Colony fragments of one well of a 6-well plate were transferred to a 6 cm culture dish for co-culture with mitomycin C (10 μ g/ml) mitotically inactivated END-2 cells (60,000 cells/cm²). END-2 cells were kindly provided by Prof. C. Mummery (Department of Anatomy and Embryology, Leiden University Medical Center).

2.1.8 Human embryonic and induced pluripotent stem cells (hESCs and hiPSCs)

2.1.8.1 *Propagation*

Human pluripotent ES and iPS cells were propagated by manual dissection every 5-7 days. For propagation approximately 50 colonies were dissected using the grid-cut method. Thereby individual un-differentiated colonies were cut into 9-16 equally sized pieces using a sterile needle [Costa, Sourris et al. 2007]. Colony pieces were collected and transferred to a fresh 3.5 cm culture dish, and maintained in knockout-Dulbeccos Modified Eagle Medium (KO-DMEM) containing Serum Replacement (SR, 20%, v/v), L-glutamine (2 mM) and non-essential amino acids (NEAA; 1x), β -ME (100 μ M), bFGF (4 ng/ml) at 37°C in 5% CO₂ incubator conditions. Medium was changed every 2 days. Remaining pre-differentiated colonies were used for differentiations. H1 and H9 hESCs were provided by Prof. J.A. Thomson, (Wisconsin Regional Primate Research Center, University of Wisconsin, Madison, USA) and WiCell research Institute, Madison, USA, iPSCs were provided by Dr. Dr. T. Saric and Dr. A. Fatima (Institute for Neurophysiology, University of Cologne, Germany).

2.1.8.2 *Cardiac Differentiation*

hESCs and hiPSCs were differentiated into CMs using END-2 protocols [Mummery, van Achterberg et al. 1991, Mummery, Ward-van Oostwaard et al. 2003, Fatima, Xu et al. 2011]. CM containing clusters of all human cell lines used herein were kindly prepared by C. Böttinger.

2.1.9 EB size assay

Pictures of EBs taken on the respective days using Axiovert 10, Axiovert 25 or Axiovert 200 microscopes (Carl Zeiss, Jena, Germany) were analyzed using the commercial Carl Zeiss software AxioVision LE 4.5 (Carl Zeiss, Jena, Germany). Depending on the microscope and magnification of objectives, pictures were calibrated to analyze EB cross-sections as a measure for cell proliferation and growth.

2.1.10 Ratio of beating clusters

For quantification of beating ratios, the EBs were plated on 6-well plates (15-25 EBs per well) at day 6 and the drug was refreshed following the respective protocol until the end of the experiment. 6-well culture dishes were coated with 0.1% gelatine to improve attachment of

the EBs. Using a microscope total numbers and numbers of EBs containing beating clusters were counted by eye and ratios were calculated.

2.2 Flow cytometry

2.2.1 *Cell preparation*

100-200 EBs were harvested at corresponding days, washed three times with phosphate-buffered saline (PBS, 0 mM Ca²⁺; 0 mM Mg²⁺) and enzymatically dissociated to a single-cell suspension using 2 ml trypsin/EDTA (0.05%) for 10 min at 37°C in a water bath with shaking every 2 min. The trypsin reaction was inhibited by addition of 10 ml IMDM + FBS (20%). Cell suspension was further dissociated by up- and down-pipetting and filtered by passing through a 40 µm cell strainer before cells were counted (life-dead staining with trypan blue). Approximately 0.5*10⁶ cells were washed in PBS and subsequently resuspended in 1 ml cell-wash solution (BD Biosciences, Franklin Lakes, USA).

2.2.2 *Measurement*

Quantification of eGFP expressing ESCMs was performed by flow cytometry using a FACScan flow-cytometer (BD Biosciences, Franklin Lakes, USA). For each sample 10,000-50,000 living cells were gated. Dead cells were stained with propidium iodide (PI, Sigma). Data was analyzed using Cyflogic (v 1.2.1, Turku, Finland).

2.3 Immunohistochemistry

2.3.1 *Cryosliced EBs*

20-40 EBs from the culture were fixated in 4% paraformaldehyde (Roth, Karlsruhe, Germany) for 30 min at room temperature and incubated in 30% sucrose solution over night at 4°C prior to embedding in Tissue Tek® O.C.T.™ Compound (Sakura® Finetek Japan Co., Tokyo, Japan). Embedded EBs were shock frozen, stored at -80°C and subsequently cryosliced. The 8 µm cryosections were then placed on silanized Histobond cover slips (Paul Marienfeld GmbH, Lauda-Königshofen, Germany) for the staining procedure.

2.3.2 Single cells/whole EBs

Two days prior to staining EBs were plated on 1% gelatine coated cover slips. For single cell stainings, EBs were enzymatically dissociated first. EBs/cells were cultivated in 12-well culture dishes and incubated at 37°C and 5% CO₂ in the respective differentiation medium (for mouse or human ESCMs). After EBs/cells were allowed to attach, they were fixated with 4% paraformaldehyde for 30 min at room temperature.

2.3.3 Permeabilization and immunostaining procedures

All preparations, cryosliced sections, whole EBs and single cells were permeabilized using permeabilisation solution (0.25% TritonX, 0.5 M NH₄Cl). After washing with PBS, the preparations were incubated with 1:10 Roti®Block (Roth, Karlsruhe, Germany) to prevent cross binding of antibodies. Incubation with primary antibodies was performed overnight at 4°C on a horizontal shaker. After six washing steps with phosphate-buffered saline (PBS, 0 mM Ca²⁺; 0 mM Mg²⁺), samples were incubated with secondary antibody for 2 hrs at 4°C. Nuclei were always co-stained with nucleic acid stain Hoechst (1:1,000; subtype H 33342; Sigma Aldrich; Prod# B2261). Stained samples were embedded in Prolong Gold (Invitrogen, Carlsbad, USA) and imaged using a Zeiss Axiovert 200 (Carl Zeiss, Jena, Germany). For analysis the Carl Zeiss software AxioVision LE 4.5 was used. Primary and secondary antibodies and corresponding dilutions are stated in section VIII. of the appendix.

2.4 Molecular biology

2.4.1 RNA Isolation

Approximately 100-1,000 EBs were harvested from mass culture for RNA Isolation depending on the differentiation day. Samples of EBs were collected on days 1-4, 6, 8, 10 after initiation of differentiation and on day 14 with and without puromycin treatment. Together with samples of undifferentiated α PIG44 ES cells and mouse embryonic fibroblasts (MEFs) all samples were collected in 1 ml TriZol® Reagent (Invitrogen, Carlsbad, USA) and frozen at -80°C. Following manufacturer's instructions RNA was isolated. Briefly, cells were homogenized by passing the cells through a sterile syringe and a needle and incubated for 5 min at room temperature to permit complete dissociation of nucleoprotein complexes. 200 μ l chloroform was added and samples were vigorously shaken by hand for 15 sec before they were again incubated at room temperature for 2-3 min and subsequently centrifugated at

10,500 rpm for 15 min at 4°C. The aqueous phase was transferred into a fresh tube. For precipitation of RNA the aqueous phase was mixed with 500 µl isopropanol and incubated for 10 min at room temperature. Samples were centrifuged at 10,500 rpm for 10 min at 4°C and the supernatant was removed. To wash the RNA the pellet was resuspended in 1 ml 75% ethanol by vortexing before it is again centrifuged (8,500 rpm, 5 min, 4°C). Finally, the pellet was air-dried and resuspended in DEPC water for storage at -20°C. RNA concentration was determined using the NanoDrop UV/Vis spectrophotometer (Thermo Scientific).

2.4.2 *DNase I digestion of RNA isolations*

For more reliable quantification of the gene expression we additionally digested isolated RNA using deoxyribonuclease I (DNase I), Amplification Grade (Prod#: 18068-015; Invitrogen, Carlsbad, USA), even though the isolation kit used in this work guarantees a yield of RNA devoid of genomic DNA. The digest strictly followed the manufacturer's guidelines with 15 min incubation at room temperature followed by DNase I inactivation at 65°C for 10 min in the presence of 2.5 µM EDTA. The final inactivation step was carried out in a peqSTAR 96 Universal Thermocycler (PEQLAB Biotechnologie GmbH, Erlangen, Germany).

2.4.3 *cDNA Synthesis*

cDNA was synthesized from 2 µg of RNA using the SuperScript[®]Vilo[™] cDNA Synthesis Kit (Invitrogen, Carlsbad, USA). Synthesis strictly followed manufacturer's instructions with the reverse transcriptase reaction step at 42°C for 60 min and the final inactivation step both being performed in a peqSTAR 96 Universal Thermocycler (PEQLAB Biotechnologie GmbH, Erlangen, Germany).

2.4.4 *Semiquantitative-RT-PCR*

cDNA of samples collected at different stages of differentiation and undifferentiated ES cells were analyzed for expression levels of different genes using semiquantitative reverse-transcription PCR (sqRT-PCR). PCR reactions containing JumpStart[™] REDTaq[®] ReadyMix[™] Reaction Mix (Invitrogen) or Fermentas[™] Dream Taq[™] PCR Master Mix (2X) were set up following manufacturer's instructions. False positive results caused by amplification of genomic DNA were excluded by choosing intron spanning primer pairs (see Table "Primers" in the appendix). PCRs were carried out in a peqSTAR 96 Universal Thermocycler (PEQLAB Biotechnologie GmbH, Erlangen, Germany). A standard PCR consisted of an initial

denaturation for 2 min at 98°C, an optimized number of cycles consisting of three steps: 1.) denaturation for 30 sec at 98°C, 2.) annealing for 45 sec at primer specific temperatures, 3.) extension 30-60 sec depending on product length at 72°C. PCRs ended with a 10 min final extension step at 72°C and were analyzed with 1.5% agarose gel electrophoresis. Primers were designed using the Primer3-based online tool NCBI Primer Blast [Ye, Coulouris et al. 2012]. Exon junctions were identified online by mouse BLAT search (programmed by Jim Kent; <http://genome.ucsc.edu/> [Kent 2002]).

2.4.5 *Quantitative-RT-PCR*

Quantitative real-time PCR analysis was carried out using the ABI-7500 Fast PCR system (Applied Biosystems, Weiterstadt, Germany). The PCR reaction consisted of 12.5 µl SYBR Green PCR master mix (QuantiFAST, Qiagen, Hilden, Germany), 1 µl of primer pair (0.2 µM each) and 1 µl of cDNA template made up to a final volume of 25 µl. The standard conditions for PCR were used, 95°C/5 min Taq activation, 40 cycles of 95°C/10 sec and 60°C/30 sec. A melting curve was produced to verify single PCR product amplification. The mRNA levels were normalized against β-actin levels and calculated using a relative quantitation with the cycle threshold (ct) method by 7500 Fast System SDS software 1.4.0. (Applied Biosystems, Weiterstadt, Germany). The primer sequences used in the PCR analysis are shown in the table “Primers” in the appendix. qPCR reactions were carried out in technical triplicates for each sample. Negative controls were reactions containing H₂O as template. Results are shown as mean±SD. Statistical analysis was done using paired Student’s *t*-test. *P*-values of ≤0.05 (*) were considered significant.

2.4.6 *Agarose gel electrophoresis*

Amplified DNA fragments from PCR reactions were loaded on agarose gels for electrophoretic separation. Gels were prepared using 1.5% (w/v) agarose in TAE buffer (40 mM Tris-base, 20 mM acetic acid, 1 mM EDTA). EtBr (Roth, Karlsruhe, Germany) was added to stain DNA. Because loading buffer was already contained, the used PCR kits allowed direct sample loading onto the gels. Samples were loaded together with a 100-10,000 bp ladder as a fragment size standard and run for 50-60 min at 100 V. Finally, pictures were taken by exposing gels to UV-light.

2.5 Extracellular recordings using Microelectrode Arrays (MEA)

Extracellular recordings of field potentials (FPs) with MEAs were performed using the Multichannel Systems 1060-Inv-BC amplifier and data acquisition system (Multichannel Systems, Reutlingen, Germany). Substrate-integrated MEA culture dishes contain 60 Titanium Nitride coated gold electrodes (30 μm diameter) arranged in an 8x8 electrode grid with an inter-electrode distance of 200 μm , allowing simultaneous recording of extracellular FPs from all electrodes at a sampling rate of 1 to 50 kHz by the use of the MEA amplifier system. Standard measurements were performed at a sampling rate of 2 kHz in IMDM. For the extracellular recordings we used either beating EBs directly from the mass culture or EBs that were prior plated on 1% gelatine-coated 6-well culture dishes at day 6 of differentiation (or day 7 for rESCMs). For measurements with hESCMs and hiPSCMs beating clusters from the END2 culture were used. Beating clusters were mechanically dissected and transferred to MEA dishes and subsequently allowed to attach for 2 days in the incubator at 37°C with 5% CO₂. To assure best attachment of beating clusters, MEA chambers were coated using a 1:200 dilution of fibronectin (1 mg/ml) in gelatine (0.1%). During measurements temperature was kept constant at 37°C. Applying a specialized self-programmed software tool based on LabView (National Instruments, Austin, USA) MEA data was analyzed. The tool allows analysis of MEA traces for interspike intervals (ISI) and intervals between FP_{min} and FP_{max} referred to as FP_{Dur} (Fig. 2.1). ISIs were considered to be the time interval between two consecutive FP minima (FP_{min}), thus providing a read out for beating frequency. Furthermore, FP_{Dur} intervals were analyzed under the influence of several drugs. FP_{Dur} was shown to correlate with APD₉₀ values of action potentials as derived from current-clamp measurements [Halbach, Egert et al. 2003, Stett, Egert et al. 2003, Halbach 2006].

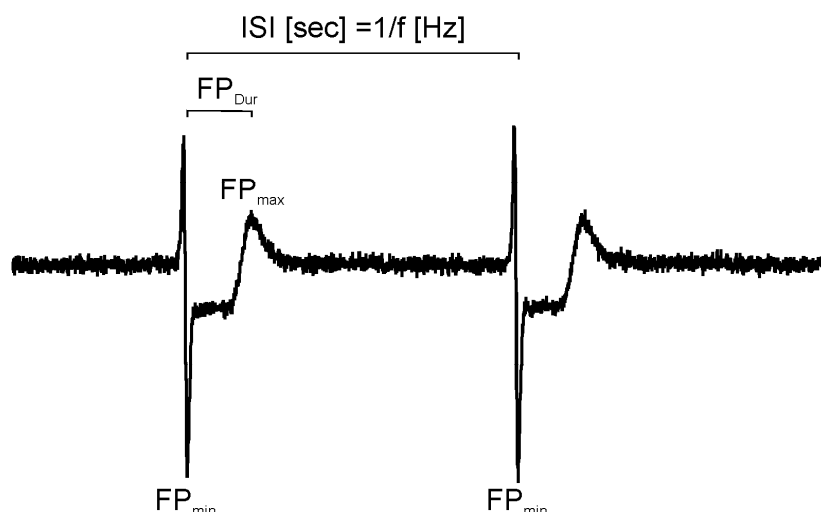


Figure 2.1: Depiction of common FP features

The interval between two consecutive FP_{\min} represents the inter-spike interval (ISI [sec]) and is the reciprocal value of the beating frequency [Hz]. The interval between FP_{\min} and FP_{\max} is referred to as the FP_{Dur} .

2.6 Impedance measurement

2.6.1 *Cell preparation*

Day 14 puromycin purified α PIG44 EBs (4 day purification; see paragraph “*Puromycin purification of cardiomyocytes*”) were harvested and washed twice with PBS (0 mM Ca^{2+} ; 0 mM Mg^{2+}) to avoid dead cells and debris. The supernatant was aspirated (with floating debris). 5 ml Trypsin/EDTA (0.05%) and DNase (5 Units) were added followed by incubation at 37°C in a water bath for 20-30 min. For better dissociation EBs were gently mixed by shaking every 2 min. After the incubation, remaining clusters were allowed to settle, and the supernatant was removed before filtration through 40 μ m cell strainer. 5-times the volume of the supernatant 20%-IMDM (cold) was added to inhibit trypsin activity. Trypsin was removed by centrifugation (100 x g) and the single cell pellet was resuspended in 20%-IMDM. This first batch of cells was kept on ice and the Trypsin/EDTA (0.05%) and DNase (5 Units) step was repeated for 15 min with the remaining pellet of un-dissociated clusters. At the end of the second dissociation round the supernatant was filtered, trypsin was removed by centrifugation, and the pellet was also re-suspended in 20%-IMDM. Both filtered single-cell suspensions were combined. Keeping cells cold helps secure the quality of the yielded single cardiomyocytes. Finally, cells were counted (live-dead staining with trypan blue) and 60,000 cells/well were seeded on specially designed 96-well microtiter plates (E-plate 96; ACEA

BIOSciences Inc., San Diego, USA) containing integrated gold microelectrodes. Cells were allowed to settle for 1 hr at room temperature before the measurement was started.

2.6.2 *Measurement procedure*

For cytotoxicity testing we used the xCELLigence RTCA Cardio system (ACEA BIOSciences Inc., San Diego, USA) allowing continuous real-time monitoring of cell viability by non-invasive impedance recording [Atienza, Yu et al. 2006, Xi, Wang et al. 2011]. The xCELLigence RTCA Cardio system consists of four hardware components: a 96-well microtiter plate (E-Plate 96); the RTCA Cardio station accommodating the E-Plate which is kept in a tissue culture incubator; The RTCA Control Unit which is necessary to operate the software and to acquire the data; the RTCA Analyzer connecting the Cardio station with the Control Unit by a cable through the sealed door of the incubator.

Dissociated CMs were treated in 3 different groups (16 wells per group, n=16): 1) control (untreated); 2) reserpine treatment starting at day 14 (10 μ M; reserpine was added at the day of seeding); 3) reserpine treatment starting at day 17 (10 μ M; reserpine was added 3 days after seeding to test if the drug itself changes adhesion and therefore the cell index (CI)). Medium was first changed after approximately at day 17 (~56 hrs) to guarantee good initial cell adhesion. Further medium changes were performed every 24 hrs during the remainder of the measurement. Within the first 56 hrs the CI of each well was recorded every 20 min. After that CIs were recorded continuously every 15 min until day 23 of differentiation. Data were recorded and analyzed using the RTCA Cardio 1.0 software (ACEA BIOSciences Inc., San Diego, USA).

2.7 Data analysis

For data analysis Student's paired or unpaired t-test and one-way ANOVA was applied, respectively. Error bars represent the standard error of the means (s.e.m.) if not stated otherwise. *P*-values ≤ 0.05 (*) were considered significant. For statistical analysis GraphPad InStat Version 3.10 software and GraphPad Prism® (GraphPad Software, Inc., San Diego, USA) were used.

3 Results

3.1 The role of catecholamines in cardiac lineage commitment in mouse ES cells

3.1.1 Cell culture and morphology

D3 α PIG44 ES cells harbor a vector expressing eGFP and a puromycin resistance gene under the control of a murine α MHC promoter. The pluripotent cells were passaged 3 times a week and propagated on a NEO-feeder layer. Fig. 3.1 depicts a representative ES cell colony as used for differentiation.

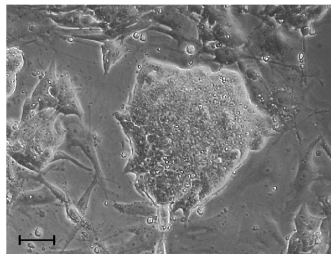


Figure 3.1: Colony of pluripotent D3 α PIG44 ES cells

Representative pluripotent α PIG44 ESC colony (scale bar: 50 μ m). Published in [Lehmann, Nguemo et al. 2013].

3.1.2 Reserpine application protocols

To study the effect of reserpine on the differentiation of α PIG44 ES cells we first tested several application schemes. Fig. 3.2 illustrates the different approaches of reserpine application used for this work. Two different approaches were used: (1) different frequency of drug refreshment: ‘d2’ (green arrows): application on days 0, 2, 4, 6, 8, 10, 12; and ‘d4’ (yellow arrows): application on days 0, 2, 4, 10; (2) different duration of reserpine application (Fig. 3.2 grey arrows): ‘until day 14’ (top) and ‘until day 6’ (bottom). In all cases reserpine or DMSO were applied starting on day 0. Fig. 3.2 further shows representative day 11 EBs of the three groups plated on 0.1% gelatine coated culture dishes on day 6 (Fig. 3.2 A-C).

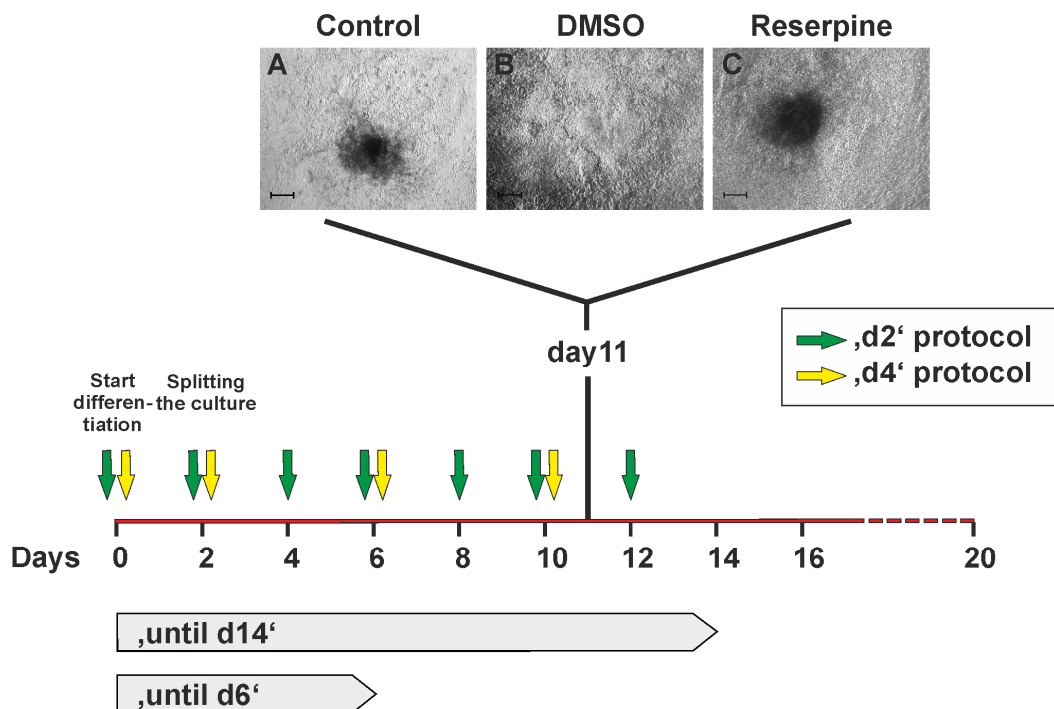


Figure 3.2: Scheme of culture protocols

Cell culture schedules: Arrows indicate the days of addition of DMSO (1:1,000) or reserpine (10 μ M in 1:1,000 DMSO) as used for the 'd2' (green) and 'd4' (yellow) protocols. For the 'd2' protocol, medium was renewed at day 6 and 12, while for the 'd4' protocol, medium changes were combined with drug application (d6 and d12): (A-C) Control (untreated), solvent control (DMSO; 1:1,000) and reserpine-treated (10 μ M in 1:1,000 DMSO) day 11 EBs plated on 0.1% gelatine-coated culture dishes (scale bars: 200 μ m). Published in [Lehmann, Nguemo et al. 2013].

Analysis of the different application protocols led to the conclusion that there are no developmental differences between the untreated and the DMSO-treated group. In comparison to these two groups, the reserpine-treated group showed a significantly reduced outcome in cardiomyocyte numbers. Because no differences between the 'd2' and 'd4' differentiation protocol was observed, all further experiments were performed following the 'd4' protocol. Also the chronic application until day 14 and the application until day 6 led to reduced cardiac development. It will be stated in the corresponding sections, if reserpine was only applied until day 6.

As a read-out for cardiomyocyte differentiation in the presence of reserpine, we first estimated the size of green eGFP-expressing CM-containing clusters within EBs, which is representative of the quantity of CMs. Therefore we used phase-contrast and fluorescence microscopy. Fig. 3.3 shows representative pictures of EBs at day 2, 4, 10 and 14. Day 2 and day 4 EBs of control and DMSO EBs were morphologically indistinguishable from reserpine-treated EBs. First eGFP expressing CMs could be observed at day 7-9 in control and DMSO-

treated EBs, whereas, in reserpine-treated EBs the cardiac differentiation was strongly reduced even at day 10. Day 14 EBs were puromycin purified to emphasize the reduction of CMs after reserpine treatment and only drastically reduced numbers of minimum-sized cardiac clusters could be observed (indicated by green arrow).

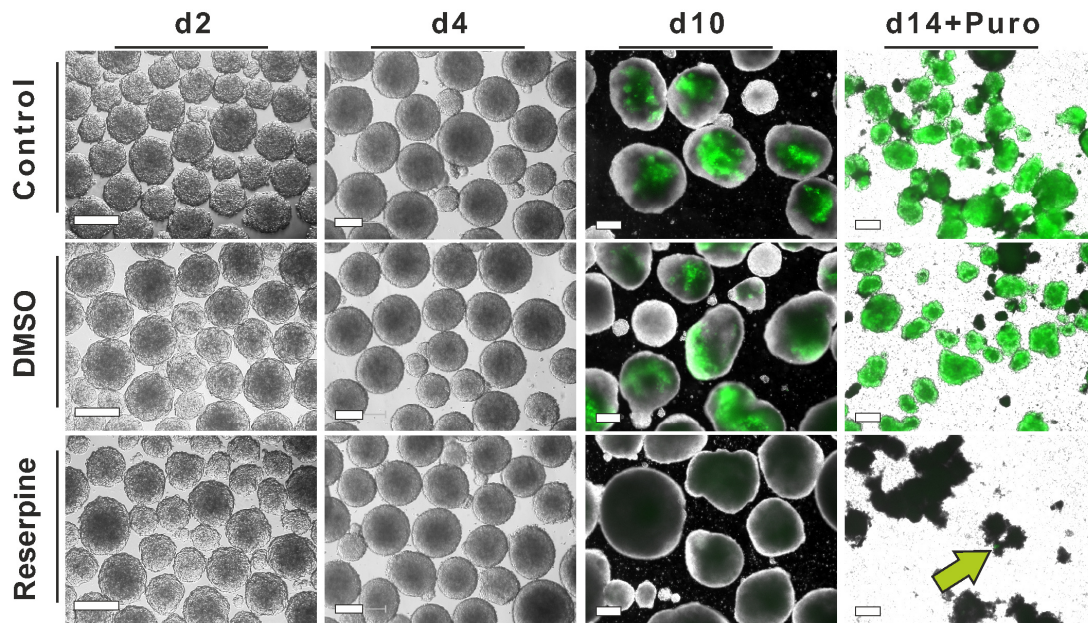


Figure 3.3: eGFP positive cardiomyocyte containing EBs representative of the time course of differentiation

Phase contrast/fluorescence overlay images of control, DMSO- (solvent control) and reserpine-treated EBs at day 2, 4, 10 and 14 of differentiation (day 14 EBs were purified with puromycin). Green: eGFP positive CMs. The reserpine-treated purified cardiac cluster is typically small in size and is highlighted by a green arrow (scale bars: d2+d4 50 μ M; d10+d14 200 μ m). Published in [Lehmann, Nguemo et al. 2013].

3.1.3 *Reserpine reduces numbers of beating clusters*

To investigate whether the reduction of cardiomyogenesis, as suggested by the reduced numbers of eGFP expressing CMs in Fig. 3.3, led to altered functionality, we quantified the ratios of beating clusters. We therefore plated EBs of the three groups on 0.1% gelatine coated culture dishes at day 6 and kept treating them following the respective protocol. Counting was performed visually and ratios of beating to non-beating EBs were calculated (Fig. 3.4). Analysis of the visual counting shows the first appearance of beating clusters with low incidence at day 12 of differentiation in reserpine-treated EBs in ‘d2’ and ‘d4’ protocols (12.2 \pm 9.8%, n=6 and 3.2 \pm 7.8%, n=7, respectively), whereas the untreated and DMSO-treated groups already show a considerable percentage of beating EBs (untreated ‘d2’: 29.3 \pm 5.7, ‘d4’: 35.8 \pm 7.3%; DMSO-treated ‘d2’: 27.0 \pm 8.0%, ‘d4’: 42.6 \pm 11.3%). Reserpine-treated EBs show their maximum of beating EBs at day 17 of differentiation (‘d2’: 36.6 \pm 9.2% and ‘d4’:

34.2±15%) before the number declines after day 20 as in the untreated and DMSO-treated group. It has to be noted that the visual counting and the eGFP expression pictures from day 14 (Fig. 3.3) are opposed, but beating clusters were counted regardless of their size or number of CMs contained in them. Since ‘d2’ and ‘d4’ protocols lead to a comparable effect of delayed start of beating during ES cell differentiation, it was decided to follow the ‘d4’ protocol for further experiments.

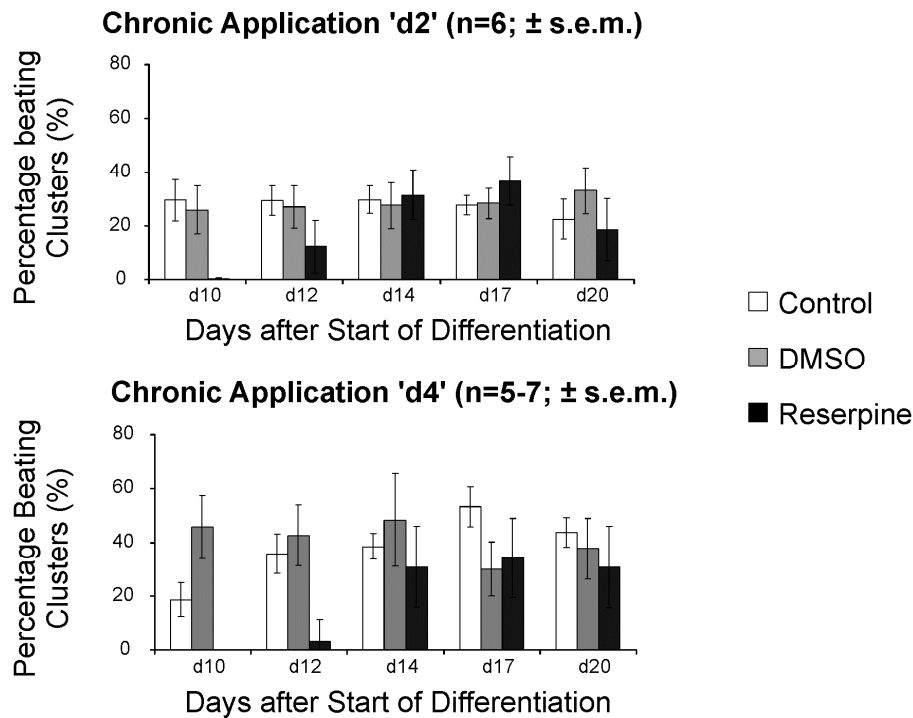


Figure 3.4: Visual counting of beating clusters

Percentages of beating vs. non-beating EBs were calculated based on visual counting of plated EBs at days 10-20. The number of experiments (n) is given on top of each panel. Published in [Lehmann, Nguemo et al. 2013].

3.1.4 Quantification of CMs in EBs using flowcytometry

For more detailed quantification of the difference of eGFP expressing CMs in control, DMSO and reserpine-treated EBs we performed flow cytometry experiments. We grew the EBs using the ‘d4’ protocol in mass cultures. Additionally, we investigated whether the period and duration of reserpine application affected cardiac differentiation. Therefore, we treated ES cells with reserpine either until day 14 (‘until d14’ application) or only until day 6 (‘until d6’ application). On day 10 and 14 of differentiation about 100-200 EBs were harvested and enzymatically dissociated. Fig. 3.5A shows representative eGFP/propidium iodide (PI) dot

plots of flow cytometry experiments. Population percentage values of the particular single measurement are given in each plot. Fig. 3.5B shows the analysis of the results. Percentages of eGFP positive CMs in treated EBs were normalized toward percentages in control EBs. Using the ‘until d14’ application (Fig. 3.5B, left), at day 10 no significant differences were found between untreated and DMSO-treated EBs (100% vs. $87.3\pm 9\%$, $n=11$ independent differentiations, $p>0.05$). In line with the morphological findings (Fig. 3.3), we found that in reserpine-treated EBs eGFP expressing CMs were reduced to $28.4\pm 13.8\%$ at day 10 ($n=11$, $***p<0.001$). At day 14 of differentiation reserpine-treated EBs contained 8% less eGFP positive CMs than control EBs ($92\pm 32\%$ vs. 100%, $n=7$ differentiations, $p>0.05$). Also DMSO-treated EBs did not show significant differences as compared to controls ($118\pm 18\%$, $n=7$, $p>0.05$). Using the ‘until d6’ application scheme demonstrated a similar outcome (Fig. 3.5B, right). At day 10 no significant difference was observed between control and DMSO (100% vs. $109\pm 17\%$, $n=7$, $p>0.05$), while after reserpine treatment the percentage of CMs was reduced to $36\pm 12\%$ ($n=6$, $**p<0.01$). As in the ‘until d14’ experiments, percentages of CMs were not significantly different between the three groups on day 14 ($n=4$, $p>0.05$).

PI was used to stain dead cells. Analyzing the values of the PI staining derived from our experiments (not shown) we did not observe significant differences of PI positive events after reserpine treatment, suggesting no significant alterations of cell viability by reserpine.

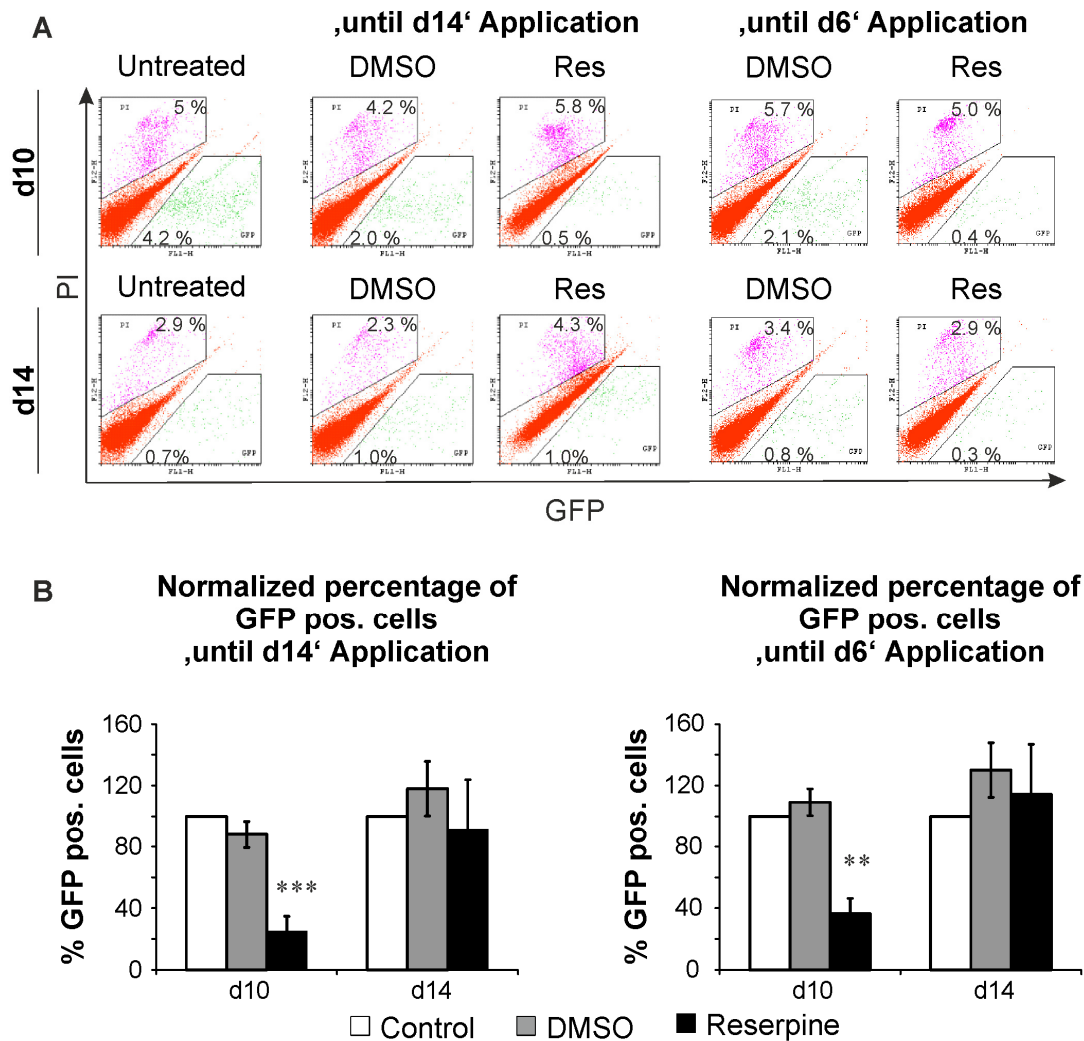


Figure 3.5: Flowcytometry for CM quantification

(A) Representative eGFP/PI dot plots of single measurements of enzymatically dissociated EBs of the control group (left) or treated with DMSO and reserpine either until day 14 or until day 6. Percentages of eGFP and PI events are given in each plot. Measurements were performed at day 10 (top row) and day 14 (bottom row) of differentiation. (B) Normalization of the percentage of CMs within EBs toward control EBs. 'until d14': d10 (n=11, *** p<0.001); d14 (n=7, p>0.05). 'until d6': d10 (DMSO n=7, Res n=6, ** p<0.01), d14 (n=4, p>0.05). Published in [Lehmann, Nguemo et al. 2013].

3.1.5 *Reserpine inhibits expression of cardiac marker proteins*

Reduced numbers of eGFP positive cells after reserpine treatment in combination with a strongly delayed initiation of contraction (Fig. 3.5) using different application protocols strongly suggests that reserpine negatively affects cardiomyogenesis. To further investigate if this observation was paralleled by alterations on different cardiac protein levels we stained EBs using anti- α Actinin and anti-cardiac TroponinT (cTnT) antibodies. Herewith it was possible to rule out the possibility that the application of reserpine unspecifically inhibited the

eGFP fluorescence or the contraction of the differentiating CMs, thus showing that reserpine in fact influences cardiomyogenesis *per se*.

Fig. 3.6 shows that in control and in DMSO-treated day 11 EBs α Actinin (red; top panel) and cTnT (red; bottom panel) are co-localized with eGFP (green). In contrast, in reserpine-treated day 11 EBs α Actinin, cTnT and eGFP are hardly expressed, supporting our previous results of reduced cardiomyogenesis.

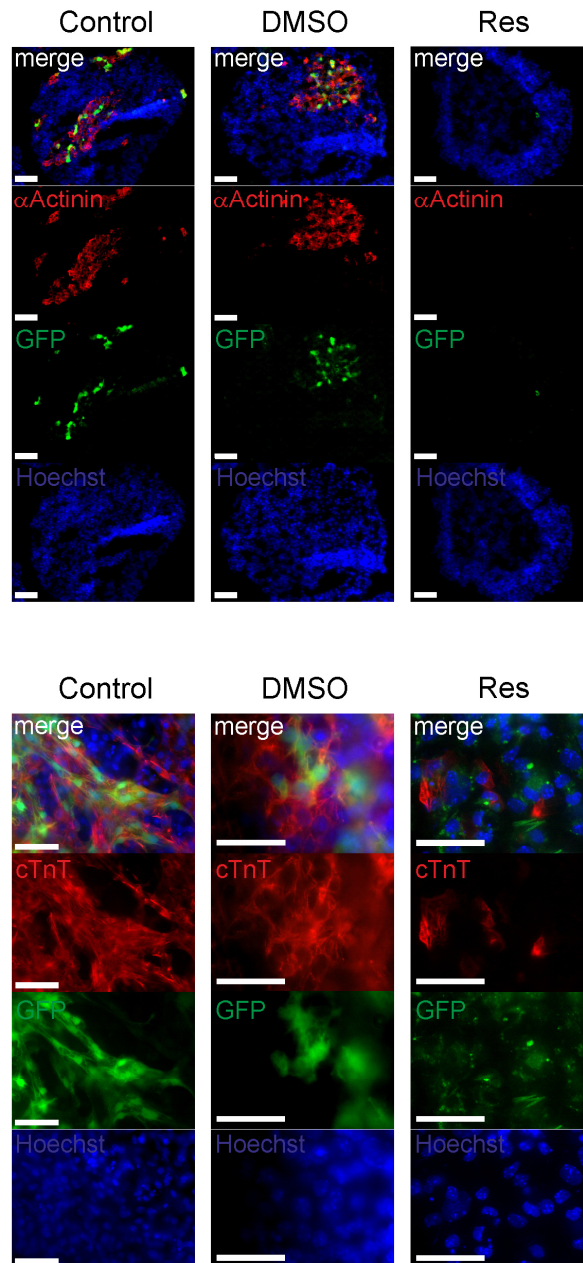


Figure 3.6: Immunocytochemical staining for cardiac markers

Immunocytochemical staining of cryosliced (top) and plated (bottom) EBs at day 11 of differentiation: eGFP positive cardiomyocytes (green), Hoechst 33342 stained nuclei (blue) and cardiac α Actinin (red; top panel) or cardiac TroponinC (red; bottom panel). Top rows represent overlay pictures. Scale bars: 50 μ m. Published in [Lehmann, Nguemo et al. 2013].

3.1.6 *Effects of reserpine on proliferation and cell viability*

3.1.6.1 *EB cross-section area measurements*

Evaluating whether reserpine affects the viability of ES cells during their differentiation would help to exclude that reserpine inhibits proliferation or might have cytotoxic and/or

apoptotic effects. In a first approach we measured the cross-section areas of spherical EBs at different days of differentiation. Fig. 3.7 represents the analysis of cross section areas of 127-230 EBs from each group of 3-4 independent differentiations at different stages during differentiation. We found no significant difference between the groups at day 2 with a mean area of $0.040\pm 0.019\text{ mm}^2$ in the untreated, $0.045\pm 0.020\text{ mm}^2$ in the DMSO-treated group and $0.046\pm 0.024\text{ mm}^2$ after reserpine treatment. Neither untreated ($0.088\pm 0.0064\text{ mm}^2$), DMSO-treated ($0.086\pm 0.0075\text{ mm}^2$), nor reserpine-treated EBs ($0.077\pm 0.0067\text{ mm}^2$) showed significant differences at day 4 of differentiation. Also at day 10 EB size did not differ significantly ($0.222\pm 0.0154\text{ mm}^2$, $0.246\pm 0.0362\text{ mm}^2$, and $0.270\pm 0.0126\text{ mm}^2$, respectively, $p>0.05$). Based on these results the cells of all three groups grow at the same proliferation rate.

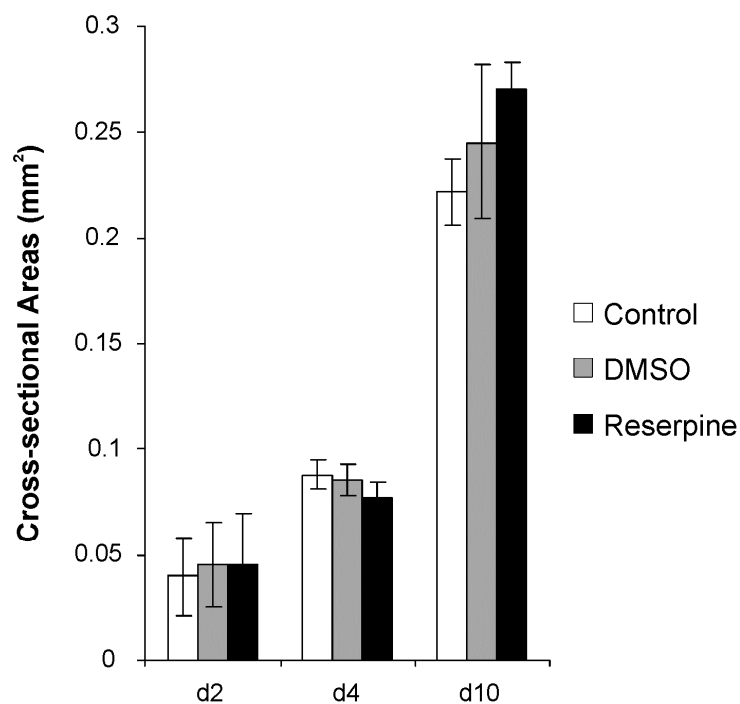


Figure 3.7: Cross-section areas during the course of differentiation

Cross-section measurements of EBs on days 2, 4, and 10 from independent differentiation experiments ($n=3-4$; \pm s.e.m.; $p>0.05$). Published in [Lehmann, Nguemo et al. 2013].

3.1.6.2 Impedance measurements

After we found that reserpine did not influence proliferation of cells during the developmental process, we further evaluated whether the reserpine-induced reduction of CMs in EBs was due to reserpine-induced cytotoxicity on CMs *per se*. For this purpose we used puromycine-purified control cardiac clusters which were enzymatically dissociated at day 14 (see section 2.6). Using the xCELLigence RTCA Cardio system enabled us to analyze the impedance of

CM monolayers. Impedance values were measured over a number of electrodes (as shown in pictures of Fig. 3.8B) and converted into the cell index (CI). The CI as an arbitrary unit reflects cell number, morphology, and attachment. For example, if a drug induces cytotoxicity fewer cells would be attached or less strongly attached to the bottom of the cell culture well covering less electrodes, and the CI would decrease over time [Xi, Yu et al. 2008, Chen, Cui et al. 2012, Otero-Gonzalez, Sierra-Alvarez et al. 2012, Weiland, Berger et al. 2012]. In this experiment we investigated if reserpine exerts cytotoxic effects on pure CMs which would decrease the CI over time. It should be noted that for this series of experiments medium and reserpine was refreshed every 24 hrs.

The results of the cytotoxicity experiment are depicted in Fig. 3.8. For each group 16 wells (n=16) of CMs were plated and the graph in Fig. 3.8A represents their averaged values. The CI of all three groups was monitored for ~222 hrs, corresponding to differentiation days 14-24. The impedance monitoring revealed that CI values increased exponentially before reaching a plateau within the first 48 hrs (d14-d16) and the plateau suggested that the cells grew a confluent layer. CI values of the single wells were within a close range indicating that the wells contained equal numbers of cells (data not shown). Finding no differences between the control and the 'Res after d14' group indicated that reserpine does not inhibit CM adhesion. In a second phase, a yet untreated group was exposed to reserpine (starting after ~72 hrs/ 'Res after d17'). Within the second phase of the monitoring the CI slowly increased in all groups. This finding strongly suggests that reserpine had no cytotoxic effect on CMs, which was further underlined by the fluorescence microscopy pictures in Fig. 3.8B, clearly showing eGFP expressing CMs after reserpine application despite more frequent reserpine refreshment (every 24 hrs instead of every 4 days).

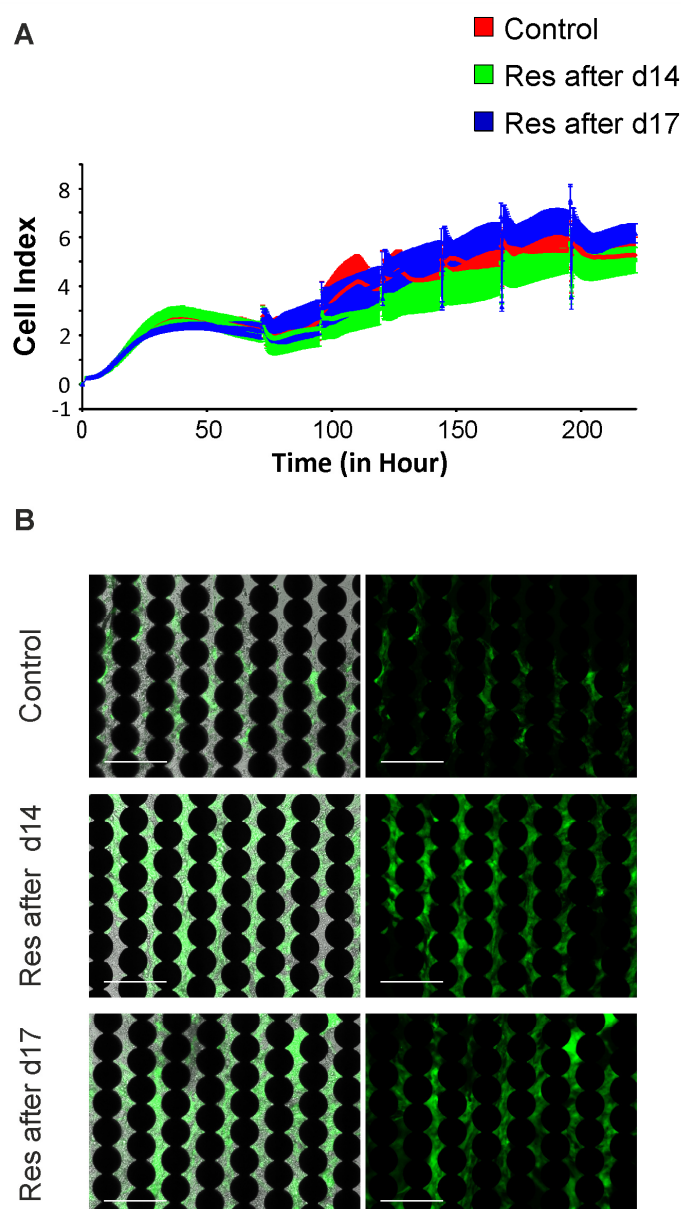


Figure 3.8: Impedance measurements to exclude cytotoxic effects of reserpine on CMs

(A) Cell index (CI)/time plot of puromycin purified day 14 CMs monitored between d14 (0 hrs) – d24 (~222 hrs) of differentiation. The plot represents averaged CI values \pm SD (n=16). Two reserpine application protocols were used: ‘Res after d14’: reserpine was applied at the day of seeding (d14); ‘Res after d17’: reserpine was applied on the third day after seeding (d17) to allow attachment without the drug. (B) phase-contrast/fluorescence overlay (left) and fluorescence (right) pictures of the CM layers at day 24 (scale bars: 200 μ m).

3.1.7 Reserpine effects on gene expression - Quantitative Real Time-PCR (qRT-PCR)

The results of the previous paragraphs provided evidence for an effect of reserpine on cardiomyogenesis. For mRNA expression level analysis we tested ES cells, d1-d14 EBs,

Results

puromycine purified EBs and mouse embryonic fibroblasts (MEFs) by qRT-PCR. All qRT-PCRs were performed in collaboration with Dr. Vilas Wagh at the University of Cologne, Institute for Neurophysiology. Used primers are listed in section VII. “Primers” of the appendix.

3.1.7.1 Pluripotency genes

To investigate if reserpine affected expression of genes important for development prior to cardiac development, we studied the expression of the pluripotency genes *Zfp42 (Rex1)*, *Oct4* and *Nanog* as well as the differentiation marker *Fgf-5* (Fig. 3.9). As a pluripotency gene, *Rex1* should be down-regulated upon the start of differentiation. Interestingly, reserpine-treated ES cells down-regulated the gene considerably faster, thus indicating that treated cells lose their pluripotency properties earlier. *Oct4* and *Nanog*, however, did not show such strong differences. *Fgf-5* is strongly expressed just prior to gastrulation followed by a dramatic cease in expression once formation of the primary germ layers is complete [Hebert, Boyle et al. 1991]. *Fgf-5* expression showed early up-regulation in both groups. But, while in the untreated group *Fgf-5* was dramatically down-regulated after day 4, this down-regulation could only be observed after day 6 in the reserpine group. Expectedly, as compared to ES cells pluripotency genes were strongly down-regulated in MEFs. *Fgf-5* expression was similar in ES cells and MEFs.

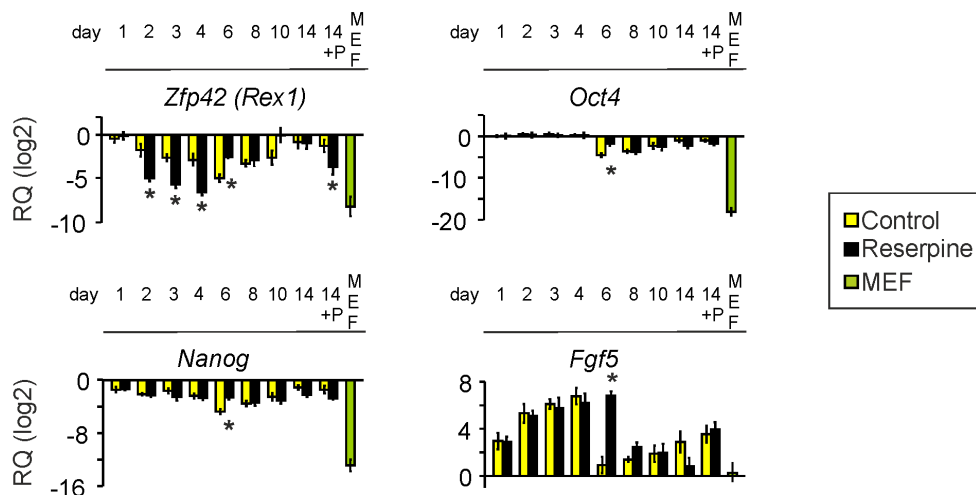


Figure 3.9: qRT-PCR results of *Zfp42 (Rex1)*, *Oct4*, *Nanog* and *Fgf-5*

Relative quantities (RQ) were calculated using the $\Delta\Delta\text{Ct}$ -method and are plotted on a log2 scale. Published in [Lehmann, Nguemo et al. 2013].

3.1.7.2 Cardiac and mesodermal marker genes

The expression of the cardiac specific genes myosin heavy chain (*Myh6*) and atrial myosin light chain 2 (*Mlc2a*) should elucidate how strong reserpine affected the CM differentiation on the gene expression level. qRT-PCR results of the cardiac genes revealed (Fig. 3.10) that *Myh6* showed a ~250-fold reduced level of expression in reserpine-treated EBs at day 10. *Mlc2a* did not even seem to be expressed until day 6-8 and expression levels never reached control EB levels (up to ~130-fold reduced expression at day 14). These results underline the finding of reserpine-inhibited cardiac differentiation. Purified CMs of the control and the treated group showed almost equal levels of gene expression. Expectedly, MEFs did not express these cardiac genes.

Investigating whether only cardiac genes or also mesodermal or early CM gene expression is altered, we tested the expression of the specific markers homeobox protein *Nkx2-5*, T-brachyury (*T-bra*), and Gata binding factor 4 (*Gata4*) (Fig. 3.10). Initial transcription of *Nkx2-5* was found to be delayed by approximately 2 days (day 8 instead of 6) in reserpine-treated EBs. Peaking at day 10 in both groups, *Nkx2-5* expression was still significantly lower in reserpine-treated EBs at each time point. Accordingly, initiation of *T-bra* expression was also delayed by about one day. The maximum expression of *T-bra* was reached at day 6 in reserpine-treated EBs instead of day 4 in control EBs. In purified day 14 CMs *T-bra* and *Gata4* expression showed higher levels in the reserpine group, whereas *Nkx2-5* expression was not altered between the groups. In MEFs *Nkx2-5*, *Gata4* and *T-bra* only showed weak expression.

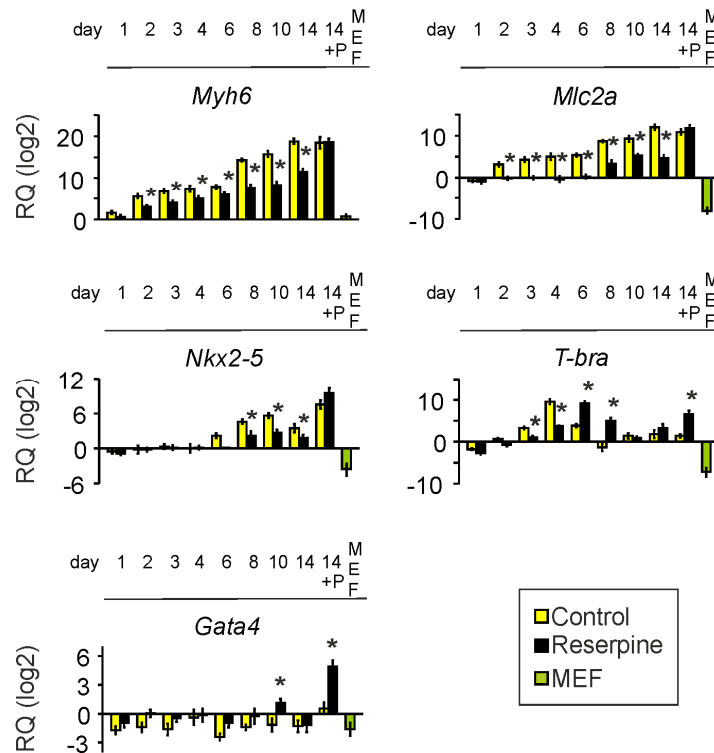


Figure 3.10: qRT-PCR results of cardiac marker genes *Myh6*, *Mlc2a* and mesodermal markers *Nkx2-5*, *T-bra* and *Gata4*

Relative quantities (RQ) were calculated using the $\Delta\Delta C_t$ -method and are plotted on a log₂ scale. Published in [Lehmann, Nguemo et al. 2013].

3.1.7.3 Catecholamine synthesis genes

Reserpine-induced depletion of catecholamines has serious effects on cardiac differentiation. However, it is not known whether reserpine also influences the expression of the genes of catecholamine synthesis. Therefore the expression of tyrosine hydroxylase (*Th*), aromatic L-amino acid decarboxylase (*Ddc*), dopamine- β -hydroxylase (*Dbh*) and phenylethanolamine N-methyltransferase (*Pnmt*) was examined using qRT-PCR (Fig. 3.11). In controls no significant expression of *Th* and *Ddc* was detected until day 6, while *Dbh* and *Pnmt* expression was not detected before day 8-10. In contrast, reserpine-treated EBs showed up-regulation of *Th*, *Ddc* and *Dbh* already on day 2. *Pnmt* showed low expression and decreasing levels during differentiation in reserpine-treated EBs, whereas in controls up-regulation of *Pnmt* expression started after day 8 and was kept up-regulated until day 14. In reserpine-treated purified day 14 EBs, expression of *Th*, *Ddc* and *DBH* was also increased, while *Pnmt* was expressed on a low level in both, controls and reserpine-treated EBs. MEFs expressed the genes on ES cell levels or below.

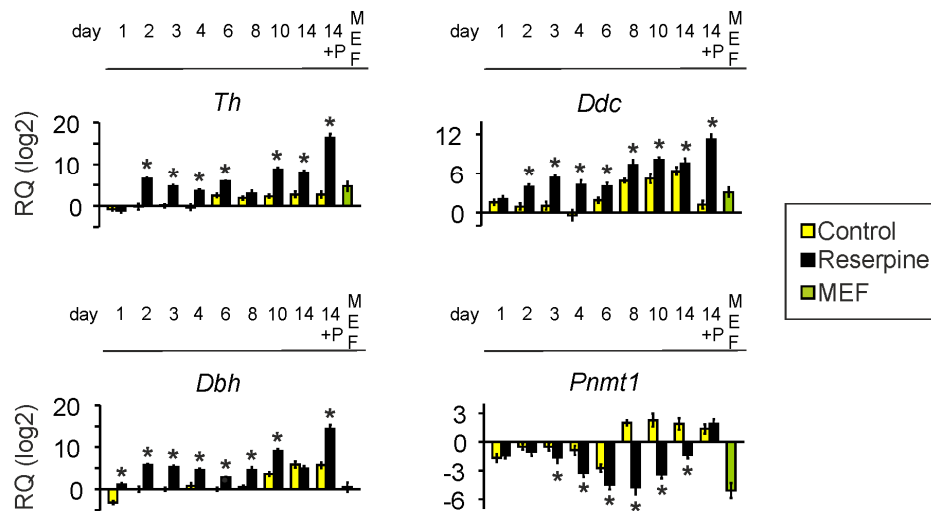


Figure 3.11: qRT-PCR results of catecholamine synthesis genes *Th*, *Ddc*, *Dbh* and *Pnmt*

Relative quantities (RQ) were calculated using the $\Delta\Delta C_t$ -method and are plotted on a log₂ scale. Published in [Lehmann, Nguemo et al. 2013].

3.1.7.4 Endodermal and Ectodermal marker genes

Given that the number of CMs was strongly reduced by reserpine although EB sizes were unaltered, compensatory or alternative lineage differentiation is conceivable. To investigate this possibility we further tested the expression of endodermal and ectodermal marker genes.

As endodermal marker genes we used *Sox17*, *Foxa2*, alpha-fetoprotein (*Afp*), hepatocyte nuclear factor 4a (*Hnf4a*) and albumin (*Alb*) (Fig. 3.12A). The most prominent discrepancies amongst the tested endodermal markers were observed in the expression patterns of the transcription factors *Sox17* and *Foxa2*. Most striking is the early up-regulation observed for both genes on day 6 instead of day 8 and day 2 instead of day 4, respectively. However, the expression of later endoderm-derived liver tissue-inducing genes *Afp*, *Hnf4a* and *Alb* revealed no such effect of reserpine. In MEFs, expression of all endodermal marker genes tested here, except for *Foxa2*, is on a level of pluripotent ES cells or below. These results suggest that reserpine may also affect certain aspects of early endodermal development.

Investigating ectodermal marker gene expression of microtubule-associated protein 2 (*Map2*), β -III-tubulin (*Tubb3*), and Nestin (*Nes*) (Fig. 3.12B), it was found that in control EBs *Map2* expression started around day 4 and stayed at a constant level between day 6 and 14. In reserpine-treated EBs *Map2* expression started already at day 1 and was 25-50-times increased within the first three days compared to controls. *Map2* expression levels were increased during the whole period. *Tubb3*, a valuable neuronal marker [Katsetos, Legido et al. 2003], was expressed from day 6 on in reserpine-treated cells, whereas in control EBs it appeared to

Results

be absent. *Nes*, a neural progenitor marker [Frederiksen and McKay 1988, Lendahl, Zimmerman et al. 1990], was expressed from day 10 on. Aberrant from expression patterns of *Map2* and *Tubb3*, *Nes* expression was rather low in reserpine-treated EBs.

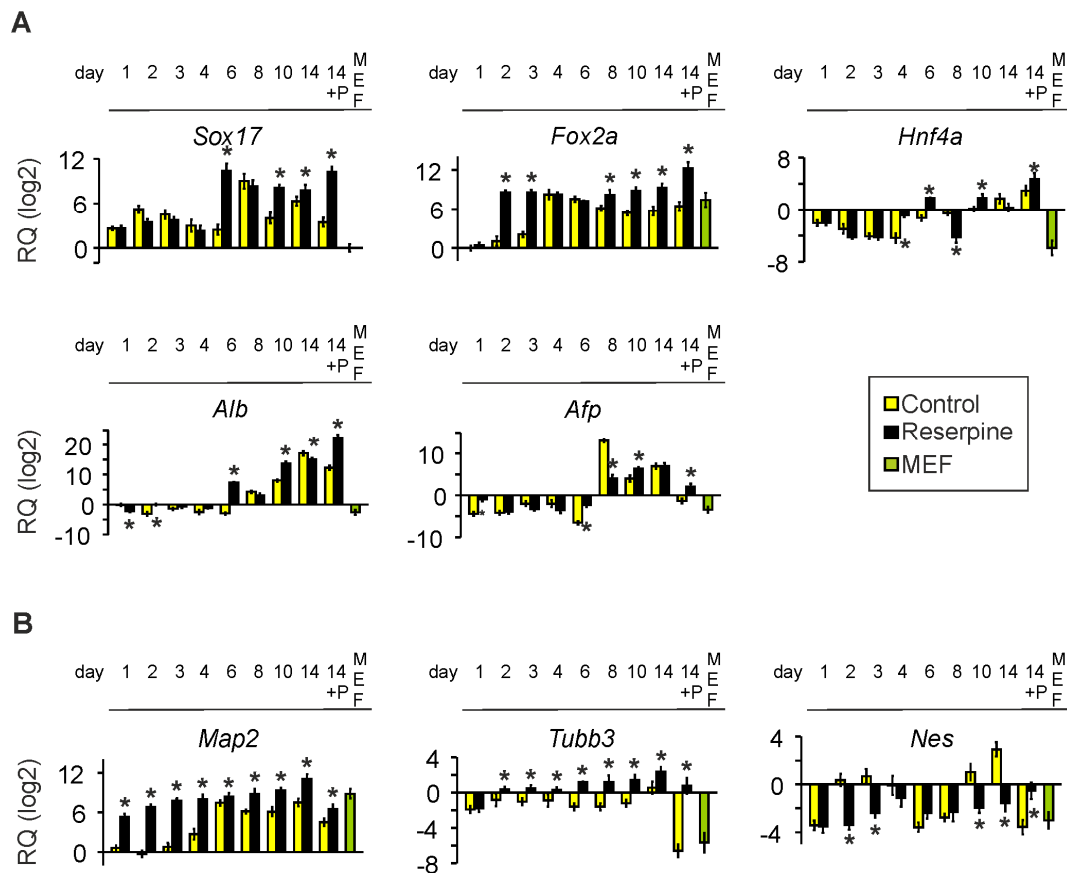


Figure 3.12: qRT-PCR results of endodermal and ectodermal/neuronal marker genes

(A) endodermal markers *Sox17*, *Fox2a*, *Hnf4a*, *Alb* and *Afp*; (B) ectodermal marker *Map2* and neuronal markers *Tubb3* and *Nes*. Relative quantities (RQ) were calculated using the $\Delta\Delta\text{Ct}$ -method and are plotted on a log₂ scale. Published in [Lehmann, Nguemo et al. 2013].

3.1.8 Expression of α - and β -adrenergic receptor subtypes

α - and β -ARs are the cellular targets of catecholamines and were therefore studied using sqRT-PCR comparing their time course expression in control and reserpine-treated EBs. Fig. 3.13 shows that in control EBs the β_1 - and the β_2 -AR expression started on day 6, while after reserpine treatment first expression was detected on day 4. However, on day 10 β_1 - and β_2 -ARs were absent in reserpine-treated EBs. Interestingly, β_3 -ARs were expressed in ES cells and their expression levels were found to be increased in reserpine-treated EBs. All α_1 -ARs were clearly expressed on day 10 in the control group, while no expression of α_1 -ARs was found in reserpine-treated EBs. A distinct transient expression of α_{1A} and α_{1D} was

detectable between days 4-8 after reserpine treatment, which even appeared to be higher than the expression in the control group. α_{1B} was not expressed at any time in reserpine-treated EBs. Expression of the α_{2A} receptor was similar in both groups, while α_{2B} expression strongly differed. In control EBs expression of α_{2B} receptors started by day 6 while in reserpine-treated EBs no expression was detectable. Like the β_1 - and β_2 receptors, α_{2C} was expressed transiently by day 4-6, but was absent on day 10 in reserpine-treated EBs, while in control EBs its expression started at day 6 and increased until day 10. Thus, reserpine induced alterations in AR-expression. Particularly remarkable was the absence of most ARs in day 10 reserpine-treated EBs, while others were expressed prematurely (β_1 , β_2 , α_{1A} , α_{1D} and α_{2C}).

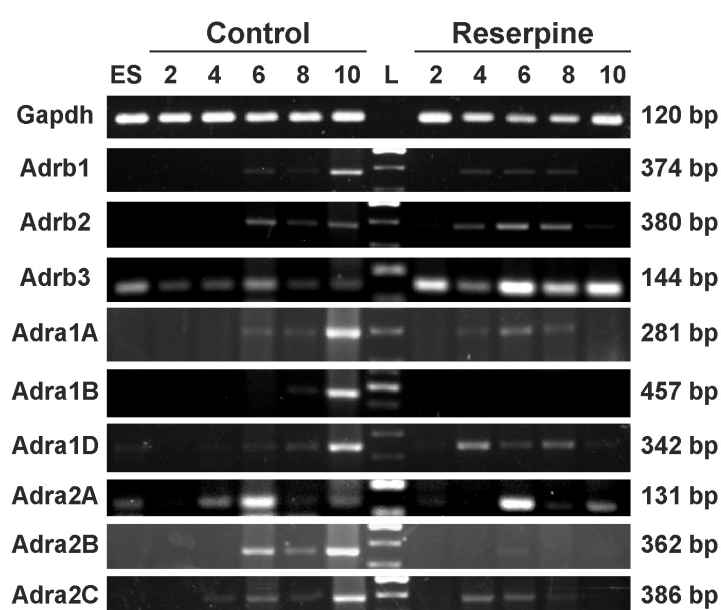


Figure 3.13: Time course of α - and β -AR subtype expression

Semiquantitative reverse-transcription PCRs (sqRT-PCRs) from ES cells (ES), control and reserpine-treated EBs during differentiation day 2 to day 10 representative of the mRNA expression of α - and β -AR subtypes (β_1 , β_2 , β_3 , α_{1A} , α_{1B} , α_{1D} , α_{2A} , α_{2B} , α_{2C} ; *Gapdh* was used as house-keeping control). L: DNA Ladder. Amplified fragment sizes are stated on the right of each pane. Primers are listed in section VII. “Primers” of the appendix. Published in [Lehmann, Nguemo et al. 2013].

3.1.9 Positive effects on neuronal differentiation

As already indicated by qRT-PCRs of ectodermal and neuronal markers (see paragraph 3.1.7.4 and Fig. 3.12B), reserpine treatment promoted differentiation of the neuronal lineage. Using a cell culture protocol originally optimized for cardiomyogenic differentiation, we frequently observed the appearance of cells with a neuronal morphology in the presence of reserpine (Fig. 3.14). These cells appeared already at day 11 and were mostly observed in the periphery of EBs. Control EBs never showed similar cells.

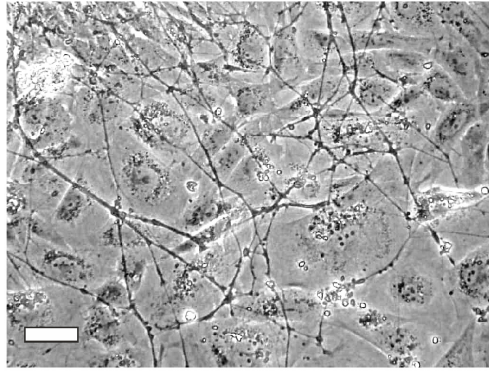


Figure 3.14: Neuronal cells in reserpine-treated EBs

Representative phase contrast image of a day 11 reserpine-treated EB showing cells with typical neuronal morphology (scale bar: 50 μm). Published in [Lehmann, Nguemo et al. 2013].

3.1.10 Immunohistochemical stainings for β -III-tubulin and DBH

To confirm our molecular biology and microscopy findings, immunohistochemical stainings with antibodies specific for TUBB3 (β -III-tubulin) and DBH were carried out (Fig. 3.15). In all day 11 EBs TUBB3 positive cells were found. However, we observed differences in cell morphology between control and reserpine-treated EBs. While the cells in control EBs were of round or elongated shape, reserpine-treated EBs contained a high number of neuronal-like cells with elongated outgrowth, presumably axons and dendrites (Fig. 3.15, top). This finding clearly underlined our phase contrast microscopy observations. DBH expressing cells were found in all three groups showing slightly increased numbers in reserpine-treated EBs (Fig. 3.15, bottom). The cells were of round shape as previously described for intracardiac adrenergic (ICA) cells [Huang, Friend et al. 1996]. Taken together our qRT-PCR and immunocytochemistry experiments investigating the presence of the DBH enzyme showed congruent findings (Fig. 3.11 and Fig. 3.15): 1. qRT-PCR for *Dbh* at day 10 proved elevated expression levels in reserpine-treated EBs confirming the IHC results (from day 11 EBs); 2. Reserpine-treated purified day 14 CMs showed a distinctly increased *Dbh* expression, suggesting that *Dbh* synthesizing cells were present.

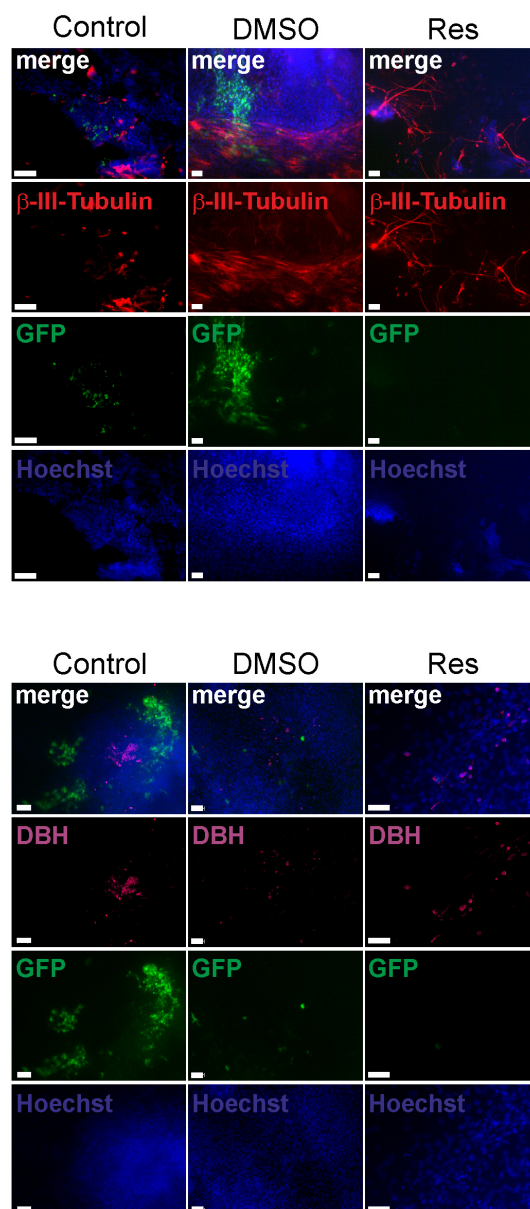


Figure 3.15: Immunohistochemical staining with anti- β -III-tubulin and anti-DBH antibodies

Immunolocalization of (top) neuronal marker β -III-Tubulin (red) and (bottom) catecholamine synthesis enzyme dopamine- β -hydroxylase (DBH; violet) in day 11 EBs: eGFP positive cardiomyocytes (green), Hoechst 33342 stained nuclei (blue). Top row represents overlay pictures. Scale bars: 50 μ m. Published in [Lehmann, Nguemo et al. 2013].

3.1.11 Functional expression of the adrenergic and muscarinic system

For functional analysis, contracting eGFP positive EBs were collected to perform extracellular recordings of field potentials (FPs) using microelectrode arrays (MEAs). Reserpine itself already confers a negative chronotropic effect when applied on CMs, because of its catecholamine depleting action and consequent lack of β_1 -AR stimulation. Therefore, the cell culture conditions applied to generate the EBs we used for functional analysis

contained reserpine only until day 6 for two reasons: 1. To slightly increase the number of beating clusters, 2. To avoid the direct effects of reserpine on CMs and their beating rates enabling us to analyze developmental changes in their beating properties. Whether the ‘until day6’ protocol led to decreased cardiac differentiation comparable to the ‘until d14’ protocol was verified by flowcytometry quantification of eGFP positive CMs (Fig. 3.5). We found that the ‘until day6’ protocol yielded slightly increased CM numbers compared to the ‘until d14’ protocol. Moreover, we observed moderately more contracting EBs. Yet, the ‘until day6’ protocol obviously still strongly inhibits cardiac differentiation compared to the untreated protocol (see Fig. 3.5; ‘until d6’). Therefore, we were able to derive sufficient numbers of contracting EBs for functional analysis using the ‘until day6’ protocol.

The β -adrenergic and muscarinic systems are crucial for heart function *in vivo*. Investigating whether both systems are functionally active *in vitro*, the respective specific receptor agonists, isoprenaline (1 μ M ISO) and carbachol (1 μ M CCH) were applied. We analyzed their effect on beating frequencies of untreated and reserpine-treated day 15-16 EBs (Fig. 3.16). An EB adhesively grown on a MEA culture chamber for two days and recorded FP traces of all 60 electrodes are depicted in Fig. 3.16A. Fig. 3.16B shows 10 sec FP traces (on top) and dot plots of the beating frequencies of representative 60 sec intervals (bottom) during the course of the experiment. Each dot represents a calculated frequency derived from values of inter-spike intervals (ISIs). Only rhythmically beating EBs were considered for analysis (n=4 for each group from 3 independent differentiations). Drugs were co-applied as follows: 1) baseline: no drug (3 min), 2) ISO (1 μ M; 6 min), 3) CCH (1 μ M; 6 min), 4) washout with repeated medium changes to confirm drug effects through frequency recovery effect.

EBs averaged beating frequencies during the conditions 1-4 of: 3.89 ± 0.75 Hz, 5.67 ± 1.06 Hz, 4.47 ± 1.14 Hz, and 5.13 ± 1.11 Hz. In comparison, reserpine-treated EBs averaged frequencies of 2.23 ± 0.34 Hz, 2.87 ± 0.36 Hz, 2.58 ± 0.41 Hz, and 2.62 ± 0.38 Hz (Fig. 3.16C). Altogether, reserpine-treated EBs showed lower beating frequencies than control EBs at baseline conditions, adding to the reserpine-induced inhibitory effect on cardiac differentiation [Banach, Halbach et al. 2003, Kuzmenkin, Liang et al. 2009, Pfannkuche, Liang et al. 2009]. Statistical analysis further showed that only in control EBs (and not in reserpine EBs) ISO treatment led to a significant positive chronotropic effect (Fig. 3.16 C+D, $\times p < 0.05$). This observation suggested a weaker responsiveness of reserpine-treated EBs towards β -adrenergic stimulation. Finding that under ISO conditions absolute frequency values were significantly different between both groups further added to the suggestion of

weaker responsiveness (Fig. 3.16C, * $p < 0.05$). Nevertheless, this significant difference between the two groups disappeared when values were normalized (Fig. 3.16D).

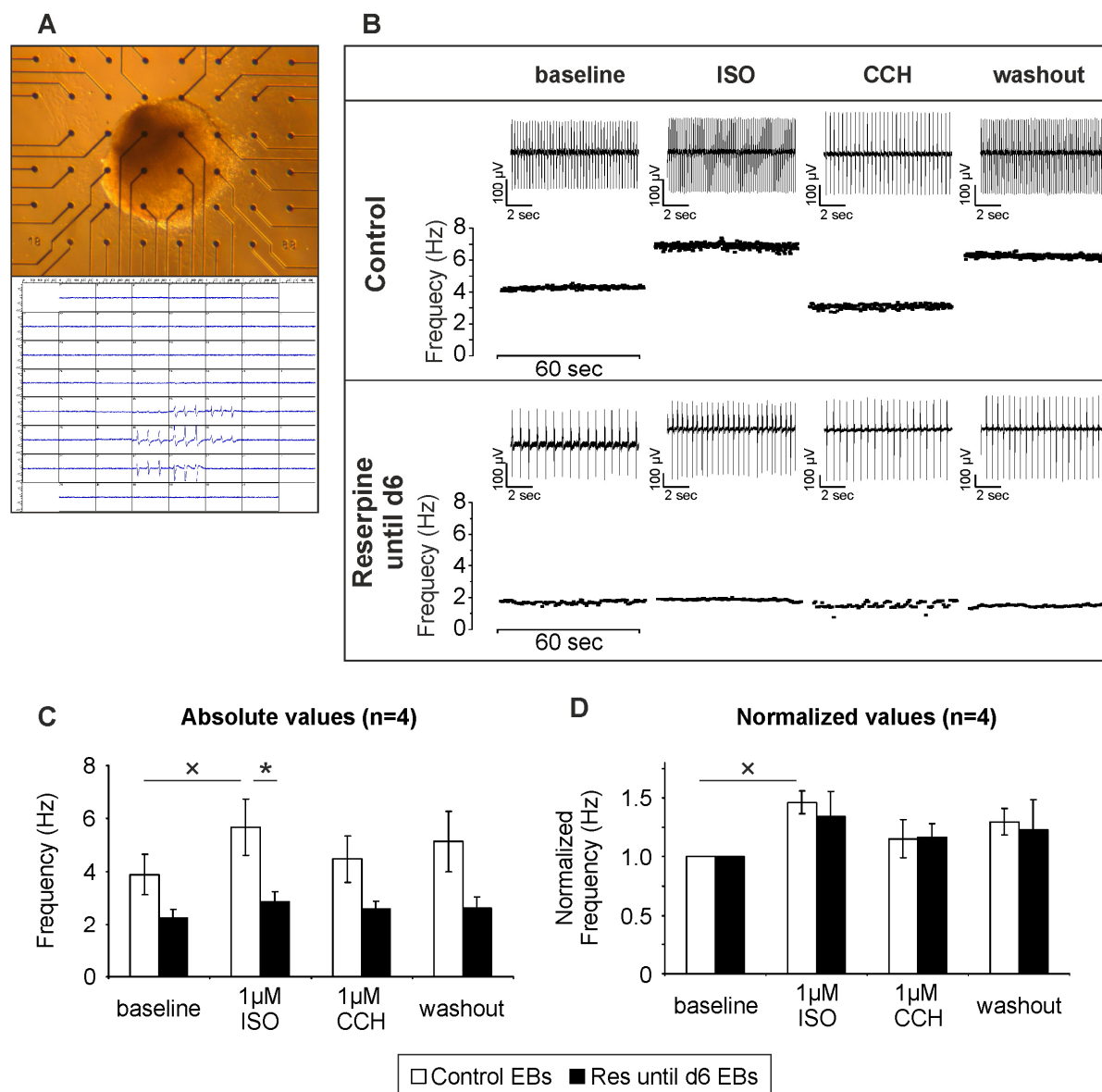


Figure 3.16: Comparison of β -adrenergic and muscarinic modulation of beating rate in control and reserpine-treated ES cell-derived cardiomyocytes

(A) Spontaneously contracting EB plated on MEA chamber for two days. (B) Representative beating frequencies demonstrating effects of β -adrenergic agonist isoprenaline (ISO, 1 μ M) and muscarinic agonist carbachol (CCH, 1 μ M) on cardiac clusters generated under control (top panel) and reserpine-treated (bottom panel) conditions. Original FP traces (10 sec) of each indicated condition are showcased (on top of each plot). (C+D) Statistical analysis of absolute and normalized FP frequencies from MEA measurements (n=4). (* $p < 0.05$: significant difference between baseline and 1 μ M ISO in ctrl EBs; * $p < 0.05$: significant difference between ctrl and reserpine-treated EB under ISO). Published in [Lehmann, Nguemo et al. 2013].

3.1.12 Prove of reserpine's catecholamine depleting action

Even though the exact mechanism of reserpine action is not fully understood yet, it has been established that reserpine is a potent drug inhibiting vesicular transport of catecholamines by the vesicular monoamine transporter (VMAT) leading to a depletion of catecholamine stores and at the same time preventing re-uptake of catecholamines [Carlsson, Lindqvist et al. 1957, Bezard, Imbert et al. 1998, Bezard and Przedborski 2011]. Extracellular and intracellular catecholamines are quickly degraded by the action of the enzymes MAO and COMT. Since reserpine inhibits vesicular transport and, thus, synthesis of NE and EPI as well as secretion of the catecholamines DA, NE and EPI, it leaves no extracellular catecholamines for paracrine action (reviewed in [Eisenhofer, Kopin et al. 2004]).

To investigate the gradual depletion of catecholamines and the subsequent negative chronotropic effect on the beating rate, we performed extracellular recordings of FPs with MEAs on untreated day 11-12 beating clusters in EBs. Two days prior to measurements EBs were plated and medium was renewed after the first 24 hrs. Fig. 3.17 depicts representative FP measurements. Baseline beating was recorded for 3 min (2.5 Hz – 4 Hz) before reserpine (10 μ M) was added. EBs were kept in the presence of reserpine until the maximum negative chronotropic effect was reached or until a complete halt of contraction was observed. We never observed a complete stop of beating within the first 8 min, while beating frequencies were already clearly reduced in all EBs tested. Of all EBs (n=16), 7 stopped beating, while 9 showed significant negative chronotropy (1 Hz or below) until 30 min after reserpine application. 5 EBs showed arrhythmia. Co-applying adrenergic receptor agonists ISO (1 μ M; Fig. 3.17A), EPI (100 nM; Fig. 3.17B) and NE (100 nM; Fig. 3.17C) quickly recovered the beating frequencies in 13 of the EBs. Washout proved that effects were drug induced. All results are summarized in Table 1.

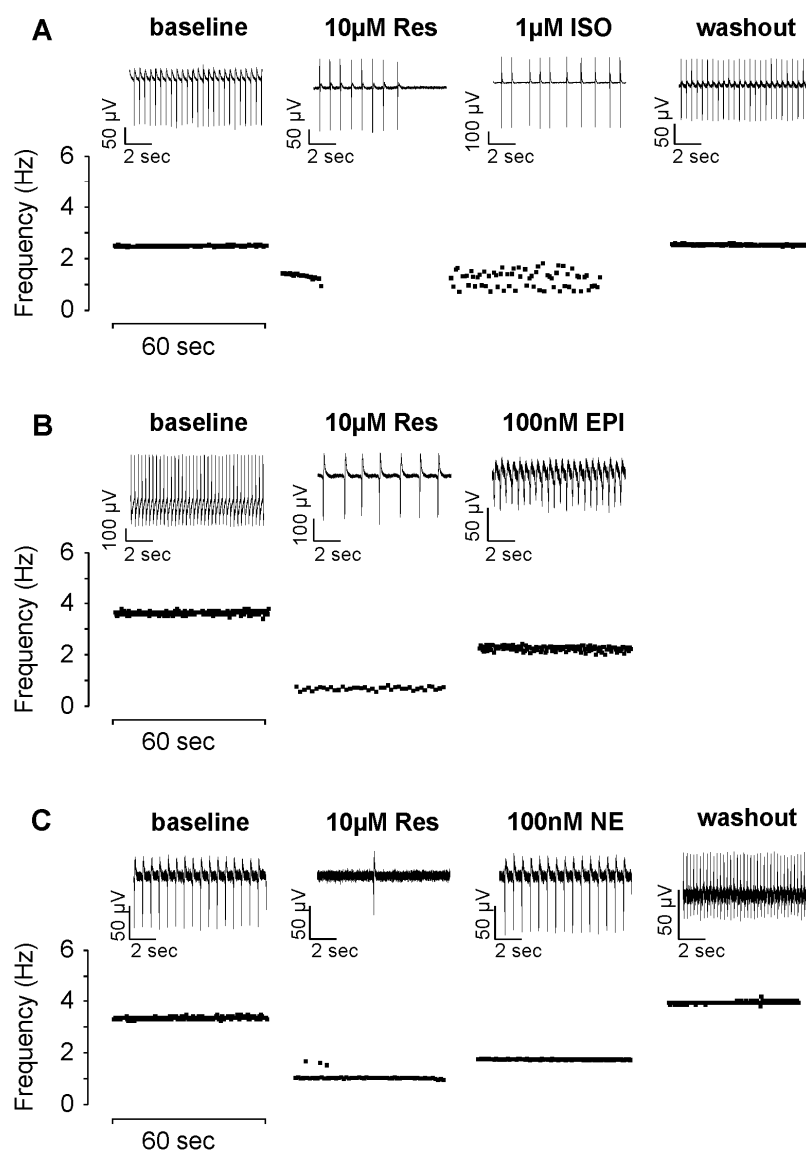


Figure 3.17: Effect of catecholamines on spontaneously beating clusters of EBs after acute application of reserpine

Representative FP frequencies of day 11 to 12 beating cardiac clusters under the acute presence of reserpine (10 μ M) and after co-application of adrenergic receptor agonists (A) ISO (1 μ M), (B) epinephrine (EPI, 100 nM) and (C) norepinephrine (NE, 100 nM). EBs were incubated with reserpine until maximum negative chronotropic effects were observed (between 8-30 min) before application of the adrenergic agonists. Depicted are frequency-time plots of representative 60 sec intervals during the experiment. 10 sec FP traces are showcased on top of each plot. Note: After rescue with epinephrine no washout could be recorded. Full summary of all EBs measured is shown in Table 1. Published in [Lehmann, Nguemo et al. 2013].

Table 3.1: Summary of reserpine application experiments and adrenergic receptor (AR) agonist stimulated recovery (from Fig. 3.17A-C)

| | N= | Reserpine | | | | AR Agonist | | | Washout | | |
|-----------|----|-------------------------|------|-----------|------------|------------|----|-----------|---------|----|-----------|
| | | Negative chronotropy | Stop | No effect | Arrhythmia | Yes | No | Undefined | Yes | No | Undefined |
| Res + ISO | 7 | 4 | 3 | 0 | 3 | 5 | 1 | 1 | 5 | 2 | 0 |
| Res + EPI | 5 | 3 | 2 | 0 | 2 | 5 | 0 | 0 | 2 | 3 | 0 |
| Res + NE | 4 | 2 | 2 | 0 | 0 | 3 | 1 | 0 | 2 | 2 | 0 |
| Overview | 16 | 9 | 7 | 0 | 5 | 13 | 2 | 1 | 12 | 7 | 0 |

Shown are the numbers of control EBs and their responses during: 1. Reserpine: Acute Reserpine application (i.e. EBs responding by negative chronotropy, stop of beating, no effect and arrhythmia). 2. AR Agonist: AR Agonist stimulation following reserpine application (EBs which reacted with positive (yes), neutral (no) or very weak (undefined) chronotropy). 3. Washout: After repeated medium changes (showing recovery toward baseline beating rate). Published in [Lehmann, Nguemo et al. 2013].

3.1.13 Isoproterenol (ISO) partially rescues the long-term effects of reserpine

The results of the “short-term” rescue experiments (Fig. 3.17) showed that reserpine-induced catecholamine depletion and resulting effects on cardiac functionality can be reversed by application of endogenous adrenergic agonists (ISO, EPI and NE). Yet, it remains to be investigated whether adrenergic agonists are able to rescue the long-term effects of reserpine on ESCM differentiation.

We developed cell culture conditions to perform a “long-term” rescue experiment. One of the major limiting factors for long-term catecholamine-containing culture conditions is the fact that catecholamines may induce apoptosis in cardiac cells by activation of the β -adrenergic receptors after only 24 hrs of incubation [Communal, Singh et al. 1998, Communal, Singh et al. 1999]. Moreover, due to their susceptibility to oxidation catecholamines are very unstable molecules. For these reasons long-term rescue experiments were performed using ISO as β -adrenergic agonist instead of the natural agonists EPI or NE. To avoid apoptotic cell death, we added ISO and also reserpine only until day 6. Whereas reserpine was applied at day 0 and refreshed at day 2, ISO, after application on day 0, had to be refreshed every 24 hrs until day 6 to keep ISO availability in the medium constant during that period.

Fig. 3.18 shows phase contrast/fluorescence overlay pictures. For evaluation of the long-term rescue effect of ISO (1 μ M) on CM development the occurrence of eGFP positive cells in day 10, day 14 and day 14 purified EBs was tracked. Untreated control EBs represented a normal differentiation with a normal yield of eGFP positive CMs (Fig. 3.18, left

column). Day 14 purified control EBs mainly consisted of eGFP positive CMs. Treating differentiating ES cells with ISO (1 μ M) during the first six days of culture did at least not reduce the eGFP positive CM yield after 10 days (data not shown). Reserpine treatment during the same period of differentiation expectedly decreased CM yield and cluster size in every setting (d10, d14, d14+puro, Fig. 3.18, middle column). Combined application of reserpine (10 μ M) and ISO (1 μ M) induced a distinct reversal of the strongly reduced CM yield in reserpine-only treated EBs (Fig. 3.18, right column). Comparing puromycin purified CM clusters at day 14, the rescue effect became most obvious (middle and right bottom; green arrows indicate CM clusters). ISO induced rescue led to an estimated 2- to 3-fold increase of CM containing EBs as compared to only reserpine treatment. Taken together, the results suggested that the reserpine effect could at least partially be reversed using the β -adrenergic agonist ISO and, thus, it can be claimed that catecholamines play an essential role in cardiac development of ESCs. The result may suggest that the effect is, at least in part, transduced by the β -adrenergic receptor system and its downstream effectors.

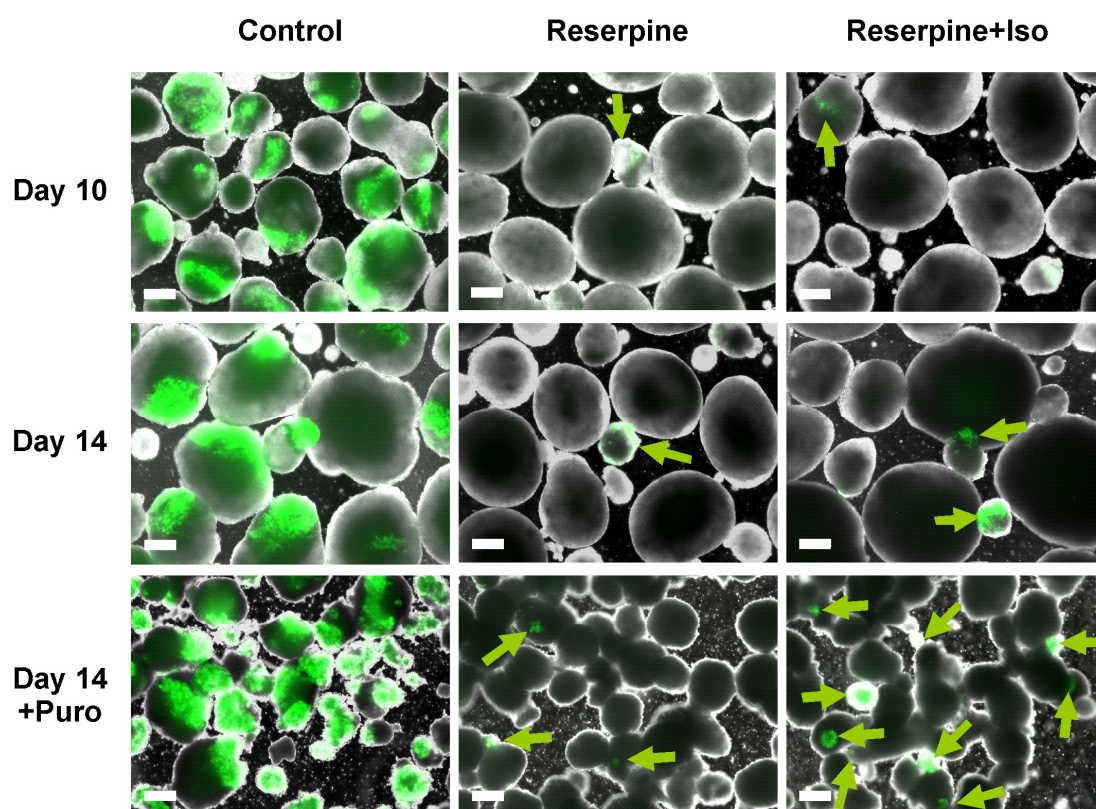


Figure 3.18: Long-term rescue experiment with ISO

EBs were cultured in the presence of reserpine and combined presence of reserpine and β -adrenergic agonist ISO. Fluorescence pictures depict eGFP positive CM clusters (green) at different stages of differentiation and after purification of EBs with puromycin (bottom row). Green arrows indicate small eGFP positive clusters. Scale bars: 200 μ m.

Reserpine applied during ES cell development induced two obvious changes of differentiation: 1. reduced CM differentiation, and 2. increased neuronal differentiation (Fig. 3.14+3.15). Whether the latter effect can also be reversed by ISO application was further investigated as depicted in Fig. 3.19. Untreated control, reserpine until day 6 and ISO + reserpine until day 6 treated EBs were plated on culture dishes at day 7 and were allowed to attach before phase contrast pictures were taken at day 10. Comparing control to reserpine-treated EBs clearly showed neuronal cells only in the reserpine group. Combined application of reserpine and ISO yielded comparable numbers of neuronal cells as in only reserpine-treated EBs. Thus, the neuronal inducing reserpine effect did not seem to be mediated by the paracrine β -adrenergic receptor signaling pathway.

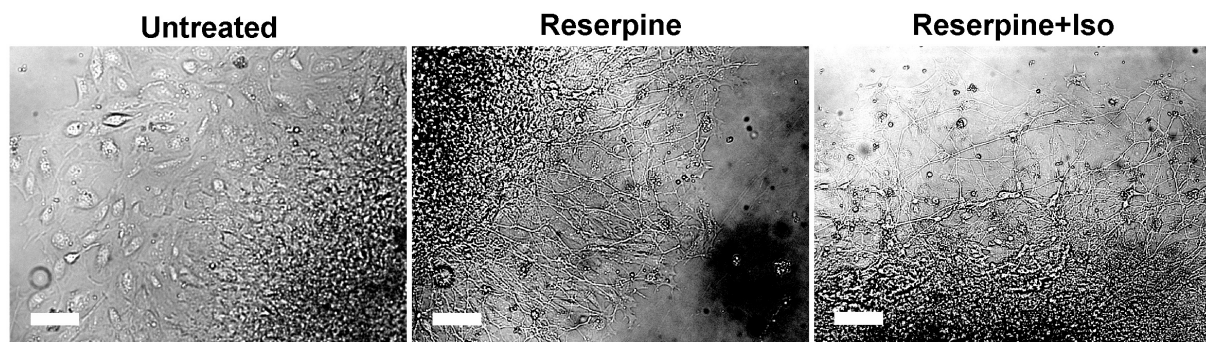


Figure 3.19: Isoprenaline long-term rescue effect on neuronal development

The same EBs as in Fig. 3.18 were plated on culture dishes to track appearance of neuronal cells at day 10. In both, reserpine only (Res) and Res+Iso-treated EBs, neuronal cells in outgrowths of plated EBs were observed. Scale bars: 100 μ m.

3.1.14 α - and β -AR antagonists mimic the reserpine effect

Catecholamines specifically target all α - and β -AR subtypes (α_{1A} , α_{1B} , α_{1D} , α_{2A} , α_{2B} , α_{2C} , β_1 , β_2 , β_3). As the sqRT-PCR results (Fig. 3.13) showed, reserpine application alters the expression of most α - and β -AR subtypes and the reserpine effects are, therefore, certainly not limited to β -ARs and their downstream effectors. If that had held true, the ISO rescue experiment (paragraph 3.1.13) would have shown complete recovery when ISO and reserpine were co-applied. To investigate whether the α - or β -AR system is responsible for cardiomyogenesis, we established differentiation conditions containing the α -AR specific antagonist phentolamine and the β -AR specific antagonist propranolol. This experiment further helps to distinguish between catecholamine-induced AR-dependent effects and possible unspecific reserpine actions on cardiac differentiation.

In Fig. 3.20 the results of the antagonisation experiments are depicted as phasecontrast/fluorescence overlay pictures at days 8-14. Control EBs showed the normal yield of eGFP expressing CMs starting on day 8. The reserpine-treated group was expectedly strongly reduced in their number of CMs. In the groups treated with either 10 μ M phentolamine or 5 μ M propranolol, numbers of CMs were slightly decreased already at day 8. Phentolamine had a stronger negative effect on cardiomyogenesis than propranolol. Co-application of phentolamine and propranolol led to even stronger inhibition of cardiomyogenesis, mimicking the effect of reserpine. The co-application led to delayed appearance of eGFP positive CMs. Starting from day 10 cardiac clusters could be observed, but were reduced in size and number as compared to control EBs. Nevertheless, EB size and shape of all groups was comparable suggesting normal growth and proliferation.

The bottom panel of Fig. 3.20 shows further control experiments. Doubling the concentration of propranolol shows that the negative effect on cardiomyogenesis was concentration-dependent. Furthermore, doubling phentolamine concentration inhibited ES cell growth and proliferation. Prolonged application of the drugs until day 10 also led to reduced cardiomyogenesis, while EB growth was not changed. Co-application of double concentrations of both drugs expectedly also led to significant reduction in EB growth which was most likely due to phentolamine action. Thus, α -ARs affect stem cell growth and proliferation or their viability. However, in conclusion these experiments show that α - as well as β -ARs are critically involved in cardiomyogenesis.

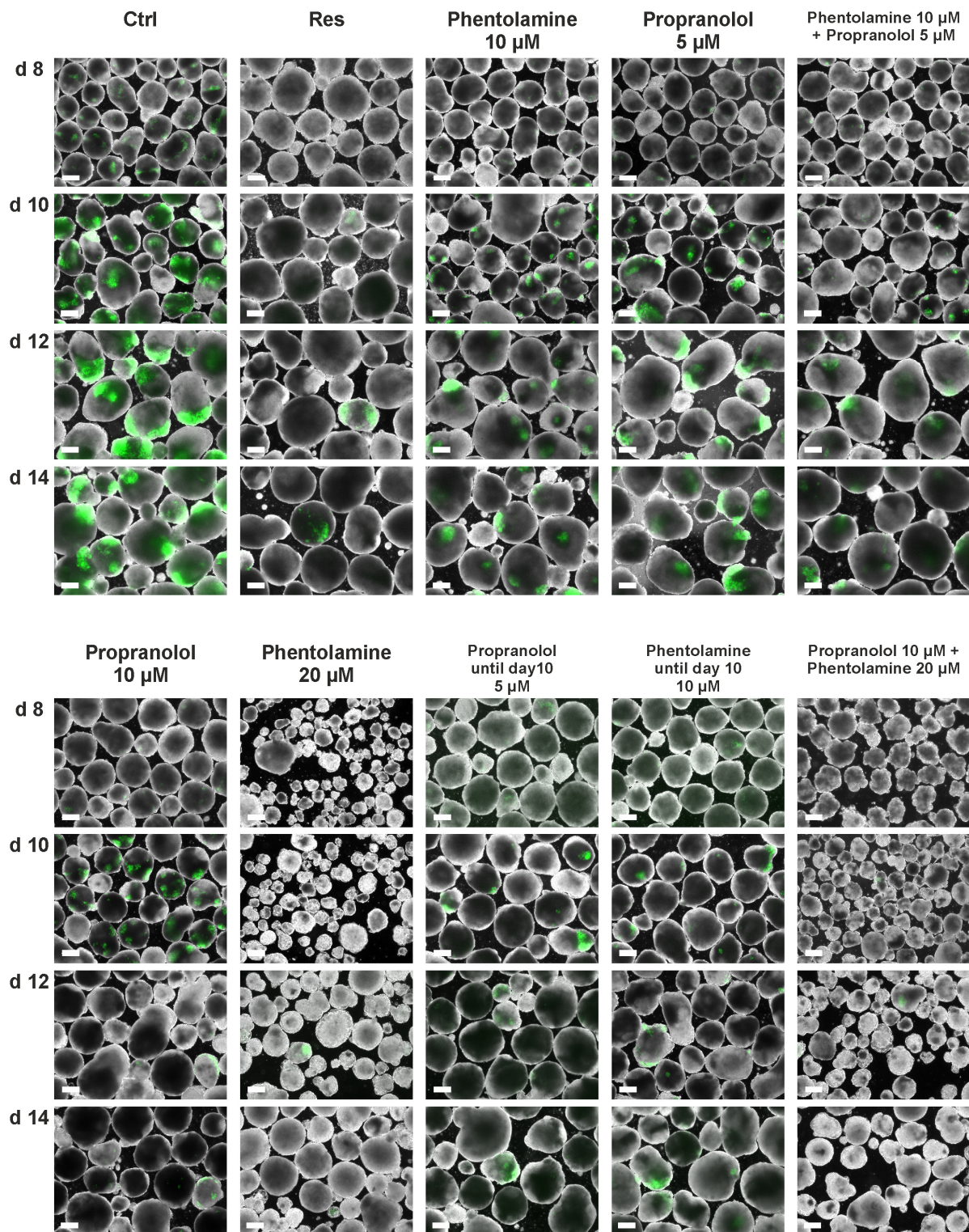


Figure 3.20: Blocking of α - and β -ARs mimics the reserpine-induced effect on cardiomyogenesis

Top: Fluorescence pictures of EBs treated with the unspecific α - and β -blockers phentolamine and propranolol and the combination of both showing the respective expression of eGFP positive CMs on days 8 to 14 of differentiation. Bottom: Additional control experiments. For details see text (Scale bars: 200 μm). Published in [Lehmann, Nguemo et al. 2013].

3.2 MEA-based QT-screen using pluripotent stem cell derived CMs

Development of drugs is cost intensive. Several drugs had to be withdrawn from the market even after implementation into clinical settings and recommendations, because they were found to cause severe and sometimes even fatal cardio-active side effects.

After establishment of the MEA and ES cell system as valuable drug-screening tool, it was approached to screen known pharmaceutical compounds for those unwanted side effects. Such a system would not only help to reduce costs, but also to largely reduce the need for laboratory animals. Therefore, we sought to use the advantages of the MEA technique in combination with rhesus monkey and human ES cell- as well as iPS cell-derived CMs. Using human ES and iPS-derived cardiomyocytes (iPSCMs) eliminates the risk of false conclusions due to species differences compared to rhesus monkey stem cell-derived CMS (rESCMs).

3.2.1 *Rhesus monkey cell culture*

As described in paragraph 2.1.3, rESCs were propagated in the presence of bFGF twice per week to maintain them in a pluripotent state and to prevent spontaneous differentiation. The undifferentiated state of pluripotent ESCs is characterized by strong expression levels of the enzyme alkaline phosphatase (AP) [Pease, Braghetta et al. 1990]. To guarantee identical pluripotent states of the rESC colonies used for propagation as well as differentiations we performed AP stainings as shown in Fig. 3.21. Both, R366.4 and MF12 rESCs stained positively for AP and were therefore shown to present a pluripotent state.

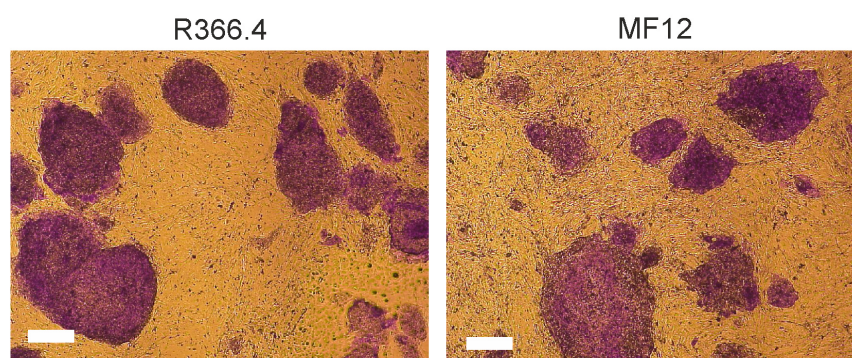


Figure 3.21: Alkaline phosphatase staining of R366.4 and MF12 rESCs

Alkaline phosphatase staining (violet) of rESC lines R366.4 and MF12 showing their pluripotent state as used for propagation on ICR-feeder layers and used for differentiation (scale bars: 200 μm).

3.2.2 *rESC differentiation using mass culture and END2 protocols*

Initially a cardiac differentiation protocol for R366.4 rESCs was published by C. Schwanke et al. in 2006 [Schwanke, Wunderlich et al. 2006]. Differentiation of MF12 rESCs into CMs (rESCMS) was known to follow the same protocol. However, the published protocol only yielded insufficient numbers of CMs and beating clusters for drug-screening purposes. Therefore alternative differentiation protocols were tested. In a first approach we applied a modified mass culture protocol with horizontal shaking as used for mESCM differentiation. Secondly, we approached to improve the CM yield by differentiating the cells on END2 feeder layers as commonly used for hESCM differentiations. Fig. 3.22 shows microscopy pictures of both approaches. Due to the mechanical stress caused by the constant shaking, the mass culture protocol did not result in any improvement, with large numbers of dead cells and very little numbers of EBs of sufficient size. Still, some EBs that were plated grew to normal size. Nevertheless, EBs did not start contracting. Also application of an END2 protocol did not improve the outcome. From human ESCM END2 differentiation we know that derived EBs are rather small, but rhesus EBs were even smaller in comparison and no contractions could be observed.

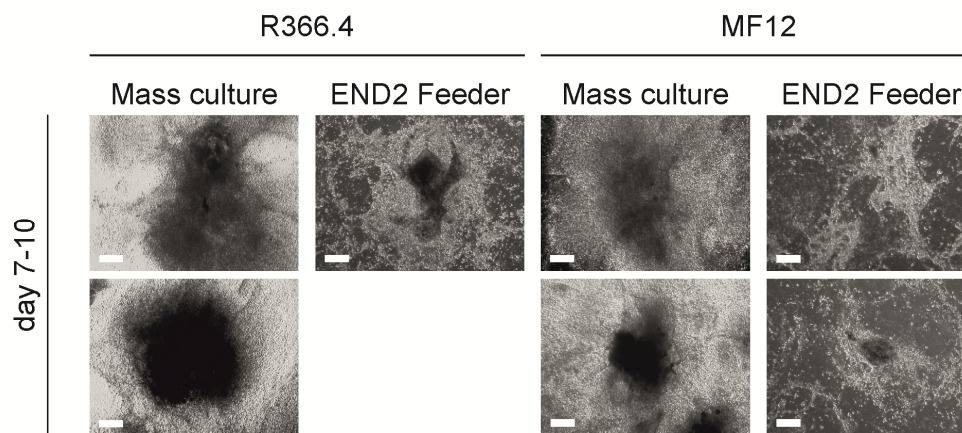


Figure 3.22: Optimization of rESCM differentiation by mass culture and END2 differentiation protocols

Representative brightfield microscopy pictures of plated EBs derived from R366.4 (left) and MF12 (right) rESC differentiation using a mass culture protocol and an END2 feeder protocol, respectively (scale bars 200 μ M).

3.2.3 *rESC differentiation applying activinA/BMP4*

Several groups showed enhancement of murine as well as human ES cell cardiac differentiation by the addition of the growth factors activinA and bone morphogenic protein 4 (BMP4) [Laflamme, Chen et al. 2007, Nostro, Cheng et al. 2008, Yang, Soonpaa et al. 2008, Kattman, Witty et al. 2011, Xu, Police et al. 2011, Sa and McCloskey 2012]. It became

evident that each cell line still required individual adaption of the concentrations as well as the stages and durations of application of both growth factors. Fig. 3.23 depicts brightfield microscopy observations of R366.4 and MF12 rESC differentiations with and without activinA and BMP4. We found that especially the R366.4 line could efficiently be directed into the cardiac lineage by activinA and BMP4, yielding increased numbers of beating clusters compared to the protocol published by Schwanke and co-workers. Also MF12 rESC differentiation into CMs was enhanced by growth factor application. Still, compared to the MF12 rESCMs, R366.4 contracting rESCMs could be observed as early as day 10-11. Thus, we decided to perform MEA QT-screen measurements with R366.4 rESCMs.

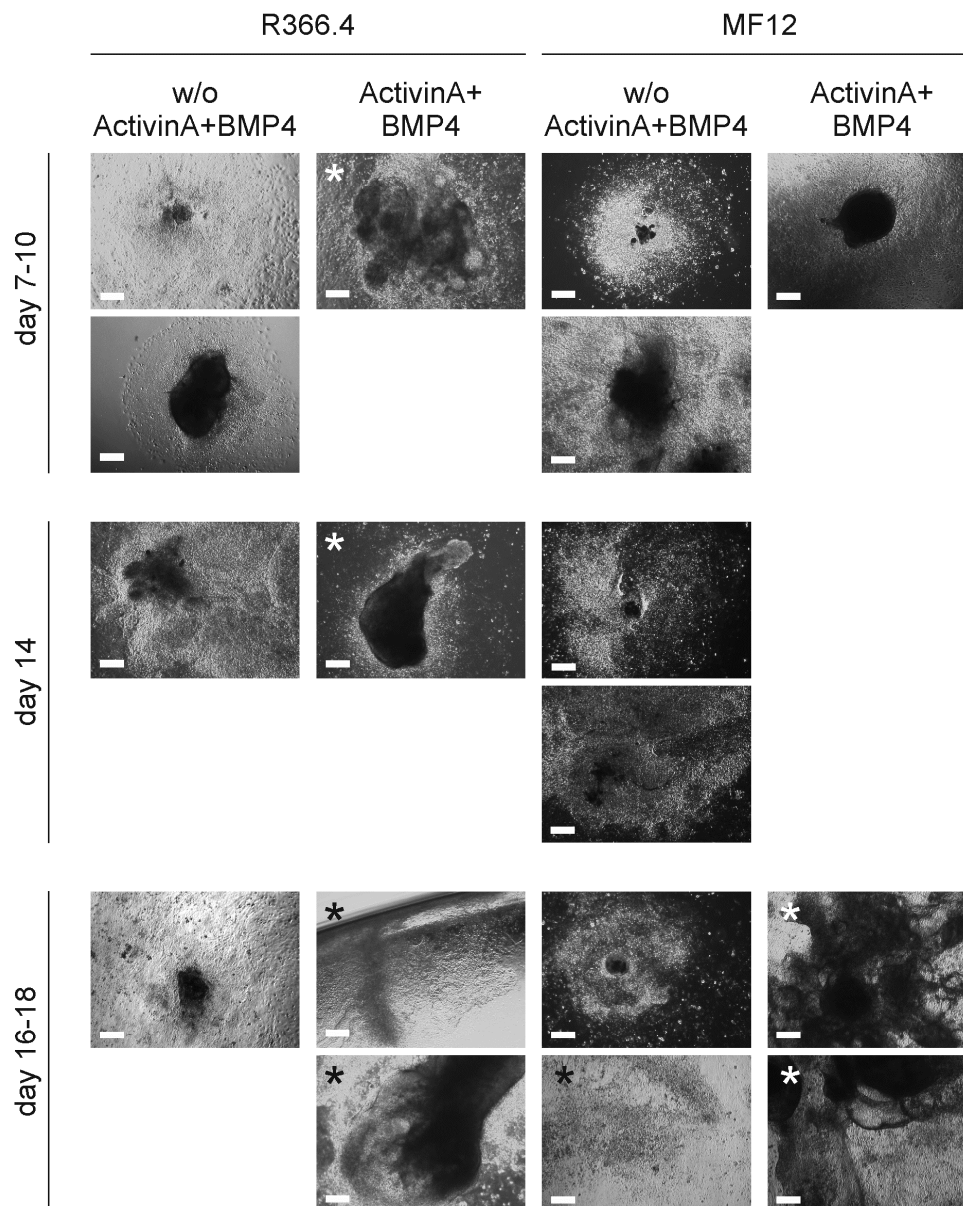


Figure 3.23: Optimization of rESCM differentiation protocols by activinA and BMP4

Representative pictures of R366.4 (left) and MF12 (right) EBs during rESC differentiation using the protocol published by C. Schwanke et al. (w/o ActivinA+BMP4; [Schwanke, Wunderlich et al. 2006]) and the same protocol modified by stage-specific addition of activinA and BMP4 (ActivinA+BMP4). EBs were plated on 1% gelatine-coated culture dishes on day 7 of differentiation and pictures were taken on different days as stated. Asterisks (*) indicate spontaneously contracting EBs (scale bars 200 μ M).

3.2.4 *Summary of the optimized differentiation*

Fig. 3.24 summarizes the optimization approach with activinA and BMP4 showing a scheme of the resulting rESCM activinA/BMP4 differentiation protocol the way it was used for subsequent MEA measurements. In brief, we combined the differentiation protocol of

Schwanke *et al.* [Schwanke, Wunderlich *et al.* 2006] with an incubation of rESCs with activinA for the first 24 hrs followed by addition of BMP4 until day 7. During this period EBs were cultivated in culture dishes coated with 1% agarose preventing adhesion to ensure proper EB formation. After day 7, EBs were collected and transferred to 0.1% gelatine-coated multi-well culture dishes and further cultivated for MEA measurements.

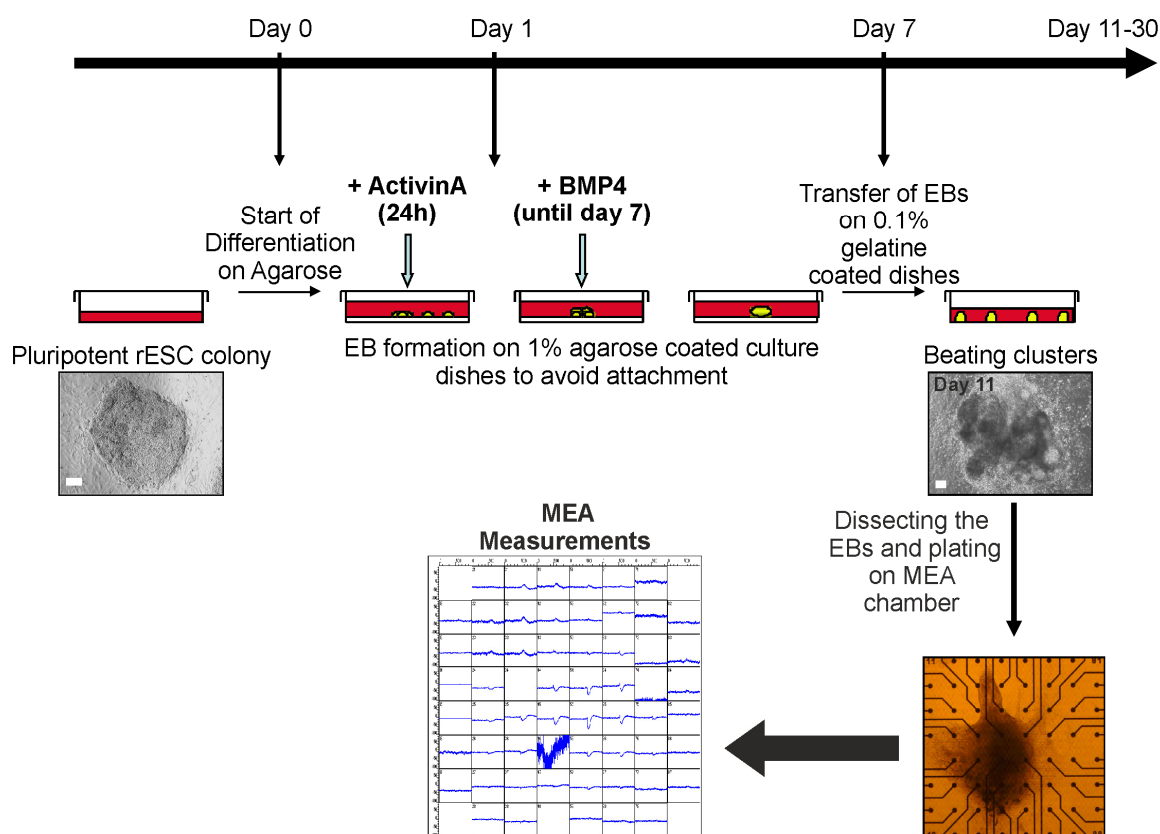


Figure 3.24: Scheme of the rESC cardiac differentiation protocol using growth factors activinA and BMP4 for MEA QT-screen

Scheme of the optimized rESC activinA/BMP4 differentiation protocol (scale bars: rESC colony, 100 μm ; beating cluster, 200 μm). Further shown is a R366.4 spontaneously contracting EB plated on a MEA chamber and a picture representative of the 8x8 grid of FP traces recorded from that EB by the recording software MCRack[®] (Multichannel Systems, Reutlingen, Germany).

3.2.5 Efficiency of the optimized differentiation

Fig. 3.25 shows the quantification of the efficiency of our differentiation protocol. The graph represents the number of contracting EBs appearing as a ratio of the total number of EBs derived from our protocol at different stages of the culture. The combined group is representative of all differentiations using the activinA/BMP4 protocol (as shown in Fig. 3.24). Between day 10 and 14 about 9% of the EBs started contracting, while between days 15-19 we yielded 5.9%. On days 20-24 another 5.4% EBs were observed that started

contracting relatively late after the initiation of differentiation. Altogether, we were able to reach about 20% differentiation efficiency using our protocol. Yet not fully understood, preliminary experiments using NEO-MEF feeders instead of ICR-feeders (as proposed by Schwanke *et al.*, 2006) for propagation of undifferentiated rESC colonies indicate a strong increase in the differentiation efficiency. Using NEO-feeders yielded over 40% efficiency of contracting EBs, compared to 4.1% between days 10-14 when rESCs were propagated on ICR-feeders. In both groups hardly any new contracting EBs appeared after day 24.

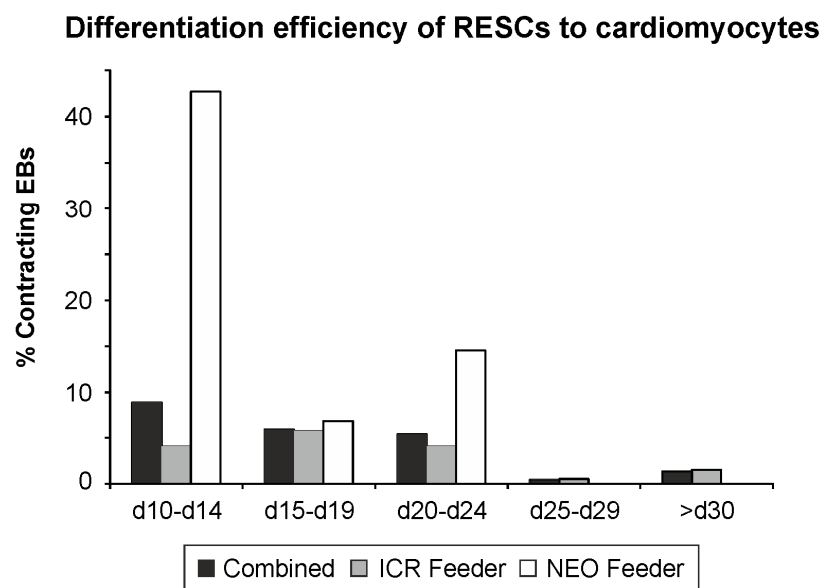


Figure 3.25: Efficiency of rESC differentiation into contracting EBs

The graph represents the ratio of contracting to total EBs derived from the activinA/BMP4 protocol between days 10 and 39 after initiation of differentiation in percent. Shown are the newly appearing contracting EBs in each phase during cultivation. It further shows preliminary results of the yield of contracting EBs depending on the feeder MEFs (ICR or NEO, respectively) that were used for rESC propagation.

3.2.6 *rESCMs express cardiac α Actinin*

In addition to the quantification of the differentiation efficiency, we performed immunohistochemical stainings of rESCM containing EBs with cardiac-specific anti- α Actinin antibodies. The result of fluorescence microscopic observations of a cryosliced rESC-derived EB is depicted in Fig. 3.26. It was found that CMs yielded using the activinA/BMP4 protocol stained positive for the cardiac marker α Actinin.

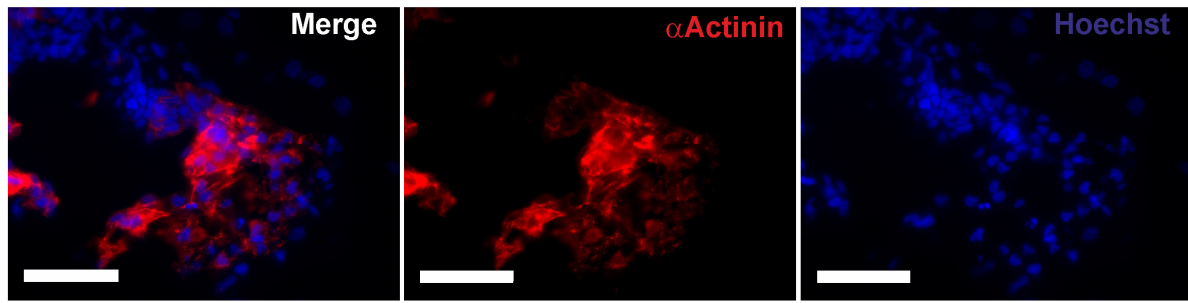


Figure 3.26: Anti- α Actinin immunohistochemical staining of an rESC-derived contracting EB

Representative fluorescence picture of a cryosliced day 15 R366.4 rESC-derived contracting EB. The slice was stained with a mouse-anti- α Actinin primary antibody (red) and Hoechst 33342 for nuclei staining (blue). Scale bars: 50 μ m.

3.2.7 *Negative FP_{Dur} /frequency (FP/f) correlation in hESCMs under physiologic conditions*

We know from human physiology that QT-time and RR-intervals are positively correlated, i.e. the longer the RR-interval the longer QT-time and vice versa. In turn this means that the higher the frequency the shorter the QT-interval (negative correlation), because the RR-interval is the multiplicative inverse of the frequency. Similarly, the action potential duration (APD) is negatively correlated with the action potential frequency. Therefore, we hypothesize that under physiological conditions also the FP duration (FP_{Dur}) must be negatively correlated with the frequency [Halbach, Egert et al. 2003, Halbach 2006].

To investigate FP_{Dur} /frequency (FP/f) correlations we first performed MEA measurements with hESCMs and iPSCMs at untreated conditions and further stimulated with the β -adrenergic agonist ISO, inducing a positive chronotropic effect. Because ISO mimics the natural sympathetic adrenergic stimulation of CMs, this stimulation can still be considered physiological. Resulting FP/f correlations should therefore provide a “normal” baseline for further experiments that investigate effects of drugs with QT-time and repolarization prolonging effects (e.g. E4031, Sotalol, etc.).

In Fig. 3.27 MEA recordings of day 30-35 H1 hESCMs treated with ISO are shown. Each panel depicts the same data set plotted under different aspects. And, each dot represents the value pairs of FP_{Dur} and frequency values averaged over a 60 sec interval under the stated conditions. Fig. 3.27A represents absolute FP/f values. Comparing all baseline (blue trapezoid) with ISO value pairs (pink, red, turquoise) shows that ISO application induced a shift of the value pairs to the top left section of the chart, thus, indicating a negative FP/f correlation. This negative correlation persisted within each single EB measurement (Fig. 3.27B). At baseline conditions beating frequency was between 1 to 1.5 Hz, while maximum

rates under ISO did not exceed 2.5 Hz, which was considered physiologic beating. However, using absolute values revealed an EB-to-EB variation typical for biological preparations. To circumvent the variation, FP/f values were normalized per EB toward their baseline value (untreated condition) as depicted in Fig. 3.27 C+D. Normalization made recordings from different EBs far more comparable and shows that a single drug affects different EBs in a relatively similar way in respect to their FP/f correlation. In this case FP/f correlations were negative to the almost same degree in each EB. Furthermore, when averaged, the FP/f values also showed negative correlation and further suggest that the correlation was almost linear within a physiological beating frequency range (~1 to 2.5 Hz). Taken together we show that, 1) FP_{Dur} and frequency are negatively correlated, and 2) Averaging of normalized FP/f value pairs represents the FP/f correlation of a population of EBs. Therefore, only averaged and normalized FP/f plots will be used for presentation of further data.

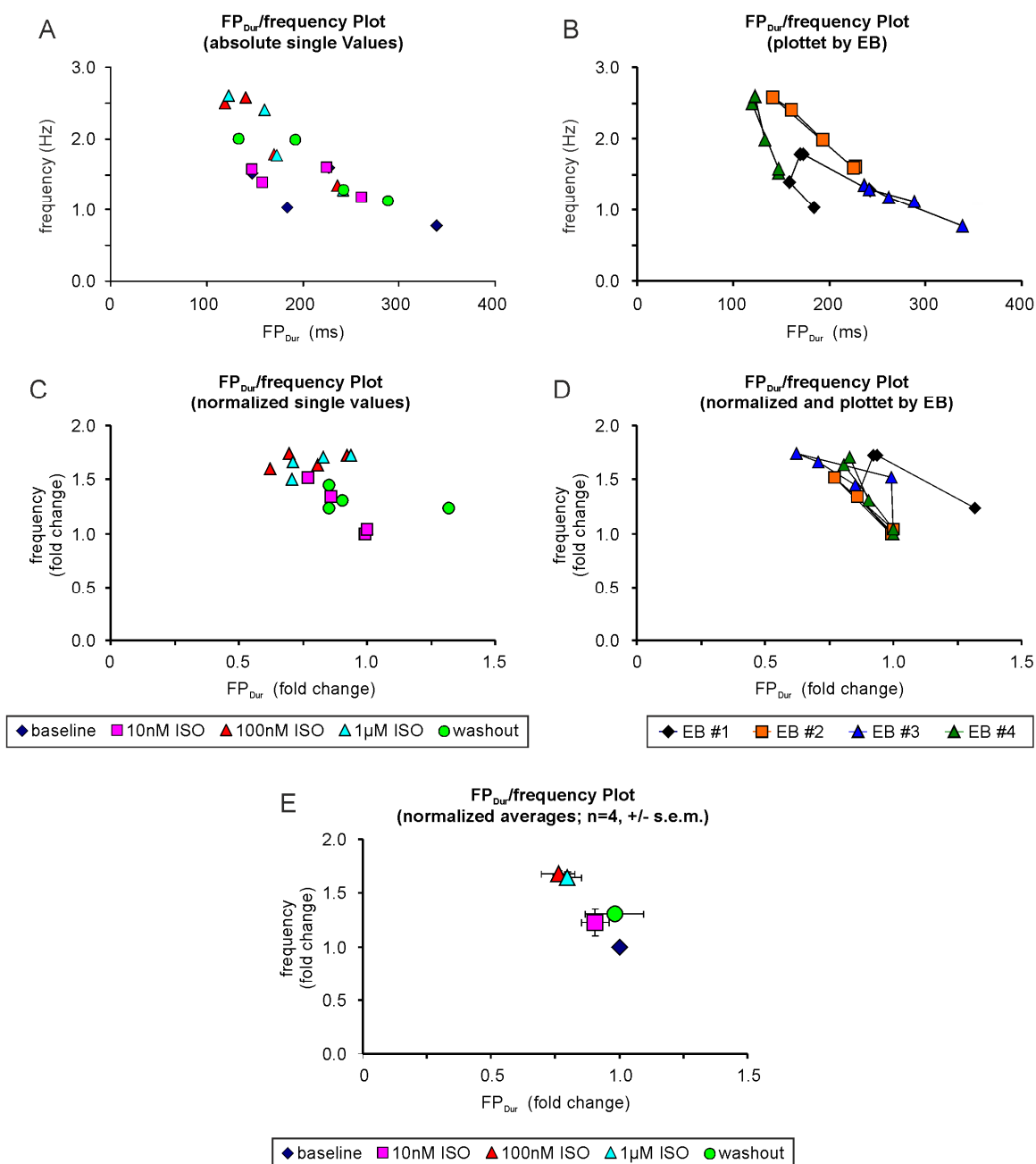


Figure 3.27: Negative FP/f correlation in H1 hESCMs under physiological positive chronotropic conditions

Day 30-35 H1 hESCMs were treated with different concentrations of β -adrenergic agonist ISO and analyzed by extracellular MEA recordings. Each dot represents the averaged value pairs of FP_{Dur} and frequency analysis of a representative 60 sec interval under the different conditions (baseline, ISO application, washout). All $FP_{Dur}/\text{frequency}$ plots represent the same data set, but different aspects: A+C: absolute and normalized single values sorted by treatment, respectively; B+D: absolute and normalized single values sorted by measurement, respectively; D: normalized and average values of all measurements. For details see text.

3.2.8 *Negative FP/f correlation in hiPSCMs under physiologic conditions*

The negative FP/f correlation was now shown in H1 hESCMs. However, to show that this negative correlation was not only a cell line- or cell type-specific phenomenon, but a general relationship, we performed MEA recordings to investigate the influence of the frequency on the FP_{Dur} in further pluripotent cell derived CMs. Fig. 3.28 shows the results of ISO application on FP/f correlations in NP0017, NP0014c5 and Royan hiPSCMs (cells were kindly provided by Dr. Dr. T. Saric and Dr. A. Fatima, University of Cologne, Institute of Neurophysiology). In accordance with the results of H1 hESCMs under the influence of ISO, also hiPSCMs showed negative FP/f correlations.

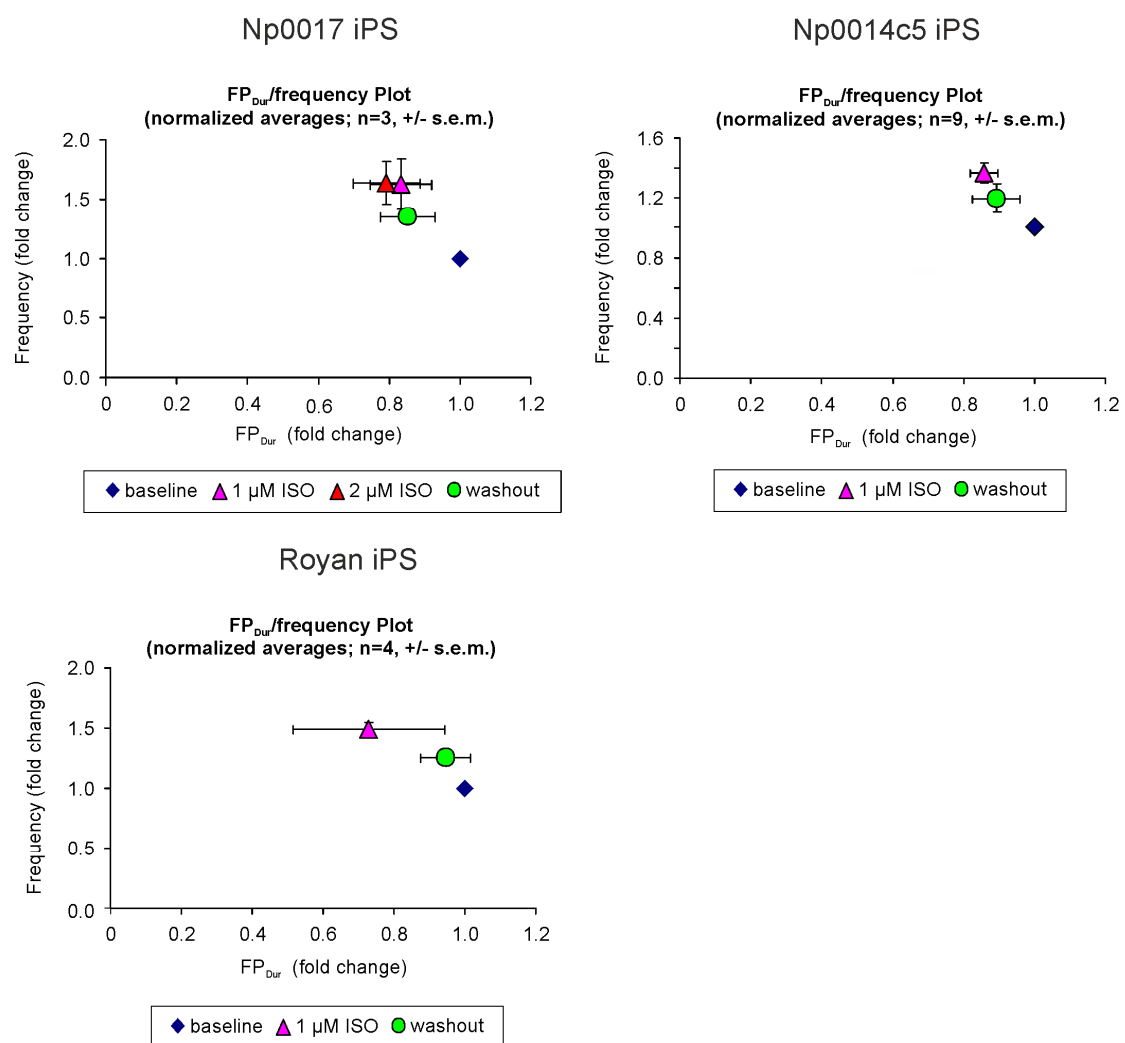


Figure 3.28: Negative FP/f-correlation in hiPSCMs under physiological positive chronotropic conditions FP_{Dur} /frequency plots representative of ISO treatment of NP0017, NP0014c5 and Royan d25-35 hiPSCMs.

3.2.9 Negative FP/f correlation during negative chronotropic stimulation

So far we showed by positive chronotropic stimulation that FP_{Dur} and frequency of EBs correlated negatively. However, it remained unclear whether the negative correlation persisted when EBs are stimulated in the opposite direction. Therefore, we used carbachol (CCH), a muscarinergic agonist, to induce a negative chronotropy in H1 hESCMs. Fig. 3.29 shows the FP_{Dur} /frequency plot of averaged and normalized values of MEA recordings during the application of increasing concentrations of CCH. The results showed that under the influence of 1 μ M and 10 μ M CCH, the frequency was decreased by ~40% while the FP_{Dur} increased by ~25%. Thus, the negative FP_{Dur} /frequency correlation persisted also after negative chronotropic stimulation.

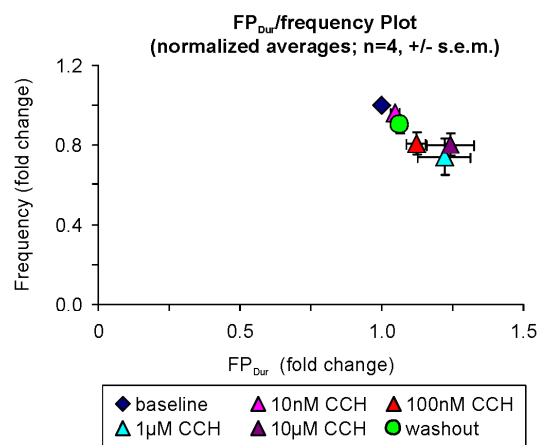


Figure 3.29: Negative FP/f correlation in hESCMs under physiologic positive chronotropic conditions FP_{Dur} /frequency plots representative of CCH treatment of H1 d25-35 hESCMs.

3.2.10 FP/f correlation during successive positive and negative chronotropic stimulations

It was further necessary to know if the negative FP_{Dur} /frequency correlation could be observed during consecutive positive and negative chronotropic stimulation. For that reason we treated H1 hESCMs first with ISO (positive chronotropic) and subsequently with the β -blocker Metoprolol (negative chronotropic). MEA analysis, shown in Fig. 3.30, again revealed the negative FP_{Dur} /frequency correlation and thus strongly indicates that FP_{Dur} and frequency are dependent on each other.

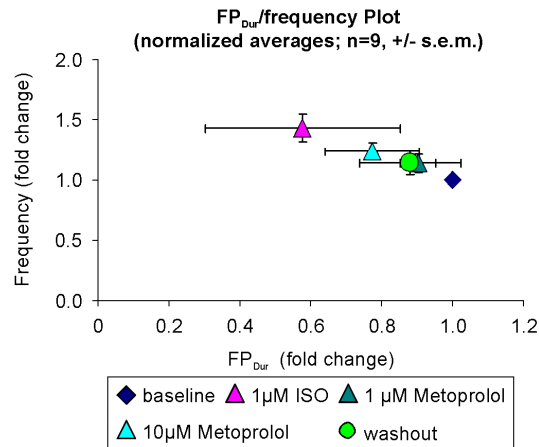


Figure 3.30: Negative FP/f correlation in hESCMs under physiologic positive and negative chronotropic conditions

FP_{Dur}/frequency plots representative of ISO and Metoprolol co-application in H1 d25-35 hESCMs.

3.2.11 Effects of class III antiarrhythmic drugs on FP/f correlations in hESCMs and rESCMs

According to our findings and publications by others [Reppel, Igelmund et al. 2007, Caspi, Itzhaki et al. 2009], we hypothesized that drugs such as class III (Vaughan Williams classification) antiarrhythmic agents (K⁺ channel blockers) should change the FP/f correlation. Since class III antiarrhythmic drugs increase AP and FP durations, we assumed a less negative or even positive FP/f correlation. To test this hypothesis, we recorded FPs of EBs during E4031 and sotalol treatment. Fig. 3.31 depicts the results of MEA measurements in H1 hESCMs and R366.4 rESCMs treated with increasing concentrations of both class III agents. Unlike during ISO treatment, FP_{Dur} increased during E4031 treatment even though the frequency increased. This was reflected by a positive FP/f correlation in H1 and R366.4. FP/f value pairs shifted to the top right of the diagram in a concentration-dependent manner (Fig. 3.31A+B). Also sotalol induced a positive FP/f correlation, even though the effect was rather weak in H1 (Fig. 3.31C+D). Furthermore, washout partially recovered this effect.

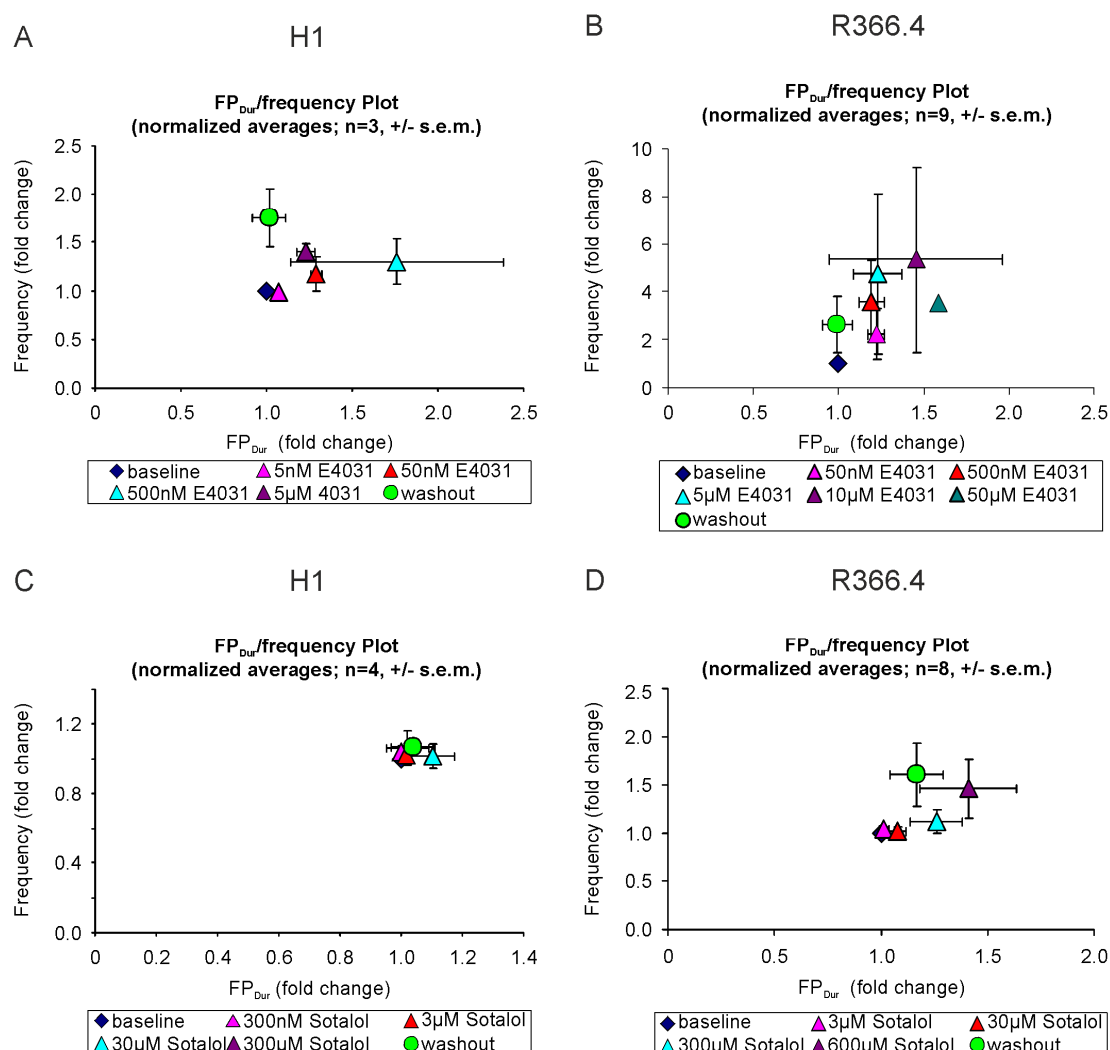


Figure 3.31: Positive FP/f correlation in hESCMs and rESCMs induced by class III antiarrhythmic drug application

FP_{Dur}/frequency plots representative of E4031 (A+B) and sotalol (C+D) application in H1 and R366.4 d25-35 ESCMs, respectively.

To demonstrate that positive FP/f correlations are generally detected in the presence of substances altering QT-time, we performed further series of measurements using different of such drugs. Accordingly, Fig. 3.32 shows the FP/f plots. Amiodarone belongs to the group of class III antiarrhythmics while quinidine actually is a class I (Na⁺-blocker) antiarrhythmic drug. However, quinidine also blocks K⁺-channels and, thus, exhibits QT-prolonging activity. Both drugs were applied with increasing concentrations in R366.4 rESCMs and H1 hESCMs, respectively (Fig. 3.32A+B). We found that amiodarone induced a positive FP/f correlation at concentrations above 25 μ M and that it could be washed out. Quinidine, however, only showed a mild effect on FP/f correlation. Lidocain, being a class Ib antiarrhythmic drug (Na⁺-blocker), is known to decrease the QT-time and AP_{Dur} by extending the depolarization on one

Results

side, but even more shortening the repolarization. To investigate if this effect can be detected with the help of FP/f correlations we performed yet another series of measurements. Lidocaine was the only antiarrhythmic compound where we could not confirm QT-time and AP_{Dur} observations, which suggests that further measurements are needed for final validation. Finally, we treated MF12 rESCMs with E4031 showing that this cell line also reacted with a positive FP/f correlation upon treatment with a class III antiarrhythmic agent (Fig. 3.32D).

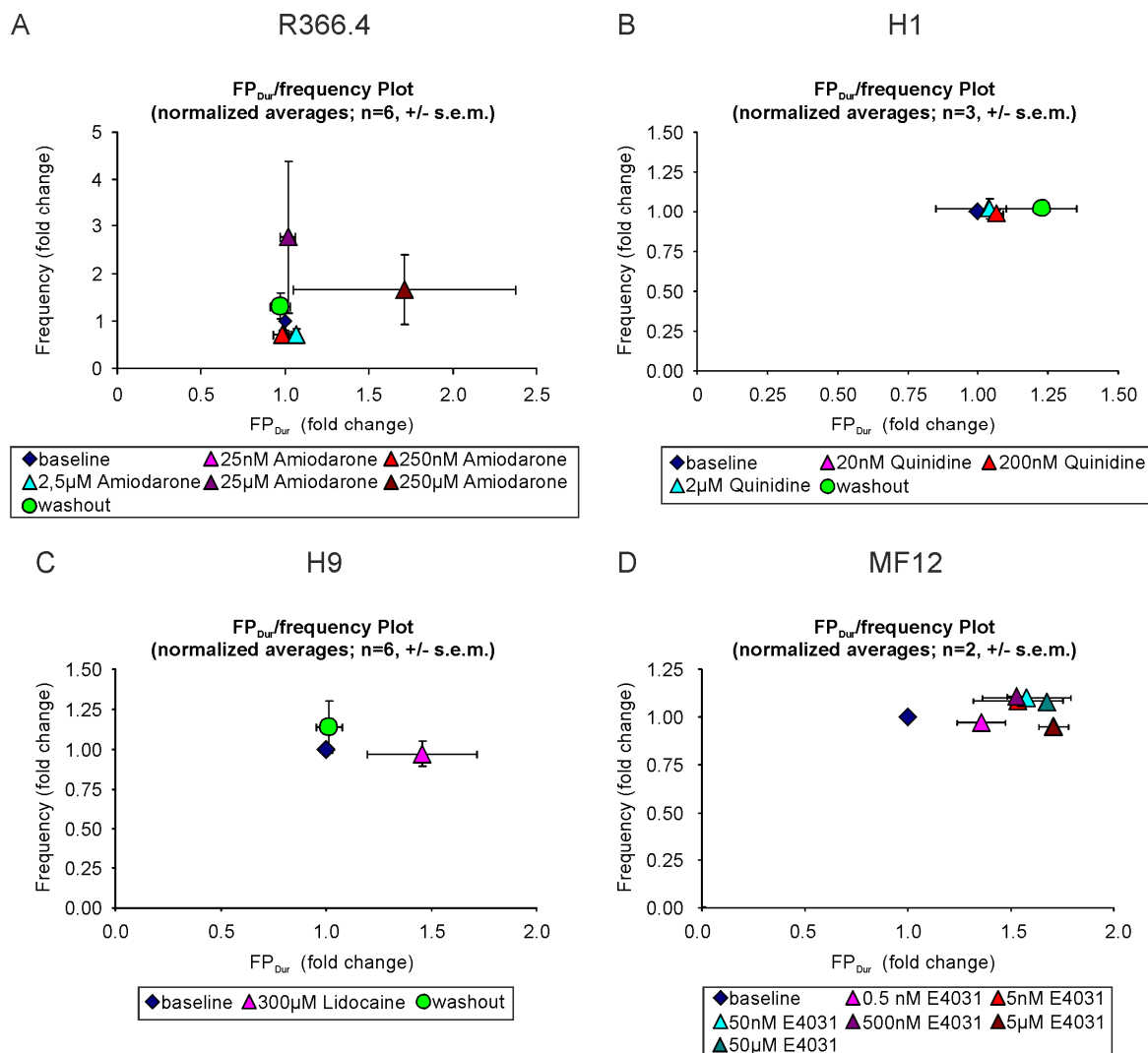


Figure 3.32: Positive FP/f correlation in hESCMs and rESCMs induced by different antiarrhythmic drug applications

FP_{Dur}/frequency plots representative of amiodarone (A), quinidine (B), lidocaine (C) and E4031 (D) application using different pluripotent ESC derived CMs (R366.4, H1, H9 and MF12, respectively).

Of the MEA data presented in the previous sections, three important conclusion can be drawn: 1) A screen for potential AP_{Dur} increasing and QT-time-prolonging compounds is feasible based on positive and negative FP/f correlations; 2) The screen is independent of the type of

pluripotent cell lines and species (rhesus monkey or human) the ESCMs were derived from;
3) The experiments showed that hiPSCMs are well suited for this purpose.

4 Discussion

4.1 **Role of catecholamines in cardiac lineage commitment in mouse ES cells**

Catecholamines have been found to be essential not only for the regulation of adult heart function but also for embryonic heart development [Kobayashi, Morita et al. 1995, Thomas, Matsumoto et al. 1995, Zhou, Quaipe et al. 1995, Ebert and Taylor 2006]. Approaching to investigate the role of catecholamines in stem cell development pluripotent murine D3 α PIG44 ES cells were treated with reserpine, a drug blocking storage and re-uptake of catecholamines thereby depleting their extracellular availability [Carlsson, Lindqvist et al. 1957, Schuldiner 1994, Bezard, Imbert et al. 1998, Bezard and Przedborski 2011]. The results clearly showed reduced and delayed cardiomyogenesis and further suggested a critical role of catecholamines in stem cell differentiation. Yet, reserpine did not negatively affect cell proliferation as was demonstrated by EB size evaluation and impedance monitoring. Apart from reduced cardiac lineage direction, application of reserpine also affected the time course and expression quantities of pluripotency, catecholamine synthesis as well as germ-layer marker genes. Of special interest was the finding of high numbers of spontaneously differentiating neuronal cells in reserpine-treated EBs, which was further strengthened by qRT-PCR results showing increased ectodermal and neuronal marker gene expression. Further supporting the finding of reserpine-induced delayed cardiac development, we observed significantly reduced beating rates in reserpine-treated EBs [Kuzmenkin, Liang et al. 2009, Pfannkuche, Liang et al. 2009]. Co-applying reserpine with NE, EPI and isoproterenol, a β -adrenergic agonist, we found a rescue of the reserpine induced effect on cardiac function, suggesting at least a partial involvement of the adrenergic system in cardiac development. Moreover, we co-applied reserpine with ISO during the first 6 days of differentiation finding distinctly rescued numbers of eGFP expressing CMs. Interestingly we could show that α - and β -AR antagonists mimic the effect of reserpine in terms of reduced cardiac development, leading to the assumption that not only β -ARs but also α -ARs are crucial for cardiomyogenesis. In conclusion, the current work presents evidence for a reserpine-induced reduction of cardiomyogenesis via catecholaminergic signal transduction, i.e. α - and β -adrenoceptors.

4.1.1 Effects of reserpine on cardiac differentiation

To directly identify the influence of catecholamines on cardiomyogenesis, determining catecholamine levels in the EBs would have been desirable. Since catecholamines possess an extremely short half-life due to their susceptibility to oxidation, we indirectly demonstrated the role of catecholamines by ISO rescue and AR antagonization. For the same reason we were not able to answer the question, if cardiomyogenesis could be enhanced by AR stimulation. To investigate this beneficial effect, further experiments will have to be performed using adrenergic agonists with increased chemical stability.

Showing severe developmental defects, several studies have been performed investigating the effect of genetic knock-outs of catecholamine synthesis enzymes in mouse models. In 1995, Thomas et al. published their results of DBH knock-out mice being unable to synthesize NE and EPI [Thomas, Matsumoto et al. 1995]. Strikingly, all of the homozygous embryos died in utero when bred from homozygous mothers and only 5% of homozygous embryos from heterozygous mothers reached adulthood. This survival probably depended on placental catecholamine transfer from their mothers. They further suggested that mortality was caused by a lack of NE rather than EPI, because it could be prevented by treatment with dihydroxyphenylserine which can be converted to NE without the activity of DBH. The majority of DBH^{-/-} embryos died of probable cardiovascular failure even before formation of adrenal glands and maturation of the sympathetic nervous system, suggesting different primary sources of catecholamine biosynthesis between embryos and adult mice [Thomas, Matsumoto et al. 1995]. The idea of an important role of catecholamines in embryonic development was strengthened by establishing mouse models deficient of intact TH being unable to synthesize the catecholamines DA, NE and EPI. Two independent publications provided strong evidence for catecholamines being essential for fetal development and postnatal survival [Kobayashi, Morita et al. 1995, Zhou, Quaife et al. 1995]. Both groups reported significant fetal mortality after E12.5 and E11.5, respectively, with even increasing mortality rates during the progression of development, very low postnatal survival (maximum P21 [Zhou, Quaife et al. 1995]) and runting of the neonates. Whereas Kobayashi et al. could not identify any “gross deformity” in any of the organs at least in embryos, Zhou et al. suggested cardiovascular failure as the cause of embryonic fatality after TH knockout [Kobayashi, Morita et al. 1995, Zhou, Quaife et al. 1995]. Nevertheless, L-DOPA rescue [Zhou, Quaife et al. 1995] and genetic rescue with human TH [Kobayashi, Morita et al. 1995] confirmed their finding of the essential developmental role of catecholamines. Both groups

suggested a paracrine action of catecholamines at a developmental stage before neuronal innervation is established.

Deleting PNMT, the enzyme catalyzing the biosynthetic step from NE to EPI, on the other side, did not lead to embryonic mortality contrasting the effects of TH and DBH deletions [Ebert, Rong et al. 2004]. This finding added to the assumption that NE is the most critical catecholamine regarding cardiac development. Our reserpine treatment model strongly resembles a DBH knock-out situation. Our observation of strongly inhibited cardiac differentiation after reserpine induced catecholamine depletion appears plausible and underlines the comparability of our stem cell model with *in vivo* models with respect to the influence of catecholamines. Nevertheless, we cannot conclude whether NE or EPI is more important. Reported severe effects on embryo survival in knock-out models is also reflected in the gene expression studies shown here (Fig. 3.9-3.13). Interestingly, we also showed that depleting catecholamines, further leads to unexpected miscellaneous timely and quantitative alterations of the expression of different groups of genes, related to e.g. pluripotency, germ layer development, catecholamine biosynthesis and α - and β -ARs. Such changes could certainly also lead to severe embryonic malformations and death as described in the aforementioned *in vivo* knock-out models.

While our *in vitro* ES cell culture system allows defined experimental conditions, the situation in terms of cell/cell interplay, hormonal regulation, and maternal/fetal interaction is far more complex *in vivo* [Schlumpf and Lichtensteiger 1979]. Placental transfer of catecholamines from the heterozygous mothers to homozygous embryos might rescue at least some embryos from prenatal death or may uphold, at least in part, the cardiac differentiation program [Kobayashi, Morita et al. 1995, Thomas, Matsumoto et al. 1995, Zhou, Quaipe et al. 1995]. The importance of placental transfer was nicely shown by Thomas et al. in 1995. They reported that 12% of their DBH^{-/-} embryos from heterozygous mothers survived until birth, whereas all DBH^{-/-} embryos from homozygous mothers died before E13.5 [Thomas, Matsumoto et al. 1995]. The same study also nicely showed that heterozygous embryos (DBH^{+/-}) from homozygous mothers synthesized NE almost at wild-type levels. Whether maternal or embryonic catecholamines are more important for development remains unclear. However, if maternal catecholamine levels would *per se* supersede the levels released by the embryo, embryonic cardiac development would be strongly dependent on the mother's catecholamine levels (e.g. stress exposure, etc.). Therefore, it is hypothesized here, that a local regulatory system might control catecholamine concentrations within the blastocyst and/or the embryo, at least during the earliest steps of cardiac development.

It was also found that excessive exposure of catecholamines or β -adrenergic agonists leads to congenital heart failure in chick embryos [Hodach, Gilbert et al. 1974]. Since, only early application (E4 to E5) led to these malformations in chicken, and embryonic mortality appeared between E9.5 and E13.5 in murine catecholamine biosynthesis gene knock-out models, a “critical period” for catecholamine action was suggested. During this period embryos are “hypersensitive” to exposure with catecholamines (reviewed in [Ebert and Taylor 2006]). This suggested that depletion as well as over-application of catecholamines leads to alteration of cardiac development *in vivo*. Reserpine applied continuously (‘until day 14’) but also only until day 6 in our respective culture protocols is already enough to induce strongly reduced cardiac development. This obviously suggests, that in our *in vitro* ES cell system the critical period was before day 6. Even though the *in vivo* knock-out models (TH and DBH knock-out) suggested the critical period in terms of embryonic lethality to be between E9.5 and E13.5 [Kobayashi, Morita et al. 1995, Thomas, Matsumoto et al. 1995, Zhou, Quaipe et al. 1995], the mechanistic changes leading to that certainly appear before E9.5. Hence, the critical periods would be more or less overlapping in the *in vivo* and the *in vitro* model of this work. Thus, reduced cardiac development in ESCs could be based on the “critical period” for catecholamine action. In this period catecholamines whether in very low or in excessive concentrations were simply shown to negatively alter cardiac development *in vivo*. Based on our results, we suggest that in the ES cell differentiation model this critical period is likely to be within the first 6 days of differentiation.

In the present study we showed results from qRT-PCR experiments quantifying the expression of catecholamine synthesizing enzymes (see Fig. 3.11). Expression of the genes *Th*, *Ddc* and *Dbh* began on day 2 when reserpine was present. *Pnmt*, on the other side, did not seem to be expressed in reserpine-treated EBs at all or were at least strongly down-regulated. In control EBs, expression of neither of these enzymes could be detected before day 6 or day 8. Already in the 1930’s people hypothesized that catecholamines are important regulators of heart rate even at early pre-innervation stages of development [Markowitz 1931] and further suggested a humoral control of the heart rate in embryos before inception of the nervous system [Hsu 1933]. In accordance, catecholamines (NE and EPI) were detected in chicken hearts as early as day 3 of incubation. In whole chick embryos, L-DOPA and DA were even present from day 1 on [Ignarro and Shideman 1968]. Consequently, the question arose what the source of the catecholamines at this pre-innervation stage of development would be. In rat [Ebert and Thompson 2001], mouse [Ebert, Rong et al. 2004] and human [Huang, Friend et al. 1996] hearts or primary cardiomyocyte isolates, intrinsic cardiac adrenergic (ICA) cells

were found. These ICA cells are present long before neuronal β -adrenergic innervation occurs and were described to have important functions in embryonic heart development and also neonatal cardiac β -adrenergic functionality. Initially it was suggested that ICA cells would only be related to cardiac conduction system development [Ebert and Thompson 2001], whereas a further study by Ebert and colleagues in 2008 proposed that also atrial and ventricular myocytes originate from the same kind of cells [Ebert, Rong et al. 2008].

Reserpine-induced depletion of catecholamines leading to reduced cardiomyogenesis indicates that catecholamines stimulate cardiomyogenesis. Moreover, our results showed higher expression of catecholamine biosynthesis genes while reserpine is present. Those results suggested higher levels of L-DOPA, DA, and NE, which would in turn contradict the hypothesis of catecholamines having inducing effects on cardiomyogenesis. Immunohistochemical staining with DBH antibodies (Fig. 3.15) revealed the increased presence of catecholaminergic cells in reserpine-treated EBs and strengthened the qRT-PCR results (Fig. 3.11). As described for ICA cells [Huang, Friend et al. 1996], catecholaminergic DBH expressing cells are small, roundish and were found in isolated groups but basically do not look like neuronal cells. Our DBH expressing cells look like ICA cells, but are not surrounded by cardiac cells in the reserpine-treated group. Nevertheless, the reserpine reduced vesicular transport and resulting lower levels of NE and EPI may have activated expression of the preceding enzymes (e.g. *Th*, *Ddc* and *Dbh*) in a feedback regulation/activation loop, as commonly seen in anabolic biosynthetic pathways. Hence, the catecholamine synthesizing enzymes are up-regulated, while effectively, catecholamine levels are low through the action of reserpine, and for that reason cardiac development may be hampered.

Higher numbers of ICA cells as seen in immunohistochemical stainings (Fig. 3.15) could have a similar reason. So far, it is unclear which mechanisms control ICA cell growth and proliferation. We show that ICA cells are present, but hypothesize that they are catecholamine-depleted by the action of reserpine. Therefore the catecholamines' cardiac-inducing effect in reserpine-treated EBs is lacking. Increased ICA cell proliferation could as well be induced by a missing feed-back inhibition mechanism. While reserpine depletes ICA cells of catecholamines and changes the cells' gene expression, in compensation it could induce a signal cascade that induces ICA cell proliferation above the normal level, leading to our observation of slightly increased numbers of those cells.

The previous discussion about the presence and the role of ICA cells is interesting in respect to a recent publication, providing evidence of those cells reducing ischemia/reperfusion injury [Huang, Nguyen et al. 2009].

4.1.2 *Underlying mechanisms*

Activation of adrenergic receptors activates highly complex intracellular signaling cascades. ARs are well known to belong to the G protein-coupled receptor superfamily (GPCRs) [Caron and Lefkowitz 1993]. Upon catecholamine binding to their specific receptor subtypes, dissociation of the G-protein heterotrimers regulates a variety of second messengers, e.g. cAMP, cGMP, Ca²⁺, inositol 1,4,5-trisphosphate (IP₃), nitric oxide (NO), arachidonic acid (AA), etc. Subsequently, protein kinases and phosphatases regulate the phosphorylation status of proteins involved in almost all areas of cellular function. These functions can roughly be divided into short-term and long-term modulating effects. Short-term effects include for example ion channel activity, receptor sensitivity, general metabolism or neurotransmitter synthesis and release, whereas, long-term modulations include synthesis of channels, receptors and intracellular messengers, synaptogenesis and generally gene expression (reviews: [Keys and Koch 2004, Zheng, Han et al. 2004]). However, many details of the adrenergic network are still unclear.

During the course of differentiation, CMs undergo various changes regarding their functional properties [Hescheler, Fleischmann et al. 1999, Janowski, Cleemann et al. 2006, Kuzmenkin, Liang et al. 2009, Pfannkuche, Liang et al. 2009]. As has been shown before, also the frequency with which CMs contract varies strongly between the developmental stages. Murine ESCMs have been demonstrated to increase their beating rates during the course of development [Banach, Halbach et al. 2003, Kuzmenkin, Liang et al. 2009]. The MEA experiments presented in Fig. 3.16 show that reserpine-treated EBs contracted with reduced frequencies and underlined our overall finding of delayed cardiac differentiation. Upon ISO stimulation, absolute values of beating rates of control EBs were significantly higher (Fig. 3.16C) than beating rates of reserpine-treated EBs, whereas, normalization of the beating rates did not lead to a significant difference (Fig. 3.16D). Even more, the normalized ISO stimulated frequency in reserpine-treated EBs is lower and could, therefore, imply a decreased responsiveness and an immature β -adrenergic system in these cells [Kuzmenkin, Liang et al. 2009, Pfannkuche, Liang et al. 2009]. The conclusion of this functional MEA experiment was also reflected by the sqRT-PCR results for β -AR expression (Fig. 3.13). Both findings further support the hypothesis that reserpine delays cardiac differentiation, but they also show that reserpine treatment changes the expression of β -ARs (and α -ARs) providing a first idea for the underlying mechanism.

The sqRT-PCRs and the MEA experiments pointed toward a possible role of ARs in ESCM differentiation. To further elucidate the mechanism underlying the reserpine-induced developmental effect, short-term rescue experiments were performed (Table 1 and Fig. 3.17). First, we used MEAs to confirm that reserpine depletes the catecholamine stores, thereby gradually reducing the beating rate of spontaneously beating clusters. Recovery of the beating rate, by application of β -adrenergic agonist ISO and natural AR agonists NE and EPI, showed that the reserpine effect on beating rates is catecholamine-dependent. Thus, the experiment confirmed that reserpine depletes intracellular catecholamine stores and suggested that the reduced cardiac development may depend on reduced levels of catecholamines causing a lack of AR stimulation (mainly β_1 -ARs in the heart). Also the increase in neuronal cells may be dependent on reduced catecholamine levels. However, whether the α -AR, the β -AR system or both systems together are responsible for the effects could not be concluded.

The previous findings laid the basis for the long-term rescue experiment. Cultivating ES cells in medium containing reserpine and ISO at least partially reversed the inhibiting effect of reserpine on cardiac development (Fig. 3.18). Thus, it can be hypothesized, that β -AR signaling partially modulates cardiac development. Since the specific β -AR subtypes are coupled to different G-protein complexes (activating as well as inhibiting) application of the unspecific β -AR agonist ISO could induce partially opposite intracellular effects that might inhibit complete rescue. It is possible that more complete rescue might be accomplished with subtype-specific β -AR agonists. In this regard, it has to be further considered that ISO has a limited half-life. Due to their even shorter half-life, the native β -AR agonists, NE and EPI, were tested for their potential rescue effects, however without providing revealing results. Also sqRT-PCRs (see Fig 3.13) did not explain which β -AR subtype determines cardiac cell fate, because expression of all subtypes was somewhat changed after reserpine treatment.

Evidence from previous work implied the conclusion that the β_1 - and the α_2 -adrenoreceptor systems are the most likely candidates for developmental inhibition. *In vivo* knockout experiments showed that those ARs negatively impact embryonic development when being deleted [Rohrer, Desai et al. 1996, Hein, Altman et al. 1999, O'Connell, Ishizaka et al. 2003]. This work showed, that applying phentolamine and propranolol to antagonize α - and β -adrenergic receptor signaling negatively affects cardiomyogenesis, mimicking the negative effects of reserpine (Fig. 3.20). This observation was in line with the above mentioned knockout experiments. The results shown here strongly suggest catecholamine-induced α - and β -AR-mediated signaling to be critical for cardiac development in ES cells. This finding may, at least partially, be extrapolated to the *in vivo* situation. Our sqRT-PCR

results point toward α_{1D} , α_{2C} and the β -ARs as possible candidates promoting the catecholamines' effects on cardiomyogenesis, because their expression patterns showed the most obvious deviations. However, also α_{2A} being prematurely expressed might be a candidate, in line with AR knockout models [Rohrer, Desai et al. 1996, Hein, Altman et al. 1999, O'Connell, Ishizaka et al. 2003]. Most striking was the rather unexpected strong expression of β_3 in reserpine-treated EBs. Except for α_{2A} and β_3 , all ARs are absent at day 10 after reserpine treatment. Therefore our data suggest that a wide-spread role of catecholamines on the differentiation of a variety of cell types (all those expressing ARs) is conceivable.

4.1.3 Effects on neuronal Differentiation

Beside the reserpine-induced inhibition of cardiomyogenesis, the present work also provides evidence for alterations in ectodermal gene expression (Fig. 3.12B). Even in our cell culture, being optimized for cardiac differentiation, reserpine-treated ES cells obviously develop into EBs containing remarkable numbers of neuronal cells (Fig. 3.14, 3.15 and 3.19). Of the genes tested, especially *Map2* is significantly up-regulated already at day 1 of differentiation. *Tubb3* also shows higher expression levels compared to untreated EBs. Together with the immunohistochemical staining with β -III-tubulin antibodies and the phase contrast microscopy pictures, the inducing effect of reserpine on neuronal development is quite striking [Theurkauf and Vallee 1982, Harada, Teng et al. 2002, Katsetos, Legido et al. 2003]. The neuronal cells found in reserpine-treated EBs are not only increased in their number, but also appear more mature based on their morphology with typical axonal and dendritic outgrowths. So far, not many details of the effects of catecholamines on neuronal development are described.

In vivo studies with heterozygous TH mutant mice ($TH^{+/-}$) with moderate 73-80% of wild-type NE levels revealed impairments in different learning and memory tasks but no morphological changes in brains [Kobayashi, Noda et al. 2000]. Another *in vivo* study by Kobayashi and colleagues worked with genetically modified mice resulting in a complete loss of TH expression only in dopaminergic neuronal cells [Kobayashi and Sano 2000]. With resulting significantly lower levels of dopamine produced in the brain (probably during the embryonic and maturation phase), three weeks after birth these mice were described to have brain weights reduced to 87% compared to control mice. These mutant mice showed impaired spontaneous locomotor activity and cataleptic behavior. Kobayashi et al. concluded that the abnormalities in motor control resulted from the combined loss of the two major

dopaminergic pathways, the nigrostriatal and the mesocorticolimbic pathway and not from a loss of dopaminergic cells in the brain [Kobayashi and Sano 2000]. In line with the *in vivo* experiments by Kobayashi *et al.* and based on our findings, catecholamine biosynthetic enzymes and their products, especially DA and NE, are also important for the development of neuronal cells. The data shown here suggest that in ES cell culture catecholamines seem to exhibit a negative regulatory effect when present. We hypothesize that reserpine reduces/depletes catecholamine concentrations and may therefore abolish this negative regulating effect, thus leading to increased neurogenesis.

Another possible reason for the positive effect of reserpine on neuronal development could be based on a more global drug effect. As discussed in a review of Zorn and colleagues, endoderm and mesoderm are derived from a transient progenitor cell population known as the mesendoderm [Zorn and Wells 2009]. In parallel to these progenitors, the ectodermal lineage arises and in the further course of development differentiates into neuronal cells (besides other cell types). Several publications provided good evidence for Nodal being an important central switch responsible for mesendodermal on one side (induced by Nodal) or ectodermal cell fate on the other side (induced when Nodal is inactivated) [Vallier, Reynolds *et al.* 2004, Ben-Haim, Lu *et al.* 2006, Camus, Perea-Gomez *et al.* 2006, Mesnard, Guzman-Ayala *et al.* 2006]. Strikingly, our results indicated that reserpine affects early developmental gene expression, of e.g. *Rex1* and *Fgf5* and, thus, suggested a very early effect during cell fate decision (Fig. 3.9). Thus, the reserpine-induced mesodermal inhibition could indirectly promote neurectodermal development by altering the regulation of a central switch such as Nodal. However, further experiments are necessary to ultimately prove this hypothesis.

Furthermore, *Fgf5* has not only been described to be a marker for the embryonic gastrulation, but it has also been suggested that its expression is somehow linked to ectodermal germ layer cells during this stage [Hebert, Boyle *et al.* 1991]. Thus, *Fgf5* is certainly involved in gastrulation, which is the process in which a population of cells is transformed into a three-layered structure forming the three germ layers. Our results show that 6 days after the start of differentiation a remarkably stronger expression of *Fgf5* was detected, when cells were treated with reserpine (Fig. 3.9). This finding suggests that the reserpine effects were influencing cell fate decisions very early during development and strengthens the hypothesis that the reduction in mesodermal differentiation might be compensated by increased ectodermal differentiation.

Adding to this hypothesis a publication by the group of Toyooka provided evidence that *Rex1*-/*Oct3/4*+ cells undergo differentiation into neurectoderm more efficiently than

Rex+/*Oct3/4+* cells [Toyooka, Shimosato et al. 2008]. qRT-PCR results presented here indicated that between day 2 and day 4 *Rex1* was strongly down-regulated in reserpine-treated cells, whereas *Oct4* expression was similar in control and reserpine-treated cells. This *Rex1/Oct4* ratio found in reserpine-treated cells resembled a *Rex1-/Oct3/4+* situation, thus, maybe promoting more efficient differentiation into neurectoderm.

4.1.4 Conclusions

In the first part of this thesis murine ES cells were treated with reserpine to elucidate a possible role of catecholamines in cardiomyogenesis. This data describes the effect of reserpine-induced catecholamine depletion and suggests several important conclusions: 1) Catecholamine depletion strongly reduces cardiac development, 2) it induces alterations of diverse gene expressions not only limited to cardiomyogenesis, 3) Catecholamines are crucial for development already at very early developmental stages, even before neuronal innervations, 4) Catecholamine depletion leads to alterations of cardiomyocyte electrophysiology, and 5) the α - as well as β -adrenergic signaling cascade seem to be involved in early stage catecholamine action. It can be assumed that the results shown here will help provide a deeper insight into the role of catecholamines and adrenergic signaling in ES cell differentiation. Our reserpine-catecholamine-depletion model shows alterations in cardiac as well as neuronal developmental processes. This will potentially help to identify new targets for directed stem cell differentiation protocols. Finally, the results indicate that high dose α - and β -blocker therapy during early pregnancy needs clear indications [Meidahl Petersen, Jimenez-Solem et al. 2012].

4.2 MEA-based QT-screen using pluripotent stem cell-derived CMs

In the second part of the thesis it was approached to establish a pharmacological screening tool, suitable for the detection of possible cardio-active side effects such as repolarization prolongation. The advantages of extracellular recordings with MEA were combined with the properties of pluripotent cells to provide large numbers of CMs and the good comparability of this *in vitro* model with the *in vivo* situation of diseased hearts. Similar to QT-times from ECGs and AP durations from intracellular recordings, we also hypothesized FP_{Dur} from MEAs to be strongly frequency dependent. Applying several compounds with known pharmacological effects we concluded that: 1) under physiological conditions the FP/f correlation is negative; 2) if class III antiarrhythmic agents are present, FP/f correlations are shifted to less negative or positive values; 3) these findings represent a general correlation since they were confirmed in rESCMs, hESCMs as well as hiPSCMs.

4.2.1 Optimization of rESC culture and differentiation

Optimization of the rES cell culture and their differentiation towards CMs was initially a crucial step. Using our newly established activinA/BMP4 protocol it was possible to derive sufficient numbers of beating clusters. This protocol clearly improved the yield of CMs as compared to the other protocols tested. While activinA/BMP4 treatment for directed differentiation of hESCMs was published before [Laflamme, Chen et al. 2007], to our knowledge here it was shown for the first time that these factors have the same pro-cardiomyogenic effect on rESCs.

Nevertheless, rESC cardiac clusters derived using our protocol showed certain downsides compared to hES or hiPS cardiac clusters. Most adverse was the low ratio of CMs within rESC EBs. hES and hiPS were differentiated using END2 protocols and generally yield comparatively small EBs, yet containing a more beneficial ratio of CMs. Low CM ratios in rESC EBs negatively affect FP signal amplitudes and make EBs prone to arrhythmia and sensitive to minor temperature oscillations. Arrhythmic behavior was most likely caused by the increased force that is needed from CMs to agitate the non-CM cells the EBs are predominantly composed of. Because arrhythmic beating reduces the quality of MEA recordings and those EBs were therefore not used for analysis, numbers of potentially good rESCM EBs were still not very high.

4.2.2 *Qualitative classification of drug effects by FP/f correlation*

In this work it was shown that the FP_{Dur} is dependent on frequency. It was further shown that under physiologic conditions FP/f correlations are negative, while they became more positive when K^+ -channel blocking class III agents were present. A graphical method representing normalized and averaged FP_{Dur} /frequency plots was chosen to illustrate changes of FP/f correlations under the influence of different types of drugs. The idea was to classify drug effects on the basis of FP/f correlations.

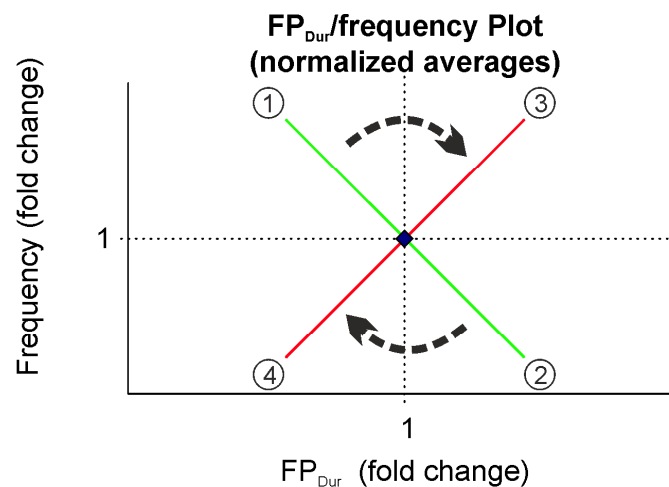


Figure 4.1: Illustration of drug effect classification based on positive and negative FP/f correlations

The FP_{Dur} /frequency plot is subdivided into quadrants (dotted lines) to classify FP_{Dur} /frequency value pairs. Normalized baseline value pairs are represented by the blue rhombus (center). The green line indicates a negative FP/f correlation shift, as detected under physiological positive (1) or negative (2) chronotropic stimulation. The red line indicates a positive FP/f correlation shift. Class III antiarrhythmic drugs E4031 and sotalol shifted value pairs to the top right quadrant (3) indicating frequency independent FP_{Dur} increase (and AP_{Dur} /QT-time prolonging drug effects), while frequency independent FP_{Dur} decrease would be expected in quadrant (4). Arrows indicate the drug-induced shift. For further details see text.

Fig. 4.1 illustrates the drug effect classification idea. As stated before, FP_{Dur} and beating frequency recorded under the influence of a drug were normalized toward the respective baseline values (untreated condition). Due to normalization, the baseline FP/f value pair is always located at coordinates $x=1/y=1$ of the FP/f plot (blue rhombus). Given a hypothetical 1:1 linear correlation of FP_{Dur} and beating frequency, FP/f values pairs should align along the green line under physiological conditions revealing a negative FP/f correlation. Positive chronotropy should shift the value pairs along the green line in the direction of (1), while negative chronotropy should shift the pairs in the direction of (2). However, as was shown with ISO measurements, in reality the steepness of the lines varied (Fig. 3.27). The variation

of the steepness was due to FP signal morphology variation, but also caused by biological variations within the analyzed parameters. Therefore, classification of drug effects should rather be made based on the quadrant in which the value pairs align. Four quadrants are indicated by dotted lines in Fig. 4.1. During positive chronotropic stimulation (ISO), FP/f value pairs were found in the top left (1), while under negative chronotropic stimulation value pairs were found in the bottom right quadrant (2) (also see Fig. 3.27-3.30). Similarly, in our hypothetical conditions, positive FP/f correlation indicating value pairs would align along the red line or in the top right (3) or bottom left (4) quadrant. E4031 and sotalol measurements (Fig. 3.31) nicely showed that classification on the basis of the quadrants is feasible. Nevertheless, it is not expected that all potentially harmful agents tested within a high-throughput screen induce effects as strong as classical K⁺-channel blockers like E4031 and sotalol. Therefore, the sensibility of such a screen needs to be further improved.

4.2.3 *Limitations and suggested improvements*

Improvement of sensibility of the screening approach presented here can be achieved in several ways. Probably most important is standardization of the experimental setup and measurement procedure, including the used cell lines, the differentiation protocol, the model system and the measurement routines. Those points will be discussed in more detail hereafter.

The results of the work demonstrated that our screen worked independent of the used cell lines (R366.4+MF12 rESCMs, H1+H9 hESCMs and several hiPSCMs). As mentioned before, work with hES cells poses ethical problems but provides cells from human origin as compared to rES cells. hiPS cells avoids ethical as well as problems resulting from inter-species differences. Furthermore, hiPSCMs have been shown to possess functional properties very similar to hESCMs and primary CMs [Zhang, Wilson et al. 2009, Germanguz, Sedan et al. 2011]. Therefore we suggest that from today's point of view iPSCMs are most applicable for such a screen. For drug screening a hiPS cell line representative of humans of all genders, races and ages will have to be established to be used as a standard.

Optimized and standardized cell culture conditions are absolutely crucial for reliable screening, not only to ensure the availability of sufficient numbers of CMs, but also, to guarantee that the CMs derived from a pluripotent origin are of the same kind (atrial, ventricular or conduction system) and at the same stage of development at all times to make results comparable. Several publications showed that CMs undergo continuous change during *in vitro* differentiation [Maltsev, Ji et al. 1999, Reppel, Boettinger et al. 2004, Pfannkuche, Liang et al. 2009]. This consequently means that all CMs used, not only have to be in the

same state, but also, that this state has to closely resemble or be the same as the mature state of CMs [Dolnikov, Shilkrot et al. 2006, Khan, Lyon et al. 2013]). For that reason detailed understanding of the maturation processes is essential.

Interestingly, early stage ES cell-derived CMs were found to resemble failing cardiac myocytes [Brito-Martins, Harding et al. 2008]. It was hypothesized that re-expression of an embryonic gene profile and function might serve as a rescue program [Liang, Halbach et al. 2010]. Characteristics of heart failure are cytosolic Ca^{2+} overload, structural changes of the myofilaments as well as alteration in neurohormonal regulation [Kho, Lee et al. 2012].

Pharmacological screening can potentially be used to identify drugs that help to reduce symptoms of certain heart diseases. Several hiPS disease models have already been established [Moretti, Bellin et al. 2010, Fatima, Xu et al. 2011, Itzhaki, Maizels et al. 2011, Jung, Moretti et al. 2012], and, in the future, can be used to identify and optimize patient-specific therapy strategies.

However, to further improve our drug-screening model it would have to be considered which grade of purification the cells should have for MEA measurements. In the current work an EB based culture and measurement was used. EBs not only consist of CMs, but to a major proportion of non-cardiac cells. In the EB cell-cell interactions upon drug application cannot be controlled and can cause bias. Therefore, a homogenous tissue-like construct of identical cells would be preferable. The demand for large amounts of specialized cells is increasing and technologies will be developed to provide the cells in the near future [Hattori, Chen et al. 2010]. During this project initial experiments were conducted using monolayers of purified CMs for MEA measurements. Though those monolayers were grown from mouse ESCMs, they still showed great promise in regard to their applicability and signal quality (data not shown) and will be potentially the optimal format for the MEA-based drug-screen. The major disadvantage of EBs, especially of the rES EBs, was the low ratio of CMs to non-cardiac cells. This ratio directly influences the signal amplitude of FPs [Halbach 2006]. In turn, low signal amplitudes lead to poor signal-to-noise ratios which exacerbated data analysis and subsequently lead to increased impreciseness particularly of FP_{Dur} . Additionally, CM monolayers are preferable to EBs in respect to possible conduction analysis. Describing conduction speeds between distant areas of the monolayer adds extra information of drug-effects to the same experimental setup.

Another way of improvement of the screening sensibility can be achieved by establishing a suitable quantification. The method we used to evaluate drug-effects is based on graphical FP/f correlation classification. This approach provided rather qualitative than

quantitative results. One possible solution for quantification was the adaption of heart-rate adjustment of QT-times (QTc) as used clinically for ECG normalization. Also tested and evaluated in humans, we calculated in analogy to QTc, frequency-corrected FP_{Dur} values using the clinically most relevant Bazett's formula [Bazett 1920]. Furthermore, we calculated QT-corrections after Fridericia's formula [Fridericia 1920] and a formula derived from the "Framingham Heart Study" involving more than 5,000 patients [Sagie, Larson et al. 1992]. All these formulas were empirically determined on the basis of a non-linear relationship of QT- and RR-intervals. However, all QT-time correction algorithms were questioned because of inaccuracy in respect to their universal applicability of the resulting QTc's [Ahnve 1985, Sagie, Larson et al. 1992]. Many other groups have proposed further linear and non-linear correction algorithms, but all of them failed to represent corrections covering subjects of all genders, races, health conditions and genetic backgrounds within the complete heart-rate frequency band. There is also ongoing debate about the maximum normal QTc, ranging from 400-440 msec [Schouten, Dekker et al. 1991], to determine their predictive value. Even though not shown in this work, our corrected FP_{Dur} quantification approach partially showed consensus with the graphical results. However, depending on the correction algorithm we also found contradictions between the applied corrected quantifications (Bazett vs Fridericia vs Framingham), but also between graphical and quantitative approach. Altogether, the graphical approach provided a more universal picture of the expected drug effects and was therefore to be preferred.

4.2.4 Conclusions

In summary, we showed here that FP_{Dur} is dependent on the beating frequency in MEA recordings with pluripotent stem cell-derived CMs irrespective of their species or cell line background. We further provided evidence of a negative FP/f correlation under physiologic conditions and shift to a positive correlation in the presence of class III antiarrhythmic drugs. Based on these findings we propose a graphical classification model for potential cardio-active drugs. Yet, with the discussed standardization of our system in respect to cell lines, cell culture conditions, the format of the CM tissue-construct, etc., we suggest the possibility of a quantifiable drug-screening system based on the proposed principle of FP/f correlation. Finally, our observations can provide the basis for establishing a high- or medium-throughput screen combining the advantages of hiPSCMs and the MEA technology.

VI **References**

- Catecholamines. Encycloaedia Britannica Online Academic Edition. <http://www.britannica.com/EBchecked/topic/99345/catecholamine>, Encyclopædia Britannica Inc., 2013.
- Abbott, G. W., F. Sesti, I. Splawski, M. E. Buck, M. H. Lehmann, K. W. Timothy, M. T. Keating and S. A. Goldstein (1999). "MiRP1 forms IKr potassium channels with HERG and is associated with cardiac arrhythmia." Cell **97**(2): 175-187.
- Ahnve, S. (1985). "Correction of the QT interval for heart rate: Review of different formulas and the use of Bazett's formula in myocardial infarction." American Heart Journal **109**(3, Part 1): 568-574.
- Antzelevitch, C. (2005). "Role of transmural dispersion of repolarization in the genesis of drug-induced torsades de pointes." Heart Rhythm **2**(2 Suppl): S9-15.
- Antzelevitch, C., W. Shimizu, G. X. Yan, S. Sicouri, J. Weissenburger, V. V. Nesterenko, A. Burashnikov, J. Di Diego, J. Saffitz and G. P. Thomas (1999). "The M cell: its contribution to the ECG and to normal and abnormal electrical function of the heart." J Cardiovasc Electrophysiol **10**(8): 1124-1152.
- Araki, R., M. Uda, Y. Hoki, M. Sunayama, M. Nakamura, S. Ando, M. Sugiura, H. Ideno, A. Shimada, A. Nifuji and M. Abe (2013). "Negligible immunogenicity of terminally differentiated cells derived from induced pluripotent or embryonic stem cells." Nature **494**(7435): 100-104.
- Arch, J. R., A. T. Ainsworth, M. A. Cawthorne, V. Piercy, M. V. Sennitt, V. E. Thody, C. Wilson and S. Wilson (1984). "Atypical beta-adrenoceptor on brown adipocytes as target for anti-obesity drugs." Nature **309**(5964): 163-165.
- Atienza, J. M., N. Yu, S. L. Kirstein, B. Xi, X. Wang, X. Xu and Y. A. Abassi (2006). "Dynamic and label-free cell-based assays using the real-time cell electronic sensing system." Assay Drug Dev Technol **4**(5): 597-607.
- Banach, K., M. D. Halbach, P. Hu, J. Hescheler and U. Egert (2003). "Development of electrical activity in cardiac myocyte aggregates derived from mouse embryonic stem cells." Am J Physiol Heart Circ Physiol **284**(6): H2114-2123.
- Baruscotti, M., A. Bucchi and D. DiFrancesco (2005). "Physiology and pharmacology of the cardiac pacemaker ("funny") current." Pharmacol Ther **107**(1): 59-79.
- Bazett, H. C. (1920). "An analysis of the time-relations of electrocardiograms." Heart **7** (1920): pp. 353-370.

References

- Ben-Haim, N., C. Lu, M. Guzman-Ayala, L. Pescatore, D. Mesnard, M. Bischofberger, F. Naef, E. J. Robertson and D. B. Constam (2006). "The nodal precursor acting via activin receptors induces mesoderm by maintaining a source of its convertases and BMP4." Dev Cell **11**(3): 313-323.
- Bers, D. M. (2002). "Cardiac excitation-contraction coupling." Nature **415**(6868): 198-205.
- Bezard, E., C. Imbert and C. E. Gross (1998). "Experimental models of Parkinson's disease: from the static to the dynamic." Rev Neurosci **9**(2): 71-90.
- Bezard, E. and S. Przedborski (2011). "A tale on animal models of Parkinson's disease." Mov Disord **26**(6): 993-1002.
- Boehm, S. and S. Huck (1995). "alpha 2-Adrenoreceptor-mediated inhibition of acetylcholine-induced noradrenaline release from rat sympathetic neurons: an action at voltage-gated Ca²⁺ channels." Neuroscience **69**(1): 221-231.
- Bond, R. A. and D. E. Clarke (1988). "Agonist and antagonist characterization of a putative adrenoceptor with distinct pharmacological properties from the alpha- and beta-subtypes." Br J Pharmacol **95**(3): 723-734.
- Boyle, W. A. and J. M. Nerbonne (1991). "A novel type of depolarization-activated K⁺ current in isolated adult rat atrial myocytes." Am J Physiol **260**(4 Pt 2): H1236-1247.
- Brade, T., J. Manner and M. Kuhl (2006). "The role of Wnt signalling in cardiac development and tissue remodelling in the mature heart." Cardiovasc Res **72**(2): 198-209.
- Brand, T. (2003). "Heart development: molecular insights into cardiac specification and early morphogenesis." Dev Biol **258**(1): 1-19.
- Bravo, E. L., R. C. Tarazi, R. W. Gifford and B. H. Stewart (1979). "Circulating and urinary catecholamines in pheochromocytoma. Diagnostic and pathophysiologic implications." N Engl J Med **301**(13): 682-686.
- Brito-Martins, M., S. E. Harding and N. N. Ali (2008). "beta(1)- and beta(2)-adrenoceptor responses in cardiomyocytes derived from human embryonic stem cells: comparison with failing and non-failing adult human heart." Br J Pharmacol **153**(4): 751-759.
- Bylund, D. B. (1992). "Subtypes of alpha 1- and alpha 2-adrenergic receptors." Faseb J **6**(3): 832-839.
- Bylund, D. B., D. C. Eikenberg, J. P. Hieble, S. Z. Langer, R. J. Lefkowitz, K. P. Minneman, P. B. Molinoff, R. R. Ruffolo, Jr. and U. Trendelenburg (1994). "International Union of Pharmacology nomenclature of adrenoceptors." Pharmacol Rev **46**(2): 121-136.

- Camus, A., A. Perea-Gomez, A. Moreau and J. Collignon (2006). "Absence of Nodal signaling promotes precocious neural differentiation in the mouse embryo." Dev Biol **295**(2): 743-755.
- Cannon, W. B. (1920). Bodily changes in pain, hunger, fear and rage; an account of recent researches into the function of emotional excitement. New York, London,, D. Appleton and Company.
- Carlsson, A., M. Lindqvist and T. Magnusson (1957). "3,4-Dihydroxyphenylalanine and 5-hydroxytryptophan as reserpine antagonists." Nature **180**(4596): 1200.
- Caron, M. G. and R. J. Lefkowitz (1993). "Catecholamine receptors: structure, function, and regulation." Recent Prog Horm Res **48**: 277-290.
- Caspi, O., I. Itzhaki, I. Kehat, A. Gepstein, G. Arbel, I. Huber, J. Satin and L. Gepstein (2009). "In vitro electrophysiological drug testing using human embryonic stem cell derived cardiomyocytes." Stem Cells Dev **18**(1): 161-172.
- Chen, H., L. Cui, X. Y. Jiang, Y. Q. Pang, G. L. Tang, H. W. Hou, J. H. Jiang and Q. Y. Hu (2012). "Evaluation of the cytotoxicity of cigarette smoke condensate by a cellular impedance biosensor." Food Chem Toxicol **50**(3-4): 612-618.
- Chen, Z. J. and K. P. Minneman (2005). "Recent progress in alpha1-adrenergic receptor research." Acta Pharmacol Sin **26**(11): 1281-1287.
- Christoffels, V. M., P. E. Habets, D. Franco, M. Campione, F. de Jong, W. H. Lamers, Z. Z. Bao, S. Palmer, C. Biben, R. P. Harvey and A. F. Moorman (2000). "Chamber formation and morphogenesis in the developing mammalian heart." Dev Biol **223**(2): 266-278.
- Christoffels, V. M. and A. F. Moorman (2009). "Development of the cardiac conduction system: why are some regions of the heart more arrhythmogenic than others?" Circ Arrhythm Electrophysiol **2**(2): 195-207.
- Communal, C., K. Singh, D. R. Pimentel and W. S. Colucci (1998). "Norepinephrine stimulates apoptosis in adult rat ventricular myocytes by activation of the beta-adrenergic pathway." Circulation **98**(13): 1329-1334.
- Communal, C., K. Singh, D. B. Sawyer and W. S. Colucci (1999). "Opposing effects of beta(1)- and beta(2)-adrenergic receptors on cardiac myocyte apoptosis : role of a pertussis toxin-sensitive G protein." Circulation **100**(22): 2210-2212.
- Conlon, F. L., K. M. Lyons, N. Takaesu, K. S. Barth, A. Kispert, B. Herrmann and E. J. Robertson (1994). "A primary requirement for nodal in the formation and maintenance of the primitive streak in the mouse." Development **120**(7): 1919-1928.

- Costa, M., K. Sourris, T. Hatzistavrou, A. G. Elefanty and E. G. Stanley (2007). Expansion of Human Embryonic Stem Cells In Vitro. Current Protocols in Stem Cell Biology, John Wiley & Sons, Inc.
- Dolnikov, K., M. Shilkrut, N. Zeevi-Levin, S. Gerech-Nir, M. Amit, A. Danon, J. Itskovitz-Eldor and O. Binah (2006). "Functional properties of human embryonic stem cell-derived cardiomyocytes: intracellular Ca²⁺ handling and the role of sarcoplasmic reticulum in the contraction." Stem Cells **24**(2): 236-245.
- Ebert, S. N., Q. Rong, S. Boe and K. Pfeifer (2008). "Catecholamine-synthesizing cells in the embryonic mouse heart." Ann N Y Acad Sci **1148**: 317-324.
- Ebert, S. N., Q. Rong, S. Boe, R. P. Thompson, A. Grinberg and K. Pfeifer (2004). "Targeted insertion of the Cre-recombinase gene at the phenylethanolamine n-methyltransferase locus: a new model for studying the developmental distribution of adrenergic cells." Dev Dyn **231**(4): 849-858.
- Ebert, S. N. and D. G. Taylor (2006). "Catecholamines and development of cardiac pacemaking: an intrinsically intimate relationship." Cardiovasc Res **72**(3): 364-374.
- Ebert, S. N. and R. P. Thompson (2001). "Embryonic epinephrine synthesis in the rat heart before innervation: association with pacemaking and conduction tissue development." Circ Res **88**(1): 117-124.
- Egert, U., D. Heck and A. Aertsen (2002). "Two-dimensional monitoring of spiking networks in acute brain slices." Exp Brain Res **142**(2): 268-274.
- Eisenhofer, G., I. J. Kopin and D. S. Goldstein (2004). "Catecholamine metabolism: a contemporary view with implications for physiology and medicine." Pharmacol Rev **56**(3): 331-349.
- Erickson, J. D., L. E. Eiden and B. J. Hoffman (1992). "Expression cloning of a reserpine-sensitive vesicular monoamine transporter." Proc Natl Acad Sci U S A **89**(22): 10993-10997.
- Evans, M. J. and M. H. Kaufman (1981). "Establishment in culture of pluripotential cells from mouse embryos." Nature **292**(5819): 154-156.
- Fabiato, A. (1983). "Calcium-induced release of calcium from the cardiac sarcoplasmic reticulum." Am J Physiol **245**(1): C1-14.
- Fatima, A., G. Xu, K. Shao, S. Papadopoulos, M. Lehmann, J. J. Arnaiz-Cot, A. O. Rosa, F. Nguemo, M. Matzkies, S. Dittmann, S. L. Stone, M. Linke, U. Zechner, V. Beyer, H. C. Hennies, S. Rosenkranz, B. Klauke, A. S. Parwani, W. Haverkamp, G. Pfitzer, M. Farr, L. Cleemann, M. Morad, H. Milting, J. Hescheler and T. Saric (2011). "In vitro

- modeling of ryanodine receptor 2 dysfunction using human induced pluripotent stem cells." Cell Physiol Biochem **28**(4): 579-592.
- Fei, H., A. Grygoruk, E. S. Brooks, A. Chen and D. E. Krantz (2008). "Trafficking of vesicular neurotransmitter transporters." Traffic **9**(9): 1425-1436.
- Feng, R., S. C. Desbordes, H. Xie, E. S. Tillo, F. Pixley, E. R. Stanley and T. Graf (2008). "PU.1 and C/EBPalpha/beta convert fibroblasts into macrophage-like cells." Proc Natl Acad Sci U S A **105**(16): 6057-6062.
- Flach, F. F. (1955). "Clinical effectiveness of reserpine." Ann N Y Acad Sci **61**(1): 161-166.
- Frederiksen, K. and R. D. McKay (1988). "Proliferation and differentiation of rat neuroepithelial precursor cells in vivo." J Neurosci **8**(4): 1144-1151.
- Freis, E. D. (1954). "Mental depression in hypertensive patients treated for long periods with large doses of reserpine." N Engl J Med **251**(25): 1006-1008.
- Freis, E. D. and R. Ari (1954). "Clinical and experimental effects of reserpine in patients with essential hypertension." Ann N Y Acad Sci **59**(1): 45-53.
- Frenzel, L. P., Z. Abdullah, A. K. Kriegeskorte, R. Dieterich, N. Lange, D. H. Busch, M. Kronke, O. Utermohlen, J. Hescheler and T. Saric (2009). "Role of natural-killer group 2 member D ligands and intercellular adhesion molecule 1 in natural killer cell-mediated lysis of murine embryonic stem cells and embryonic stem cell-derived cardiomyocytes." Stem Cells **27**(2): 307-316.
- Fridericia, L. S. (1920). "Die Systolendauer im Elektrokardiogramm bei normalen Menschen und bei Herzkranken." Acta Medica Scandinavica **53**(1): 469-486.
- Gadue, P., T. L. Huber, P. J. Paddison and G. M. Keller (2006). "Wnt and TGF-beta signaling are required for the induction of an in vitro model of primitive streak formation using embryonic stem cells." Proc Natl Acad Sci U S A **103**(45): 16806-16811.
- Germanguz, I., O. Sedan, N. Zeevi-Levin, R. Shtrichman, E. Barak, A. Ziskind, S. Eliyahu, G. Meiry, M. Amit, J. Itskovitz-Eldor and O. Binah (2011). "Molecular characterization and functional properties of cardiomyocytes derived from human inducible pluripotent stem cells." Journal of Cellular and Molecular Medicine **15**(1): 38-51.
- Gilsbach, R., J. Albarran-Juarez and L. Hein (2011). "Pre- versus postsynaptic signaling by alpha(2)-adrenoceptors." Curr Top Membr **67**: 139-160.
- Gilsbach, R., M. Brede, N. Beetz, E. Moura, V. Muthig, C. Gerstner, F. Barreto, S. Neubauer, M. A. Vieira-Coelho and L. Hein (2007). "Heterozygous alpha 2C-adrenoceptor-deficient mice develop heart failure after transverse aortic constriction." Cardiovasc Res **75**(4): 728-737.

References

- Haegel, H., L. Larue, M. Ohsugi, L. Fedorov, K. Herrenknecht and R. Kemler (1995). "Lack of beta-catenin affects mouse development at gastrulation." Development **121**(11): 3529-3537.
- Halbach, M. (2006). Messung und Charakterisierung von kardialen Feldpotentialen mittels microelectrode arrays.
- Halbach, M., U. Egert, J. Hescheler and K. Banach (2003). "Estimation of action potential changes from field potential recordings in multicellular mouse cardiac myocyte cultures." Cell Physiol Biochem **13**(5): 271-284.
- Halbach, M., F. Pillekamp, K. Brockmeier, J. Hescheler, J. Muller-Ehmsen and M. Reppel (2006). "Ventricular slices of adult mouse hearts - a new multicellular in vitro model for electrophysiological studies." Cellular Physiology and Biochemistry **18**(1-3): 1-8.
- Hammerle, H., U. Egert, A. Mohr and W. Nisch (1994). "Extracellular recording in neuronal networks with substrate integrated microelectrode arrays." Biosens Bioelectron **9**(9-10): 691-696.
- Harada, A., J. Teng, Y. Takei, K. Oguchi and N. Hirokawa (2002). "MAP2 is required for dendrite elongation, PKA anchoring in dendrites, and proper PKA signal transduction." J Cell Biol **158**(3): 541-549.
- Hattori, F., H. Chen, H. Yamashita, S. Tohyama, Y. S. Satoh, S. Yuasa, W. Li, H. Yamakawa, T. Tanaka, T. Onitsuka, K. Shimoji, Y. Ohno, T. Egashira, R. Kaneda, M. Murata, K. Hidaka, T. Morisaki, E. Sasaki, T. Suzuki, M. Sano, S. Makino, S. Oikawa and K. Fukuda (2010). "Nongenetic method for purifying stem cell-derived cardiomyocytes." Nat Methods **7**(1): 61-66.
- Hebert, J. M., M. Boyle and G. R. Martin (1991). "mRNA localization studies suggest that murine FGF-5 plays a role in gastrulation." Development **112**(2): 407-415.
- Hein, L., J. D. Altman and B. K. Kobilka (1999). "Two functionally distinct alpha2-adrenergic receptors regulate sympathetic neurotransmission." Nature **402**(6758): 181-184.
- Hescheler, J., B. K. Fleischmann, M. Wartenberg, W. Bloch, E. Kolossov, G. Ji, K. Addicks and H. Sauer (1999). "Establishment of ionic channels and signalling cascades in the embryonic stem cell-derived primitive endoderm and cardiovascular system." Cells Tissues Organs **165**(3-4): 153-164.
- Hieble, J. P., D. B. Bylund, D. E. Clarke, D. C. Eikenburg, S. Z. Langer, R. J. Lefkowitz, K. P. Minneman and R. R. Ruffolo, Jr. (1995). "International Union of Pharmacology. X.

- Recommendation for nomenclature of alpha 1-adrenoceptors: consensus update." Pharmacol Rev **47**(2): 267-270.
- Hodach, R. J., E. F. Gilbert and J. F. Fallon (1974). "Aortic arch anomalies associated with the administration of epinephrine in chick embryos." Teratology **9**(2): 203-209.
- Hsu, F.-Y. (1933). "The effect of adrenaline and acetylcholine on the heart rate of the chick embryo." Chin J Physiol **VII**: 243-252.
- Huang, M. H., D. S. Friend, M. E. Sunday, K. Singh, K. Haley, K. F. Austen, R. A. Kelly and T. W. Smith (1996). "An intrinsic adrenergic system in mammalian heart." J Clin Invest **98**(6): 1298-1303.
- Huang, M. H., V. Nguyen, Y. Wu, S. Rastogi, C. Y. Lui, Y. Birnbaum, H. Q. Wang, D. L. Ware, M. Chauhan, N. Garg, K. K. Poh, L. Ye, A. R. Omar, H. C. Tan, B. F. Uretsky and K. Fujise (2009). "Reducing ischaemia/reperfusion injury through delta-opioid-regulated intrinsic cardiac adrenergic cells: adrenoceptor co-signalling." Cardiovasc Res **84**(3): 452-460.
- Ieda, M., J. D. Fu, P. Delgado-Olguin, V. Vedantham, Y. Hayashi, B. G. Bruneau and D. Srivastava (2010). "Direct reprogramming of fibroblasts into functional cardiomyocytes by defined factors." Cell **142**(3): 375-386.
- Ignarro, L. J. and F. E. Shideman (1968). "Appearance and concentrations of catecholamines and their biosynthesis in the embryonic and developing chick." J Pharmacol Exp Ther **159**(1): 38-48.
- Itskovitz-Eldor, J., M. Schuldiner, D. Karsenti, A. Eden, O. Yanuka, M. Amit, H. Soreq and N. Benvenisty (2000). "Differentiation of human embryonic stem cells into embryoid bodies compromising the three embryonic germ layers." Mol Med **6**(2): 88-95.
- Itzhaki, I., L. Maizels, I. Huber, L. Zwi-Dantsis, O. Caspi, A. Winterstern, O. Feldman, A. Gepstein, G. Arbel, H. Hammerman, M. Boulos and L. Gepstein (2011). "Modelling the long QT syndrome with induced pluripotent stem cells." Nature **471**(7337): 225-229.
- Janowski, E., L. Cleemann, P. Sasse and M. Morad (2006). "Diversity of Ca²⁺ signaling in developing cardiac cells." Ann N Y Acad Sci **1080**: 154-164.
- Jensen, B. C., P. M. Swigart, T. De Marco, C. Hoopes and P. C. Simpson (2009). "{alpha}1-Adrenergic receptor subtypes in nonfailing and failing human myocardium." Circ Heart Fail **2**(6): 654-663.
- Jung, C. B., A. Moretti, M. Mederos y Schnitzler, L. Iop, U. Storch, M. Bellin, T. Dorn, S. Ruppenthal, S. Pfeiffer, A. Goedel, R. J. Dirschinger, M. Seyfarth, J. T. Lam, D.

References

- Sinnecker, T. Gudermann, P. Lipp and K. L. Laugwitz (2012). "Dantrolene rescues arrhythmogenic RYR2 defect in a patient-specific stem cell model of catecholaminergic polymorphic ventricular tachycardia." EMBO Mol Med **4**(3): 180-191.
- Jurna, I. and G. Lanzer (1969). "Inhibition of the effect of reserpine on motor control by drugs which influence reserpine rigidity." Naunyn Schmiedebergs Arch Exp Pathol Pharmacol **262**(3): 309-324.
- Katsetos, C. D., A. Legido, E. Perentes and S. J. Mork (2003). "Class III beta-tubulin isotype: a key cytoskeletal protein at the crossroads of developmental neurobiology and tumor neuropathology." J Child Neurol **18**(12): 851-866; discussion 867.
- Kattman, S. J., A. D. Witty, M. Gagliardi, N. C. Dubois, M. Niapour, A. Hotta, J. Ellis and G. Keller (2011). "Stage-specific optimization of activin/nodal and BMP signaling promotes cardiac differentiation of mouse and human pluripotent stem cell lines." Cell Stem Cell **8**(2): 228-240.
- Kent, W. J. (2002). "BLAT--the BLAST-like alignment tool." Genome Res **12**(4): 656-664.
- Keys, J. R. and W. J. Koch (2004). "The adrenergic pathway and heart failure." Recent Prog Horm Res **59**: 13-30.
- Khan, J. M., A. R. Lyon and S. E. Harding (2013). "The case for induced pluripotent stem cell-derived cardiomyocytes in pharmacological screening." Br J Pharmacol **169**(2): 304-317.
- Kho, C., A. Lee and R. J. Hajjar (2012). "Altered sarcoplasmic reticulum calcium cycling--targets for heart failure therapy." Nat Rev Cardiol **9**(12): 717-733.
- Kim, D., C. H. Kim, J. I. Moon, Y. G. Chung, M. Y. Chang, B. S. Han, S. Ko, E. Yang, K. Y. Cha, R. Lanza and K. S. Kim (2009). "Generation of human induced pluripotent stem cells by direct delivery of reprogramming proteins." Cell Stem Cell **4**(6): 472-476.
- Kim, J. B., V. Sebastiano, G. Wu, M. J. Arauzo-Bravo, P. Sasse, L. Gentile, K. Ko, D. Ruau, M. Ehrlich, D. van den Boom, J. Meyer, K. Hubner, C. Bernemann, C. Ortmeier, M. Zenke, B. K. Fleischmann, H. Zaehres and H. R. Scholer (2009). "Oct4-induced pluripotency in adult neural stem cells." Cell **136**(3): 411-419.
- Klaus, A., Y. Saga, M. M. Taketo, E. Tzahor and W. Birchmeier (2007). "Distinct roles of Wnt/beta-catenin and Bmp signaling during early cardiogenesis." Proc Natl Acad Sci U S A **104**(47): 18531-18536.
- Kobayashi, K., S. Morita, H. Sawada, T. Mizuguchi, K. Yamada, I. Nagatsu, T. Hata, Y. Watanabe, K. Fujita and T. Nagatsu (1995). "Targeted disruption of the tyrosine

- hydroxylase locus results in severe catecholamine depletion and perinatal lethality in mice." *J Biol Chem* **270**(45): 27235-27243.
- Kobayashi, K., Y. Noda, N. Matsushita, K. Nishii, H. Sawada, T. Nagatsu, D. Nakahara, R. Fukabori, Y. Yasoshima, T. Yamamoto, M. Miura, M. Kano, T. Mamiya, Y. Miyamoto and T. Nabeshima (2000). "Modest neuropsychological deficits caused by reduced noradrenaline metabolism in mice heterozygous for a mutated tyrosine hydroxylase gene." *J Neurosci* **20**(6): 2418-2426.
- Kobayashi, K. and H. Sano (2000). "Dopamine deficiency in mice." *Brain Dev* **22 Suppl 1**: S54-60.
- Kolossov, E., B. K. Fleischmann, Q. Liu, W. Bloch, S. Viatchenko-Karpinski, O. Manzke, G. J. Ji, H. Bohlen, K. Addicks and J. Hescheler (1998). "Functional characteristics of ES cell-derived cardiac precursor cells identified by tissue-specific expression of the green fluorescent protein." *J Cell Biol* **143**(7): 2045-2056.
- Kolossov, E., Z. J. Lu, I. Drobinskaya, N. Gassanov, Y. Q. Duan, H. Sauer, O. Manzke, W. Bloch, H. Bohlen, J. Hescheler and B. K. Fleischmann (2005). "Identification and characterization of embryonic stem cell-derived pacemaker and atrial cardiomyocytes." *Faseb Journal* **19**(1): 577-+.
- Kuzmenkin, A., H. Liang, G. Xu, K. Pfannkuche, H. Eichhorn, A. Fatima, H. Luo, T. Saric, M. Wernig, R. Jaenisch and J. Hescheler (2009). "Functional characterization of cardiomyocytes derived from murine induced pluripotent stem cells in vitro." *Faseb J* **23**(12): 4168-4180.
- Laflamme, M. A., K. Y. Chen, A. V. Naumova, V. Muskheli, J. A. Fugate, S. K. Dupras, H. Reinecke, C. Xu, M. Hassanipour, S. Police, C. O'Sullivan, L. Collins, Y. Chen, E. Minami, E. A. Gill, S. Ueno, C. Yuan, J. Gold and C. E. Murry (2007). "Cardiomyocytes derived from human embryonic stem cells in pro-survival factors enhance function of infarcted rat hearts." *Nat Biotechnol* **25**(9): 1015-1024.
- Lands, A. M., A. Arnold, J. P. McAuliff, F. P. Luduena and T. G. Brown, Jr. (1967). "Differentiation of receptor systems activated by sympathomimetic amines." *Nature* **214**(5088): 597-598.
- Langer, S. Z. (1974). "Presynaptic regulation of catecholamine release." *Biochem Pharmacol* **23**(13): 1793-1800.
- Lehmann, M., F. Nguemo, V. Wagh, K. Pfannkuche, J. Hescheler and M. Reppel (2013). "Evidence for a Critical Role of Catecholamines for Cardiomyocyte Lineage

- Commitment in Murine Embryonic Stem Cells." PLoS ONE **8(8)** [10.1371/journal.pone.0070913](https://doi.org/10.1371/journal.pone.0070913).
- Lendahl, U., L. B. Zimmerman and R. D. McKay (1990). "CNS stem cells express a new class of intermediate filament protein." Cell **60(4)**: 585-595.
- Liang, H., M. Halbach, T. Hannes, B. K. Fleischmann, M. Tang, H. Schunkert, J. Hescheler and M. Reppel (2010). "Electrophysiological basis of the first heart beats." Cell Physiol Biochem **25(6)**: 561-570.
- Limbird, L. E. (1988). "Receptors linked to inhibition of adenylate cyclase: additional signaling mechanisms." Faseb J **2(11)**: 2686-2695.
- Link, R. E., K. Desai, L. Hein, M. E. Stevens, A. Chruscinski, D. Bernstein, G. S. Barsh and B. K. Kobilka (1996). "Cardiovascular regulation in mice lacking alpha2-adrenergic receptor subtypes b and c." Science **273(5276)**: 803-805.
- Liu, Y., D. E. Krantz, C. Waites and R. H. Edwards (1999). "Membrane trafficking of neurotransmitter transporters in the regulation of synaptic transmission." Trends Cell Biol **9(9)**: 356-363.
- Lorenz, W., J. W. Lomasney, S. Collins, J. W. Regan, M. G. Caron and R. J. Lefkowitz (1990). "Expression of three alpha 2-adrenergic receptor subtypes in rat tissues: implications for alpha 2 receptor classification." Mol Pharmacol **38(5)**: 599-603.
- Maltsev, V. A., G. J. Ji, A. M. Wobus, B. K. Fleischmann and J. Hescheler (1999). "Establishment of beta-adrenergic modulation of L-type Ca²⁺ current in the early stages of cardiomyocyte development." Circ Res **84(2)**: 136-145.
- Manasek, F. J. (1968). "Embryonic development of the heart. I. A light and electron microscopic study of myocardial development in the early chick embryo." J Morphol **125(3)**: 329-365.
- Manner, J. (2006). "Extracardiac tissues and the epigenetic control of myocardial development in vertebrate embryos." Ann Anat **188(3)**: 199-212.
- Manner, J., J. M. Perez-Pomares, D. Macias and R. Munoz-Chapuli (2001). "The origin, formation and developmental significance of the epicardium: a review." Cells Tissues Organs **169(2)**: 89-103.
- Markowitz, C. (1931). "RESPONSE OF EXPLANTED EMBRYONIC CARDIAC TISSUE TO EPINEPHRINE AND ACETYLCHOLINE " American Journal of Physiology **97((2))**: 271-275.

- Martin, G. R. (1981). "Isolation of a pluripotent cell line from early mouse embryos cultured in medium conditioned by teratocarcinoma stem cells." Proc Natl Acad Sci U S A **78**(12): 7634-7638.
- Meidahl Petersen, K., E. Jimenez-Solem, J. T. Andersen, M. Petersen, K. Brødbæk, L. Køber, C. Torp-Pedersen and H. E. Poulsen (2012). "β-Blocker treatment during pregnancy and adverse pregnancy outcomes: a nationwide population-based cohort study." BMJ Open **2**(4).
- Mesnard, D., M. Guzman-Ayala and D. B. Constam (2006). "Nodal specifies embryonic visceral endoderm and sustains pluripotent cells in the epiblast before overt axial patterning." Development **133**(13): 2497-2505.
- Molinoff, P. B. and J. Axelrod (1971). "Biochemistry of catecholamines." Annu Rev Biochem **40**: 465-500.
- Moorman, A. F. and W. H. Lamers (1994). "Molecular anatomy of the developing heart." Trends Cardiovasc Med **4**(6): 257-264.
- Moretti, A., M. Bellin, A. Welling, C. B. Jung, J. T. Lam, L. Bott-Flugel, T. Dorn, A. Goedel, C. Hohnke, F. Hofmann, M. Seyfarth, D. Sinnecker, A. Schomig and K. L. Laugwitz (2010). "Patient-specific induced pluripotent stem-cell models for long-QT syndrome." N Engl J Med **363**(15): 1397-1409.
- Morrison, A. B. and R. A. Webster (1973). "Reserpine rigidity and adrenergic neurones." Neuropharmacology **12**(8): 725-733.
- Mummery, C., D. Ward-van Oostwaard, P. Doevendans, R. Spijker, S. van den Brink, R. Hassink, M. van der Heyden, T. Opthof, M. Pera, A. B. de la Riviere, R. Passier and L. Tertoolen (2003). "Differentiation of human embryonic stem cells to cardiomyocytes - Role of coculture with visceral endoderm-like cells." Circulation **107**(21): 2733-2740.
- Mummery, C. L., T. A. van Achterberg, A. J. van den Eijnden-van Raaij, L. van Haaster, A. Willemsse, S. W. de Laat and A. H. Piersma (1991). "Visceral-endoderm-like cell lines induce differentiation of murine P19 embryonal carcinoma cells." Differentiation **46**(1): 51-60.
- Nakagawa, M., M. Koyanagi, K. Tanabe, K. Takahashi, T. Ichisaka, T. Aoi, K. Okita, Y. Mochiduki, N. Takizawa and S. Yamanaka (2008). "Generation of induced pluripotent stem cells without Myc from mouse and human fibroblasts." Nat Biotechnol **26**(1): 101-106.

References

- Nirenberg, M. J., J. Chan, Y. Liu, R. H. Edwards and V. M. Pickel (1996). "Ultrastructural localization of the vesicular monoamine transporter-2 in midbrain dopaminergic neurons: potential sites for somatodendritic storage and release of dopamine." J Neurosci **16**(13): 4135-4145.
- Nirenberg, M. J., J. Chan, Y. Liu, R. H. Edwards and V. M. Pickel (1997). "Vesicular monoamine transporter-2: immunogold localization in striatal axons and terminals." Synapse **26**(2): 194-198.
- Nirenberg, M. J., Y. Liu, D. Peter, R. H. Edwards and V. M. Pickel (1995). "The vesicular monoamine transporter 2 is present in small synaptic vesicles and preferentially localizes to large dense core vesicles in rat solitary tract nuclei." Proc Natl Acad Sci U S A **92**(19): 8773-8777.
- Nostro, M. C., X. Cheng, G. M. Keller and P. Gadue (2008). "Wnt, activin, and BMP signaling regulate distinct stages in the developmental pathway from embryonic stem cells to blood." Cell Stem Cell **2**(1): 60-71.
- O'Connell, T. D., S. Ishizaka, A. Nakamura, P. M. Swigart, M. C. Rodrigo, G. L. Simpson, S. Cotecchia, D. G. Rokosh, W. Grossman, E. Foster and P. C. Simpson (2003). "The alpha(1A/C)- and alpha(1B)-adrenergic receptors are required for physiological cardiac hypertrophy in the double-knockout mouse." J Clin Invest **111**(11): 1783-1791.
- Okita, K., Y. Matsumura, Y. Sato, A. Okada, A. Morizane, S. Okamoto, H. Hong, M. Nakagawa, K. Tanabe, K. Tezuka, T. Shibata, T. Kunisada, M. Takahashi, J. Takahashi, H. Saji and S. Yamanaka (2011). "A more efficient method to generate integration-free human iPS cells." Nat Methods **8**(5): 409-412.
- Okita, K., N. Nagata and S. Yamanaka (2011). "Immunogenicity of induced pluripotent stem cells." Circ Res **109**(7): 720-721.
- Oliver, G. and E. A. Schafer (1895). "The Physiological Effects of Extracts of the Suprarenal Capsules." J Physiol **18**(3): 230-276.
- Otero-Gonzalez, L., R. Sierra-Alvarez, S. Boitano and J. A. Field (2012). "Application and validation of an impedance-based real time cell analyzer to measure the toxicity of nanoparticles impacting human bronchial epithelial cells." Environ Sci Technol **46**(18): 10271-10278.
- Pease, S., P. Braghetta, D. Gearing, D. Grail and R. L. Williams (1990). "Isolation of embryonic stem (ES) cells in media supplemented with recombinant leukemia inhibitory factor (LIF)." Dev Biol **141**(2): 344-352.

- Peaston, R. T. and C. Weinkove (2004). "Measurement of catecholamines and their metabolites." Ann Clin Biochem **41**(Pt 1): 17-38.
- Pera, M. F. and K. Hasegawa (2008). "Simpler and safer cell reprogramming." Nat Biotechnol **26**(1): 59-60.
- Pfannkuche, K., H. M. Liang, T. Hannes, J. Y. Xi, A. Fatima, F. Nguemo, M. Matzkies, M. Wernig, R. Jaenisch, F. Pillekamp, M. Halbach, H. Schunkert, T. Saric, J. Hescheler and M. Reppel (2009). "Cardiac Myocytes Derived from Murine Reprogrammed Fibroblasts: Intact Hormonal Regulation, Cardiac Ion Channel Expression and Development of Contractility." Cellular Physiology and Biochemistry **24**(1-2): 73-86.
- Powell, C. E. and I. H. Slater (1958). "Blocking of inhibitory adrenergic receptors by a dichloro analog of isoproterenol." J Pharmacol Exp Ther **122**(4): 480-488.
- Reppel, M., C. Boettinger and J. Hescheler (2004). "Beta-adrenergic and muscarinic modulation of human embryonic stem cell-derived cardiomyocytes." Cell Physiol Biochem **14**(4-6): 187-196.
- Reppel, M., P. Igelmund, U. Egert, F. Juchelka, J. Hescheler and I. Drobinskaya (2007). "Effect of cardioactive drugs on action potential generation and propagation in embryonic stem cell-derived cardiomyocytes." Cell Physiol Biochem **19**(5-6): 213-224.
- Rohrer, D. K., K. H. Desai, J. R. Jasper, M. E. Stevens, D. P. Regula, Jr., G. S. Barsh, D. Bernstein and B. K. Kobilka (1996). "Targeted disruption of the mouse beta1-adrenergic receptor gene: developmental and cardiovascular effects." Proc Natl Acad Sci U S A **93**(14): 7375-7380.
- Sa, S. and K. E. McCloskey (2012). "Stage-specific cardiomyocyte differentiation method for H7 and H9 human embryonic stem cells." Stem Cell Rev **8**(4): 1120-1128.
- Sagie, A., M. G. Larson, R. J. Goldberg, J. R. Bengtson and D. Levy (1992). "An improved method for adjusting the QT interval for heart rate (the Framingham Heart Study)." Am J Cardiol **70**(7): 797-801.
- Sanguinetti, M. C. and N. K. Jurkiewicz (1990). "Two components of cardiac delayed rectifier K⁺ current. Differential sensitivity to block by class III antiarrhythmic agents." J Gen Physiol **96**(1): 195-215.
- Sanguinetti, M. C. and N. K. Jurkiewicz (1991). "Delayed rectifier outward K⁺ current is composed of two currents in guinea pig atrial cells." Am J Physiol **260**(2 Pt 2): H393-399.

References

- Schlumpf, M. and W. Lichtensteiger (1979). "Catecholamines in the yolk sac epithelium of the rat." Anatomy and Embryology **156**(2): 177-187.
- Schouten, E. G., J. M. Dekker, P. Meppelink, F. J. Kok, J. P. Vandenbroucke and J. Pool (1991). "QT interval prolongation predicts cardiovascular mortality in an apparently healthy population." Circulation **84**(4): 1516-1523.
- Schuldiner, S. (1994). "A molecular glimpse of vesicular monoamine transporters." J Neurochem **62**(6): 2067-2078.
- Schwanke, K., S. Wunderlich, M. Reppel, M. E. Winkler, M. Matzkies, S. Groos, J. Itskovitz-Eldor, A. R. Simon, J. Hescheler, A. Haverich and U. Martin (2006). "Generation and characterization of functional cardiomyocytes from rhesus monkey embryonic stem cells." Stem Cells **24**(6): 1423-1432.
- Selzer, A. and H. W. Wray (1964). "Quinidine Syncope. Paroxysmal Ventricular Fibrillation Occurring during Treatment of Chronic Atrial Arrhythmias." Circulation **30**: 17-26.
- Stalsberg, H. and R. L. DeHaan (1969). "The precardiac areas and formation of the tubular heart in the chick embryo." Dev Biol **19**(2): 128-159.
- Starke, K. (1987). "Presynaptic alpha-autoreceptors." Rev Physiol Biochem Pharmacol **107**: 73-146.
- Starke, K. (2001). "Presynaptic autoreceptors in the third decade: focus on alpha2-adrenoceptors." J Neurochem **78**(4): 685-693.
- Stett, A., U. Egert, E. Guenther, F. Hofmann, T. Meyer, W. Nisch and H. Haemmerle (2003). "Biological application of microelectrode arrays in drug discovery and basic research." Anal Bioanal Chem **377**(3): 486-495.
- Stevens, D. R., A. Kuramasu, K. S. Eriksson, O. Selbach and H. L. Haas (2004). " α 2-Adrenergic receptor-mediated presynaptic inhibition of GABAergic IPSPs in rat histaminergic neurons." Neuropharmacology **46**(7): 1018-1022.
- Takahashi, K., K. Tanabe, M. Ohnuki, M. Narita, T. Ichisaka, K. Tomoda and S. Yamanaka (2007). "Induction of pluripotent stem cells from adult human fibroblasts by defined factors." Cell **131**(5): 861-872.
- Takahashi, K. and S. Yamanaka (2006). "Induction of pluripotent stem cells from mouse embryonic and adult fibroblast cultures by defined factors." Cell **126**(4): 663-676.
- Theurkauf, W. E. and R. B. Vallee (1982). "Molecular characterization of the cAMP-dependent protein kinase bound to microtubule-associated protein 2." J Biol Chem **257**(6): 3284-3290.

- Thomas, S. A., A. M. Matsumoto and R. D. Palmiter (1995). "Noradrenaline is essential for mouse fetal development." Nature **374**(6523): 643-646.
- Thomson, J. A., J. Itskovitz-Eldor, S. S. Shapiro, M. A. Waknitz, J. J. Swiergiel, V. S. Marshall and J. M. Jones (1998). "Embryonic stem cell lines derived from human blastocysts." Science **282**(5391): 1145-1147.
- Thomson, J. A., J. Kalishman, T. G. Golos, M. Durning, C. P. Harris, R. A. Becker and J. P. Hearn (1995). "Isolation of a primate embryonic stem cell line." Proc Natl Acad Sci U S A **92**(17): 7844-7848.
- Thomson, J. A. and V. S. Marshall (1998). "Primate embryonic stem cells." Curr Top Dev Biol **38**: 133-165.
- Torrealba, F. and M. A. Carrasco (2004). "A review on electron microscopy and neurotransmitter systems." Brain Res Brain Res Rev **47**(1-3): 5-17.
- Toyooka, Y., D. Shimosato, K. Murakami, K. Takahashi and H. Niwa (2008). "Identification and characterization of subpopulations in undifferentiated ES cell culture." Development **135**(5): 909-918.
- Vallier, L., D. Reynolds and R. A. Pedersen (2004). "Nodal inhibits differentiation of human embryonic stem cells along the neuroectodermal default pathway." Dev Biol **275**(2): 403-421.
- Vierbuchen, T., A. Ostermeier, Z. P. Pang, Y. Kokubu, T. C. Sudhof and M. Wernig (2010). "Direct conversion of fibroblasts to functional neurons by defined factors." Nature **463**(7284): 1035-1041.
- Wagner, B. H. and R. J. Anderson (1982). "Prevention of reserpine rigidity by alpha-2 adrenergic antagonists." Pharmacol Biochem Behav **16**(5): 731-735.
- Wang, G. Y., C. C. Yeh, B. C. Jensen, M. J. Mann, P. C. Simpson and A. J. Baker (2010). "Heart failure switches the RV alpha1-adrenergic inotropic response from negative to positive." Am J Physiol Heart Circ Physiol **298**(3): H913-920.
- Warren, L., P. D. Manos, T. Ahfeldt, Y. H. Loh, H. Li, F. Lau, W. Ebina, P. K. Mandal, Z. D. Smith, A. Meissner, G. Q. Daley, A. S. Brack, J. J. Collins, C. Cowan, T. M. Schlaeger and D. J. Rossi (2010). "Highly efficient reprogramming to pluripotency and directed differentiation of human cells with synthetic modified mRNA." Cell Stem Cell **7**(5): 618-630.
- Warren, L., Y. Ni, J. Wang and X. Guo (2012). "Feeder-free derivation of human induced pluripotent stem cells with messenger RNA." Sci Rep **2**: 657.

References

- Weihe, E. and L. E. Eiden (2000). "Chemical neuroanatomy of the vesicular amine transporters." *Faseb J* **14**(15): 2435-2449.
- Weiland, T., A. Berger, F. Essmann, U. M. Lauer, M. Bitzer and S. Venturelli (2012). "Kinetic tracking of therapy-induced senescence using the real-time cell analyzer single plate system." *Assay Drug Dev Technol* **10**(3): 289-295.
- Wernig, M., A. Meissner, J. P. Cassady and R. Jaenisch (2008). "c-Myc is dispensable for direct reprogramming of mouse fibroblasts." *Cell Stem Cell* **2**(1): 10-12.
- Wernig, M., A. Meissner, R. Foreman, T. Brambrink, M. Ku, K. Hochedlinger, B. E. Bernstein and R. Jaenisch (2007). "In vitro reprogramming of fibroblasts into a pluripotent ES-cell-like state." *Nature* **448**(7151): 318-324.
- Xi, B., T. Wang, N. Li, W. Ouyang, W. Zhang, J. Wu, X. Xu, X. Wang and Y. A. Abassi (2011). "Functional cardiotoxicity profiling and screening using the xCELLigence RTCA Cardio System." *J Lab Autom* **16**(6): 415-421.
- Xi, B., N. Yu, X. Wang, X. Xu and Y. A. Abassi (2008). "The application of cell-based label-free technology in drug discovery." *Biotechnol J* **3**(4): 484-495.
- Xu, C., S. Police, M. Hassanipour, Y. Li, Y. Chen, C. Priest, C. O'Sullivan, M. A. Laflamme, W. Z. Zhu, B. Van Biber, L. Hegerova, J. Yang, K. Delavan-Boorsma, A. Davies, J. Lebkowski and J. D. Gold (2011). "Efficient generation and cryopreservation of cardiomyocytes derived from human embryonic stem cells." *Regen Med* **6**(1): 53-66.
- Yang, L., M. H. Soonpaa, E. D. Adler, T. K. Roepke, S. J. Kattman, M. Kennedy, E. Henckaerts, K. Bonham, G. W. Abbott, R. M. Linden, L. J. Field and G. M. Keller (2008). "Human cardiovascular progenitor cells develop from a KDR+ embryonic-stem-cell-derived population." *Nature* **453**(7194): 524-528.
- Ye, J., G. Coulouris, I. Zaretskaya, I. Cutcutache, S. Rozen and T. L. Madden (2012). "Primer-BLAST: a tool to design target-specific primers for polymerase chain reaction." *BMC Bioinformatics* **13**: 134.
- Yoshida, Y. and S. Yamanaka (2010). "Recent stem cell advances: induced pluripotent stem cells for disease modeling and stem cell-based regeneration." *Circulation* **122**(1): 80-87.
- Yu, J., M. A. Vodyanik, K. Smuga-Otto, J. Antosiewicz-Bourget, J. L. Frane, S. Tian, J. Nie, G. A. Jonsdottir, V. Ruotti, R. Stewart, Slukvin, II and J. A. Thomson (2007). "Induced pluripotent stem cell lines derived from human somatic cells." *Science* **318**(5858): 1917-1920.

-
- Zhang, J., G. F. Wilson, A. G. Soerens, C. H. Koonce, J. Yu, S. P. Palecek, J. A. Thomson and T. J. Kamp (2009). "Functional cardiomyocytes derived from human induced pluripotent stem cells." Circ Res **104**(4): e30-41.
- Zhao, T., Z. N. Zhang, Z. Rong and Y. Xu (2011). "Immunogenicity of induced pluripotent stem cells." Nature **474**(7350): 212-215.
- Zheng, M., Q. D. Han and R. P. Xiao (2004). "Distinct beta-adrenergic receptor subtype signaling in the heart and their pathophysiological relevance." Sheng Li Xue Bao **56**(1): 1-15.
- Zhong, H. and K. P. Minneman (1999). "Alpha1-adrenoceptor subtypes." Eur J Pharmacol **375**(1-3): 261-276.
- Zhou, H., S. Wu, J. Y. Joo, S. Zhu, D. W. Han, T. Lin, S. Trauger, G. Bien, S. Yao, Y. Zhu, G. Siuzdak, H. R. Scholer, L. Duan and S. Ding (2009). "Generation of induced pluripotent stem cells using recombinant proteins." Cell Stem Cell **4**(5): 381-384.
- Zhou, Q. Y., C. J. Quafe and R. D. Palmiter (1995). "Targeted disruption of the tyrosine hydroxylase gene reveals that catecholamines are required for mouse fetal development." Nature **374**(6523): 640-643.
- Zorn, A. M. and J. M. Wells (2009). "Vertebrate endoderm development and organ formation." Annu Rev Cell Dev Biol **25**: 221-251.

VII Primers

| Gene | Forward-primer | Reverse-primer |
|--------------------|-------------------------|-------------------------|
| <i>Zpf42(Rex1)</i> | GAGACTGAGGAAGATGGCTTCC | CTGGCGAGAAAGGTTTTGCTCC |
| <i>Oct4</i> | CAGCAGATCACTCACATCGCCA | GCCTCATACTCTTCTCGTTGGG |
| <i>Nanog</i> | GAACGCCTCATCAATGCCTGCA | GAATCAGGGCTGCCTTGAAGAG |
| <i>Fgf5</i> | AGAGTGGGCATCGGTTTCCATC | CCTACAATCCCCTGAGACACAG |
| <i>Map2</i> | GCTGTAGCAGTCCTGAAAGGTG | CTTCCTCCACTGTGGCTGTTTG |
| <i>Tubb3</i> | CATCAGCGATGAGCACGGCATA | GGTTCCAAGTCCACCAGAATGG |
| <i>Nes</i> | AGGAGAAGCAGGGTCTACAGAG | AGTTCTCAGCCTCCAGCAGAGT |
| <i>Sox17</i> | GCCGATGAACGCCTTTATGGTG | TCTCTGCCAAGGTCAACGCCTT |
| <i>Fox2a</i> | TGGAGCTGTGTATGGTCCTGAG | GTTGGGTAAGGGAAGCCAGGAA |
| <i>Hnf4</i> | TGCGAACTCCTTCTGGATGACC | CAGCACGTCCTTAAACACCATGG |
| <i>Alb</i> | CAGTGTTGTGCAGAGGCTGACA | GGAGCACTTCATTCTCTGACGG |
| <i>Afp</i> | GCTCACATCCACGAGGAGTGTT | CAGAAGCCTAGTTGGATCATGGG |
| <i>Th</i> | TGCACACAGTACATCCGTCATGC | GCAAATGTGCGGTCAGCCAACA |
| <i>Ddc</i> | GGAGCCAGAAACATACGAGGAC | GCATGTCTGCAAGCATAGCTGG |
| <i>Dbh</i> | GAGACTGCCTTTGTGTTGACCG | CGAGCACAGTAACCACCTTCCT |
| <i>Pnmt1</i> | CAGGAGCCTTTGACTGGAGTGT | TCGATAGGCAGGACTCGCTTCA |
| <i>Myh6</i> | GCTGGAAGATGAGTGCTCAGAG | CCAGCCATCTCCTCTGTTAGGT |
| <i>Mlc2a</i> | AGGAAGCCATCCTGAGTGCCTT | CATGGGTGTCAGCGCAAACAGT |
| <i>Nkx2.5</i> | TGCTCTCCTGCTTTCCCAGCC | CTTTGTCCAGCTCCACTGCCTT |
| <i>Gata4</i> | GCCTCTATCACAAGATGAACGGC | TACAGGCTCACCTCGGCATTA |
| <i>T-bra</i> | ATCCACCCAGACTCGCCCAATT | CTCTCACGATGTGAATCCGAGG |
| <i>ACTB</i> | CATTGCTGACAGGATGCAGAAGG | TGCTGGAAGGTGGACAGTGAGG |
| <i>Adrb1</i> | GACGCTCACCAACCTCTTCA | ACTTGGGGTCGTTGTAGCAG |
| <i>Adrb2</i> | TGAAGGAAGATTCCACGCCC | CCGTTCTGCCGTTGCTATTG |
| <i>Adrb3</i> | AGGCACAGGAATGCCACTCCAA | GCTTAGCCACAACGAACACTCG |
| <i>Adra1a</i> | GAGTTTGAGGGCTCAGCAGT | AGTGACTCTCAACTTGGCCG |
| <i>Adra1b</i> | AGAACCCTTCTACGCCCTCT | GGAGCACGGGTAGATGATGG |
| <i>Adr1d</i> | ATCGTGGTGTCATGTAAGTCCG | GACGCCCTCTGATGGTTTCA |
| <i>Adra2a</i> | CAGGTGACACTGACGCTGGTTT | GACACCAGGAAGAGGTTTTGGG |
| <i>Adra2b</i> | CCCTCATCTACAAGGGCGAC | TTCGGGATCTTCAGGGGTCT |
| <i>Adra2c</i> | TCACCGTGGTAGGCAATGTG | GCGGTAGAACGAGACGAGAG |
| <i>Gapdh</i> | GGCTCATGACCACAGTCCAT | ACCTTGCCACAGCCTTG |

VIII Antibodies

| Primary antibodies | Manufacturer; Prod# | dilution |
|---|------------------------------|-----------------|
| anti- α -Actinin | Sigma-Aldrich; A7811 | 1:800 |
| anti-cardiac Troponin I | Chemicon; MAB3438 | 1:1,000 |
| anti-cardiac Troponin T | Thermo Scientific; MS-295-P1 | 1:1,000 |
| anti-HCN4 | Alomone Labs; APC-052 | 1:300 |
| anti- β -III-Tubulin | GeneTex; GTX27751 | 1:1,000 |
| anti-NCAM | GeneTex; GTX19782 | 1:200 |
| sheep-anti-dopamine- β -hydroxylase | GeneTex; 19353 | 1:200 |
| Secondary antibodies | | |
| goat-anti-mouse Alexa Fluor 555 | Invitrogen; A21081 | 1:1,000 |
| donkey-anti-sheep Alexa Fluor 647 | Molecular Probes; A-21448 | 1:200 |
| Nuclear Staining | | |
| Hochst H33342 | Sigma Aldrich; B2261 | 1:1,000 |

IX Materials

a) Cell culture supplements & consumables

| | |
|--|---|
| DMEM | Invitrogen, Carlsbad, USA |
| IMDM | Invitrogen, Carlsbad, USA |
| IMDM-GlutaMAX™ | Invitrogen, Carlsbad, USA |
| Knockout™ DMEM | Invitrogen, Carlsbad, USA |
| Knockout™ Serum Replacement | Invitrogen, Carlsbad, USA |
| FBS (Standard) | Invitrogen, Carlsbad, USA |
| MEM NEAA (100x) | Invitrogen, Carlsbad, USA |
| β-ME | Invitrogen, Carlsbad, USA |
| L-glutamine | Invitrogen, Carlsbad, USA |
| Pen/Strep | Invitrogen, Carlsbad, USA |
| Trypan blue | Invitrogen, Carlsbad, USA |
| Trypsin/EDTA (0.05%/0.25%) | Invitrogen, Carlsbad, USA |
| Collagenase IV | Invitrogen, Carlsbad, USA |
| PBS (+/+)/(/-) | Invitrogen, Carlsbad, USA |
| Geneticin® Selective Antibiotic (G418 Sulfate) | Invitrogen, Carlsbad, USA |
| Puromycin Dihydrochloride | Invitrogen, Carlsbad, USA |
| Gelatin (porcine) | Sigma-Aldrich, St. Louis, USA |
| HyClone™ FBS | Thermo Fisher Scientific Inc., Waltham, USA |
| CryoTubes 1.8 ml | Nunc® Thermo Fisher Scientific Inc., Waltham, USA |
| Nylon cell strainer (100μm) | BD Falcon™ Biosciences, Bedford; USA |
| culture dishes (3.5, 6, and 10 cm) | BD Falcon™ Biosciences, Bedford; USA |
| tubes (15 ml, 50 ml) | BD Falcon™ Biosciences, Bedford; USA |
| bacteriological culture dishes (3 and 10 cm) | Greiner Bio-One GmbH, Frickenhausen, Germany |
| multi-well culture dishes | Greiner Bio-One GmbH, Frickenhausen, Germany |
| pipettes (1 ml - 50 ml) | Greiner Bio-One GmbH, Frickenhausen, Germany |
| tubes (1.5 ml) | Greiner Bio-One GmbH, Frickenhausen, Germany |
| pipette tips | SARSTEDT AG & Co., Nümbrecht, Germany |
| facs tubes 5 ml | SARSTEDT AG & Co., Nümbrecht, Germany |
| syringes & needles | B. Braun, Melsungen, Germany |

b) Growth factors

| | |
|---|---------------------------------|
| activin A | PeptoTech, Hamburg, Germany |
| BMP4 | PeptoTech, Hamburg, Germany |
| bFGF | PeptoTech, Hamburg, Germany |
| LIF (ESGRO® Leukemia Inhibitory Factor) | Merck Millipore, Billerica, USA |

c) Molecular Biology Kits & Consumables

| | |
|---|---|
| DNA-Ladder (100 bp-10kb) | Fermentas |
| DNase I, Amplification Grade | Invitrogen, Carlsbad, USA |
| Fermentas™ Dream Taq™ PCR Master Mix (2X) | Thermo Fisher Scientific Inc., Waltham, USA |
| JumpStart™ REDTaq® ReadyMix™ Reaction Mix | Invitrogen, Carlsbad, USA |
| Multi Guard™ Barrier Tips (10µl, 100µl, 1000µl) | Sorenson Bioscience Inc. |
| PCR tubes | Bio-Rad Laboratories GmbH, München Germany |
| QuantiFAST SYBR Green PCR master mix | Qiagen, Hilden, Germany |
| SuperScript® Vilo™ cDNA Synthesis Kit | Invitrogen, Carlsbad, USA |
| TriZol® Reagent | Invitrogen, Carlsbad, USA |

d) Immunohistochemistry Materials

| | |
|---------------------------------|---|
| Cover slips (10 mm) | Paul Marienfeld GmbH, Lauda-Königshofen, Germany |
| Prolong Gold | Invitrogen, Carlsbad, USA |
| Roti®Block | Roth, Karlsruhe, Germany |
| silanized Histobond cover slips | Paul Marienfeld GmbH, Lauda-Königshofen, Germany |
| Tissue Tek® O.C.T.™ Compound | Sakura® Finetek Japan Co., Tokyo, Japan |

e) Drugs & Chemicals

| | |
|--------------------|-------------------------------|
| Amiodarone | Sigma-Aldrich, St. Louis, USA |
| CCH | Sigma-Aldrich, St. Louis, USA |
| DMSO | Sigma-Aldrich, St. Louis, USA |
| E4031 | Sigma-Aldrich, St. Louis, USA |
| EDTA | Sigma-Aldrich, St. Louis, USA |
| EtBr (1%) | Roth, Karlsruhe Germany |
| ISO | Sigma-Aldrich, St. Louis, USA |
| Lidocain | Sigma-Aldrich, St. Louis, USA |
| NH ₄ Cl | Sigma-Aldrich, St. Louis, USA |
| paraformaldehyde | Roth, Karlsruhe, Germany |
| Phentoleamine | Sigma-Aldrich, St. Louis, USA |
| Propidium Iodide | Sigma-Aldrich, St. Louis, USA |
| Propranolol | Sigma-Aldrich, St. Louis, USA |
| Resepine | Sigma-Aldrich, St. Louis, USA |
| SeaKem LE Agarose | Roth, Karlsruhe Germany |
| Sotalol | Sigma-Aldrich, St. Louis, USA |
| Sucrose | Sigma-Aldrich, St. Louis, USA |
| Tris | Roth, Karlsruhe, Germany |
| TritonX 100 | Sigma-Aldrich, St. Louis, USA |

f) Devices & Softwares

Microscopy

Axiovert 10/25/200

Carl Zeiss AG, Jena, Germany

AxioVision LE 4.5

Carl Zeiss AG, Jena, Germany

Flowcytometry

Facs Flow solution

BD Biosciences, Franklin Lakes, USA

Cell-wash solution

BD Biosciences, Franklin Lakes, USA

FACScan flow-cytometer

BD Biosciences, Franklin Lakes, USA

Cyflowic v 1.2.1

Turku, Finland

sqRT-PCR

peqSTAR 96 Universal Thermocycler

PEQLAB Biotechnologie GmbH, Erlangen, Germany

qRT-PCR

ABI-7500 Fast PCR system

Applied Biosystems, Weiterstadt, Germany

7500 Fast System SDS software 1.4.0.

Applied Biosystems, Weiterstadt, Germany

NanoDrop 1000

Thermo Fisher Scientific Inc., Waltham, USA

MEA

Multichannel Systems 1060-Inv-BC amplifier

Multichannel Systems, Reutlingen, Germany

MEA culture dishes

Multichannel Systems, Reutlingen, Germany

MCRack

Multichannel Systems, Reutlingen, Germany

MC DataTool

Multichannel Systems, Reutlingen, Germany

LabView

National Instruments, Austin, USA

Impedance measurement

E-plate 96

ACEA BIOSciences Inc., San Diego, USA

xCELLigence RTCA Cardio system

ACEA BIOSciences Inc., San Diego, USA

RTCA Cardio 1.0 software

ACEA BIOSciences Inc., San Diego, USA

Data processing/Data analysis

GraphPad InStat Version 3.10 (trial version)

GraphPad Software, Inc., San Diego, USA

GraphPad Prism®

GraphPad Software, Inc., San Diego, USA

Microsoft Office 2003+2010

Microsoft, USA

Origin7

OriginLab Corporation, Northampton, USA

CorelDraw X5

Corel Corporation, Ottawa, Kanada

Adobe Photoshop C3

Adobe Systems Incorporated, San Jose, USA

ImageJ
EndNote

National Institutes of Health, USA
Thomson Reuters, New York, USA

X Curriculum Vitae

Personal Details

Name Martin Lehmann, Dipl. Biol. t.o.
Nationality German
Date and Place of birth 14.11.1979, Hoyerswerda
Departmental address University Hospital Cologne, Institute for Neurophysiology,
Robert-Koch-Str. 39, 50931 Köln, Germany

Academic Career

PhD Thesis

2009-2013 Institute for Neurophysiology, University Hospital of the University of
Cologne

University Education

Master degree (Dipl.-Biol. technisch orientiert) in Technical Biology at the University of Stuttgart

09/07-05/08 Master Thesis at the “*Institute for Biochemistry*”, University of
Stuttgart, Stuttgart, Germany
„Studies to Characterize Components of the Gid-complex involved in
the Catabolite Degradation of FBPase in Yeast”
10/00-04/06 Bachelor Thesis at the “*BIO21 Institute for Biochemistry and
Biotechnology*”, University of Melbourne, Melbourne,
Australia
“Investigation of Purification Properties of the Monomeric Outer
Mitochondrial Membrane Translocase Tom70”

School Education

06/1999 Graduation „Erlangung der allgemeinen Hochschulreife (Abitur)“
1993-1999 Albert-Schweitzer Gymnasium, Neckarsulm
1991-1993 Hohen-Stauffen-Gymnasium, Bad Wimpfen
1987-1991 Grundschule Gundelsheim

XI Declaration

Ich versichere, daß ich die von mir vorgelegte Dissertation selbstständig angefertigt, die benutzten Quellen und Hilfsmittel vollständig angegeben und die Stellen der Arbeit - einschließlich Tabellen, Karten und Abbildungen -, die anderen Werken im Wortlaut oder dem Sinn nach entnommen sind, in jedem Einzelfall als Entlehnung kenntlich gemacht habe; daß diese Dissertation noch keiner anderen Fakultät oder Universität zur Prüfung vorgelegen hat; daß sie – abgesehen von unten angegebenen Teilpublikationen – noch nicht veröffentlicht worden ist sowie, daß ich eine solche Veröffentlichung vor Abschluß des Promotionsverfahrens nicht vornehmen werde. Die Bestimmungen dieser Promotionsordnung sind mir bekannt. Die von mir vorgelegte Dissertation ist von Herrn Prof. Dr. Dr. J. Hescheler betreut worden.

Übersicht der Publikationen: siehe Kapitel „**XII Publications**“

Ich versichere, dass ich alle Angaben wahrheitsgemäß nach bestem Wissen und Gewissen gemacht habe und verpflichte mich, jedmögliche, die obigen Angaben betreffenden Veränderungen, dem Promotionsausschuss unverzüglich mitzuteilen.

.....
Datum

.....
Unterschrift

XII Publications

Evidence for a Critical Role of Catecholamines for Cardiomyocyte Lineage Commitment in Murine Embryonic Stem Cells.

Martin Lehmann, Filomain Nguemo, Vilas Wagh, Kurt Pfannkuche, Jürgen Hescheler, Michael Reppel

PLoS ONE 8(8): e70913. doi:10.1371/journal.pone.0070913. published 02 Aug 2013

In vitro modeling of ryanodine receptor 2 dysfunction using human induced pluripotent stem cells.

Fatima A, Xu G, Shao K, Papadopoulos S, Lehmann M, Arnáiz-Cot JJ, Rosa AO, Nguemo F, Matzkies M, Dittmann S, Stone SL, Linke M, Zechner U, Beyer V, Hennies HC, Rosenkranz S, Klauke B, Parwani AS, Haverkamp W, Pfitzer G, Farr M, Cleemann L, Morad M, Milting H, Hescheler J, Saric T.

Cell Physiol Biochem. 2011;28(4):579-92. doi: 10.1159/000335753. Epub 2011 Dec 14.

Functional Expression and Regulation of Hyperpolarization-Activated Cyclic Nucleotide-Gated Channels (HCN) in Mouse iPS Cell-derived Cardiomyocytes After UTF1-Neo Selection.

Judith Semmler, Martin Lehmann, Kurt Pfannkuche, Michael Reppel, Jürgen Hescheler and Filomain Nguemo

(submitted “Journal of Cellular Physiology and Biochemistry”)

XIII Danksagungen

Mein Dank gilt:

Herrn Prof. J. Hescheler für die Überlassung der interessanten Projekte für diese Arbeit. Ich schätze mich glücklich auf dem hochaktuellen Gebiet der Stammzellbiologie arbeiten zu dürfen und am Institut für Neurophysiologie die Plattform für diese Arbeiten gefunden zu haben, die er und seine Mitarbeiter in jahrlanger Arbeit aufgebaut hat.

Mein ganz besonderer Dank gilt Herrn PD Michael Reppel, der sich trotz seiner vielen beruflichen Verpflichtungen als Arzt an der Universitätsklinik Lübeck und nicht zuletzt auch trotz seiner familiären Verpflichtungen, immer Zeit für mich genommen hat. Als mein „externer Betreuer“ hat er durch viele fachliche Diskussionen und Ratschläge, Manuskriptkorrekturen der Publikation sowie der Doktorarbeit, aber besonders durch seine sehr konstruktive und hilfreiche Art maßgeblich zum Gelingen der Arbeit beigetragen.

Meinem Gruppenleiter, Dr. Filomain Nguemo, dafür dass er mich in seine Arbeitsgruppe aufgenommen hat, fachliche Diskussionen, die Benutzung seiner Büro- und Laborräume und allem was man zum Arbeiten braucht.

Meinen Tutoren der Graduate School, Herrn Prof. Roth und Herrn Prof. Rosenkranz, für die Betreuung dieser Arbeit, und für deren Begutachtung.

Herrn Dr. Vilas Wagh und Herrn Dr. Kurt Pfannkuche für ihre Hilfe bei Experimenten (qRT-PCRs), kritische Ratschläge und wertvolle Diskussionen.

Ganz herzlich möchte ich mich bei meiner Arbeitsgruppe und meinen Arbeitskollegen für eine schöne und spannende Zeit bedanken. Besonders erwähnen möchte ich dabei meine „Kollegen der ersten Stunde“, Matthias und Judith. Neben diversen fachlichen Unterhaltungen und Erörterungen zur Laboroptimierung, war es mir immer ein besonderes Fest im Office beim Kaffee oder mal abends ein paar Gedanken mit euch auszutauschen. Ich hoffe, man verliert sich nicht aus den Augen!

Selbiges gilt auch für meine Doktoranden-Kollegen und Wegbegleiter Carlos, Christoph, Moritz und Gabriel. Vielen Dank für die gelegentliche geistige Zerstreuung im Kölner

Danksagungen

Nachtleben. Darüber hinaus bedanke ich mich auch bei meinen Arbeitskollegen Philipp, Daniel, Sven, Birte, Azra, Julius, Suresh, Antony, Raja und Jenni für ihre Hilfsbereitschaft, Unterstützung und die angenehme Arbeitsatmosphäre.

Den technischen Assistentinnen: Frau C. Böttinger für die sehr zuverlässige und stete Bereitstellung von Feedern, diversen anderen Zellen und Materialien. Susan Rohani für ihre Hilfe beim Auffinden verschwundener Aliquots und anderer täglicher Laborprobleme. Aber ein besonderer Dank geht an Rebecca (Rebi) und Annette, zum einen für eure Unterstützung bei einigen der Experimente, aber viel mehr noch für eure nette und lustige Art.

Den Technikern und Ingenieuren unserer Werkstätten und der IT Abteilung, Herrn Metzner und Herrn Stassen, und deren Hilfe in technischen Fragen. Herrn Stassen danke ich außerdem für die Bereitstellung diverser Software und die Beratung und Unterstützung bei der Handhabung der Datenberge. Ganz speziell bedanke ich mich auch bei Fabian Böde, der an der Programmierung unseres maßgeschneiderten MEA QT-Zeit Auswertungstools maßgeblich beteiligt war.

Last, but definitely not least, bedanke ich mich bei meinen Eltern. Ihr habt mich immer unterstützt, an mich geglaubt, gefördert, bei Bedarf aufgemuntert und motiviert und mir den Rücken frei gehalten. Dafür bin ich euch unendlich dankbar! Worte können nicht ausdrücken wie glücklich ich bin, Eltern wie euch zu haben.